University of Venda
Creating Future Leaders

University of Venda

EVALUATION OF MAJOR CLAY DEPOSITS FOR POTENTIAL INDUSTRIAL UTILIZATION IN VHEMBE DISTRICT MUNICIPALITY, LIMPOPO PROVINCE OF SOUTH AFRICA

Name : George Oluwole Akintola
Student Number : 16014356

Supervisor : Dr. F Amponsah-Dacosta
Co-supervisor : Mr. Sphiwe Emmanuel Mhlongo

A Dissertation Submitted to the Department of Mining and Environmental Geology, University of Venda, in Fulfillment of the Requirements for the Degree of the Master of Earth Science in Mining and Environmental Geology

February 2018

DEDICATION

To

The almighty God for making it possible to complete this degree.

To my father Pastor Jacob. A. Akintola who never cease to encourage and inspire me

To my mother of blessed memory, Deaconess Comfort. A. Akintola

To my lovely wife, Phebean Olutosin Akintola

To my wonderful son, David Olusola Akintola

To my beloved family members

And

To my supervisors without whom this work would not have been completed in record time.

DECLARATION

I, **George Oluwole Akintola** with student number 16014356 hereby declare that Evaluation of major clay deposits for potential industrial utilization in Vhembe District Municipality, Limpopo Province of South Africa is my own work except where sources are otherwise cited and acknowledged in references. Also, it has not been previously, in whole or in part, submitted to any examination or university for any degree.

Signature……. Date:……...

George. Akintola

We, the supervisors**,** certify that this declaration is correct.

Signature:……. Date:……..

Supervisor: Dr. F. Amponsah-Dacosta

Signature:…….. Date: ……

Co-supervisor: Mr Sphiwe Emmanuel Mhlongo

ACKNOWLEDGEMENTS

First, I thank the Almighty God for his matchless grace that enables me to successfully complete this thesis. The thesis could not have been possible without the support of my promoter, Francis Amponsah-Dacosta, whose scientific vigor and masterful experience are motivating and impactful. I am gratefully indebted to my co-promoter, Sphiwe Emmanuel Mhlongo, who always steered me in right direction when needed while allowing the research to be my own work. I acknowledge that I have not only been mentored and transformed into a better researcher but also received invaluable contributions and insights from the best supervisors in the world. Your financial support towards my registration, sample collection and analyses is greatly appreciated.

The full financial support received from the University of Venda research fund was greatly acknowledged and appreciated. I would also like to extend my thanks to the staff of Mining and Environmental Geology laboratory: Mr. C. Muzerengi and Nemapate; XRD and XRF unit of University of Pretoria and Johannesburg; mineralogy division of Mintek for assistance during my laboratory work. I wish to thank Manenzhe A.B, Matsiketa Khensani.E, Maluleke Rivoningo, to mention but few, for their assistance during fieldwork and sample collections.

I sincerely express my profound gratitude to my parents Pastor and Deaconess J. Akinyemi Akintola for their unflinching support. My special thanks go to my wife and son: Phebean and David for always being there for me. It is not easy to leave ones' family and travel to obtain a degree. Your encouragement, understanding, prayers and love inspire me to work harder. I cannot but just thank my siblings: Barrister Olusegun, Mr. Adekunle, Dr Akintunde, Mr. Olawale and Mrs. Adeola and other members of the family for their encouragement and prayers for the success of this work.

I am appreciative to Dr. A.I Akintola, Dr. S. Obadire, Mr. M.O Oyebanjo and Dr. J. Edokpayi for not only facilitating and supporting my commencing of this programme but also caring for me spiritually, materially and financially. I am indebted to Mr. O.M. Obijole, Mr. K.I Ekanade, Dr. T. Anyansi, Dr. Jegede and Mr. Elegbeleye for your immeasurable supports. Finally, my special thanks go to the leadership of Christ Tabernacle Church and all the members for providing a healthy and homely spiritual family for me.

ABSTRACT

Vhembe District has several clay deposits which are traditionally use for clay products such as burnt bricks without taking into account the chemical and mineralogical characteristics of clay being used. The ever-increasing market demand for these clay products cannot be met with the traditional method of clay utilization due to the paucity of scientific information on properties of the clay in the area. Consequently, there is a need to gain better understanding of the characteristics of the clay in Vhembe District and to establish the suitability of the variety of clay for different purposes.

The current study was undertaken to better understand the compositional relationship between the clay deposits and surrounding rocks present in the study area. It further aimed at characterizing the clay deposits on the basis of chemical, mineralogy, physical, mechanical, thermal and micro structural properties with a view of evaluating the clays for possible industrial use. A total of thirty-nine clay and rock samples were collected from thirteen different locations across the Vhembe District. Thirteen representative samples from each location were obtained after thorough mixing until homogenization was attained and then quartered for subsequent analyses.

The mineralogical and chemical characteristics of the clay and rock samples were determined using XRD and XRF respectively. Thin-sections of the rock samples were prepared and examined under petrographic microscope to better understand the mineral assemblages present in the rocks. The thermal and micro structural properties of the clays were determined using DTA-TGA and SEM analyses and the physical properties which include colour, cation exchange capacity (CEC) and soil pH were assessed. The particle distribution and Atterberg limits tests of the clay samples were also conducted in order to establish their mechanical properties.

The petrographic results showed that the clay deposits exhibited an intense weathering and sedimentation processes which incorporated detrital minerals from the surrounding rock units. The rock units which include basalt, granodiorite, gneiss and quartzofeldspathic gneiss were found to be differentiated from subalkaline and/or tholeiitic magmatic composition. Although the value of SiO_2 content in rock samples was higher when compared with clay samples, it indicated an ongoing desilicication and allitization processes. The high values of chemical index of alteration (CIA), low values of K/Cs (<6200), Ce* normalized value and higher values of LILE enrichment in the clay deposits indicated oxidizing environments during period of deposition.

The mineralogical composition of the studied clayey deposits showed that smectite (8.25 - 29.32%), kaolinite (14.91 - 59.26%) and chlorite (5.94 -16.54%) were present as clay minerals although associated with other non-clay minerals such quartz, plagioclase, talc and geothite. The chemical composition results revealed high silica and alumina content in most studied clay samples. Their fluxing oxides which include K_2O, Na_2O, CaO, and MgO, varied slightly from 0.06% to 1.78% in abundance while the Fe_2O_3 and TiO_2 contents in most samples averages at 9.2% and 1.3% respectively. The plasticity index of the studied deposits ranged from 9.50 to 62.00% while liquid limit ranged from 31.34 to 73.62%.

The microanalysis using SEM indicated that the microstructure framework of most studied clay exhibited a porous skeleton structure owing to numerous tiny voids. The composite results of SEM and CEC analyses suggested their possible application in water filter and chemical fertilizer industries since they provided passage for water and soil cations transmission. The particle size distribution demonstrated that the studied soils have clayey silt texture with wide range coverage of the well graded and sorted particle sizes. Compressibility and plasticity properties were found to be high in Mukondeni, Mashamba-1, Mashamba-2 and Mashamba-3 clay samples. The thermal behavior of Mukondeni, Mashamba-1, Mashamba-2 and Mashamba-3 samples showed relatively high shrinkage (>9%). The high shrinkage percentage suggests the preponderance of smectite minerals. Other samples which are rich in kaolinite and chlorite minerals exhibited low shrinkage (<2%). The drying trends of the studied clay suggest their suitability for fast drying processes like soft and hard refractoriness, sanitary wares and ceramics. Empirical assessment of most studied clay showed their suitability for pottery-making and manufacturing of roofing tiles and masonry bricks.

Keywords: *Clay deposit, Chemical index of alteration (CIA), desilicication, allitization, potential industrial utilization, scientific evaluation.*

TABLE OF CONTENT

Content **Page**

LIST OF FIGURES

LIST OF TABLES

LIST OF MEASUREMENT UNITS

˚C	Degree Celcius
g	Gram
Kg	Kilogram
%	Percentage
mL	Milliltre
meq/100g	Milliequivalent per 100 gram

LIST OF ACRONYMS AND ABBREVIATIONS

ASTM	American Society for Testing and Material
C_c	Coefficient of Uniformity
C_c	Coefficient of Curvature
CEC	Cation Exchange Capacity
CIA	Chemical Index of Alteration
CIW	Chemical Index of Weathering
Dol	Doli Clay Samples
Man	Manini Clay Samples
Mat	Matsika Clay Samples
Mas1	Mashamba1 Clay Samples
Mas2	Mashamba2 Clay Samples
Mas3	Mashamba3 Clay Samples
Mav	Mavambe Clay Samples
Muk	Mukondeni Clay Samples
PI	Plasticity Index
PL	Plasticity Limit
SEM	Scanning Electron Microscopy
Sil	Siloam Clay Samples
S_o	Coefficient of Sorting
UCC	Upper Continental Crust
USCS	Unified Soil Classification System
XRD	X-Ray Diffraction Spectroscopy
XRF	X-Ray Fluorescence

CHAPTER ONE

INTRODUCTION

1.1. Background on Clay Minerals and their Industrial Application

The utilization of raw clay for different purposes is known and acknowledged in different parts of the world. Demands of clay mineral products are ever-increasing and wide-ranging thereby making clays to have different applications in different industries such as mining, agriculture, civil and construction, engineering, environmental and processing industry (Mahmoudi *et al*., 2017). The reason for varied applications of clay minerals can be primarily attributed to their varying physical and chemical properties. According to Murray (2000), it is due to their structural arrangement and composition of octahedral and tetrahedral coordination within the layered crystal structure of clay minerals. These properties play an important role in identification and utilization of certain clay minerals for a specific purpose (Boussen *et al.,* 2016).

Mineralogical characterization of clay can be influenced by the parent rocks from which it originated (Montes *et al.,* 2016). Clay deposit derived from granitic and gneissic rocks can occur together with those derived from micaceous schist though differing in properties. The micaceous-schist derivatives impart yellow-brown color as opposed to the dull gray appearance of clay derived from gneissic and granitic rocks (Nyakairu, *et al.,* 2002). According to Ekosse (2010), kaolin can be formed from possible alteration of feldspathic arkosic-sediments which weathered from potassium-rich granitic rock and identification of kaolin has been revealed by observation of petrographic and mineralogical studies. Clay derived from gneissic and granitic rocks tend to possess property such as thermal strength which makes it suitable for refractory materials (Nyakairu, *et al.,* 2002; Mark, 2010).

The suitability of clay mineral for specific utilization can be related to the clay's physical properties as well as chemical composition (Manoharan *et al.,* 2012). Interestingly, the work noted that the engineering behavior of clay such as plasticity and strength can be influenced by its composition and physical properties such as particle size distribution. According to Dies (2003), plasticity is the most important property of clay mineral that determines its use for ceramic purposes. This is because this property ensures that different shapes are maintained before firing of ceramic products. Furthermore, M'barek-Jemai et al. (2017) indicated that clay deposits with low plasticity and high amount of finer particles can be used in ceramic industry. Therefore, it would be regarded

unsuitable to utilize same clay mineral for a particular industrial production without considering its physical and chemical properties. As a result, detailed scientific understanding of physical, chemical and engineering properties is critical to ultimate description of the utilization of any clay mineral.

There are varieties of clay mineral types and Murray (2000) has described smectite, kaolinite, and palygorskite and sepiolite to be among the World's most important due their wide traditional utilization. In general, clay is any naturally occurring fined-grained substance composed of hydrous phyllosilicate mineral with residual fragments of other minerals and colloidal materials which possesses plasticity property at appropriate water content and becomes indurated when fired (Horn and Strydom,1998; Dacosta *et al*., 2013). The origin of clay could be primary (residual deposits), hydrothermal deposit or mixed hydrothermal and residual deposits, or secondary which is the erosion, transportation and deposition of clay particles into depositional environment such as lacustrine, paludal, deltaic, glacial, loess and marine (Ekosse, 2005).

Kaolinite mineral was recognized to be found in estuarine or deltaic environment where fluvial or tidal influence can rapidly remove the Mg^{2+} and K^{+} ions from weathered solution of parent mineral (Santos and Rossett, 2006). This environment suggests tropical humid condition with alternating more pronounced wet seasons and less dry season which tend to increase water movement for rapid and adequate removal of the ions in the weathered solution (Refaey *et al.,* 2015). Conversely, smectite clay mineral is demonstrated to be present in low-lying surfaces which is indicative of marine environments under dry seasons with alternating less pronounced wet season and characterized with poor drainage or water movement (Odoma *et al.,* 2013; Ehrmann *et al.,* 2007; Schaetzl and Anderson, 2005).

Post-depositional alteration such as digenesis, reduction and oxidation, chemical dissolution processes affect the mechanical, mineralogical, geochemical and fabric properties of pre-existing clay sediment in depositional environments (Pruett, 2016). According to Ghandour *et al.* (2004), diagenetic process tends to modify pre-formed smectite into authigenic illite clay mineral during its precipitation. The precipitation from pore fluid of organic and inorganic compounds such as calcium carbonate, alkali and iron oxide, silicate causes cementation of clayey sediments (Casey, 2014). The cementation process has natural micro-structure effect on soil properties which include changes in void ratio, stiffness, brittleness, quasi preconsolidation and shear strength (Gutierrez *et al.,* 2008). Gray kaolin that pre-existed in reducing anaerobic environment can modify to cream or pink colour kaolin due to post-depositional oxidative alteration (Schroeder *et*

al., 2004). The alteration, which is not sedimentological process, removes iron sulphide (FeS) and oxidize the remaining free iron to iron oxides. Other post-depositional alteration involves conversion of mica and ilmenite to anatase during mica kaolinization. Furthermore, post-depositional weathering has been adduced to formation of bauxitic kaolin and bauxite from further weathering of pre-formed kaolin (Galan *et al.,* 2016).

Momoh *et al* (2013; 2014) and Dacosta *et al* (2013) conducted studies on the geophagic clay materials consumed by the local communities of Vhembe District and industrial purposes respectively. In furtherance to the mentioned previous researches, this study characterizes the major clay deposits in Vhembe District for their potential industrial utilization. The outcomes of this study will not only constitute an inventory of useful clay materials but also stimulate growth of clay raw material sector and thereby contribute to sustainability of the economic development in Vhembe District. In addition, it will contribute to the clay minerals body of knowledge and stimulate private investors and government for investment opportunities and policies particularly in the Vhembe District.

1.2. Statement of the Problem

The Vhembe District has several clay deposits that are used by local communities for different purposes such as making of clay bricks and traditional ceramic pots (Barker *et al.,* 2006; Dacosta *et al*., 2013). In Vhembe District, the conventional local use of clay for products such as burnt bricks and pottery is mostly considered without any scientific assessment of the raw clay to determine its suitability for the products. In practice, traditional methods of clay utilization do not take into account the chemical and mineralogical characteristics of clay being used.

There is an ever-increasing market demand for clay products. This has been primarily driven by increase in civil and construction activities as well as a ceramic water filter factory in the area. This demand cannot be met with the traditional methods of manufacturing the products due to the paucity of scientific information on properties of the clay in the area. Consequently, there is a need to gain better understanding of the characteristics of clay in the Vhembe and to establish the suitability of the variety of clay for different purposes.

1.3. Aim and Objectives of the Research

The research aimed to carrying out an evaluation of major clay deposits in the Vhembe District Municipality with the purpose of establishing their potential industrial utilization. The specific objectives were:

- To investigate the provenance of clay sediments in the study area.
- To determine the geochemical, mineralogical and engineering properties of the major clay deposits in the study area.
- To evaluate the suitability of the different clay deposits for various industrial uses.

1.4. Research Questions

The following questions were developed to address the research:

- What is the compositional relationship between the clay sediments and exposed lithology within the study area?
- What is the mineralogy composition of the major clay deposits found in Vhembe District?
- What are the physical and geochemical characteristics of the major clay deposits found in Vhembe District?
- What are the potential industrial uses of major clay deposit of Vhembe District?

1.5. Hypothesis of the Study

The research was conducted to test the following hypotheses:

- The characteristics of clay deposits can reflect the mineralogical composition of parent rock from which it originated or different source rock that contributes to the deposit.
- The engineering and mechanical properties of clay could be an expression of the interplay of combination of clays compositions.
- The physicochemical and mineralogical characteristics that clay possesses could be responsible for its suitability for specific industrial use.
- Based on the characterization and evaluation of the Vhembe clay deposits, useful, relevant and reliable scientific information about the spatial distribution of major clay types can be produced.

1.6. Justification of the Study

The Vhembe District Municipality is basically made up of Musina, Mutale, Makhado and Thulamela Municipalities. It is comparatively a rural area with economic activities ranging from agricultural, mining to tourism. Interactions with the traditional rulers and youths reflect the poor economic development and high unemployment rate despite their growing agriculture and tourism sector. Small-scale farming and pottery are mainly the income generating activities of the indigenes.

Most residents in the community are comparatively indigent and this was confirmed by the reviewed indigent policy of 2016 that recognized the need to reduce levels of poverty and enhance local economic and human capital development. The availability of vast raw clay deposits can be identified as another latent development potential for the municipality if evaluated, explored and exploited.

From academic viewpoints, comprehensive scientific evaluation and characterization of major clay deposits will not only contribute to the Clay Minerals Body of knowledge but also provide valid report upon which prospective companies, industrialists and government can leverage for decision making. While harnessing the major clay deposits in this study area, sustainable and commercially viable business opportunities can be developed for investment thus improving the local economic development and the standard of living of the residents. From economic viewpoint, this will encourage industries producing ceramics, water filters, building bricks, tiles, insulators, plastics, paints to be established in Vhembe environs thus creating job opportunities for unskilled, skilled and graduates' personnel.

1.7. Description of the Study Area

The study area is described in terms of geographical location, topography and drainage pattern, vegetation, climate condition and regional geology and structural geology.

1.7.1. Geographical location of the study area

The study area is Vhembe District and it is in the north of Limpopo Province. The province shares a border with Zimbabwe and Botswana and the capital is Polokwane. It is situated between latitude $22^0\,15'\ 00''$and $23^0 30'00''$ longitude $28^0 45'00''$and $31^0 15'00''$. Vhembe District has four local municipalities namely: Musina, Mutale, Thulamela and Makhado with a population of about 1.2 million people (Amidou, 2007).

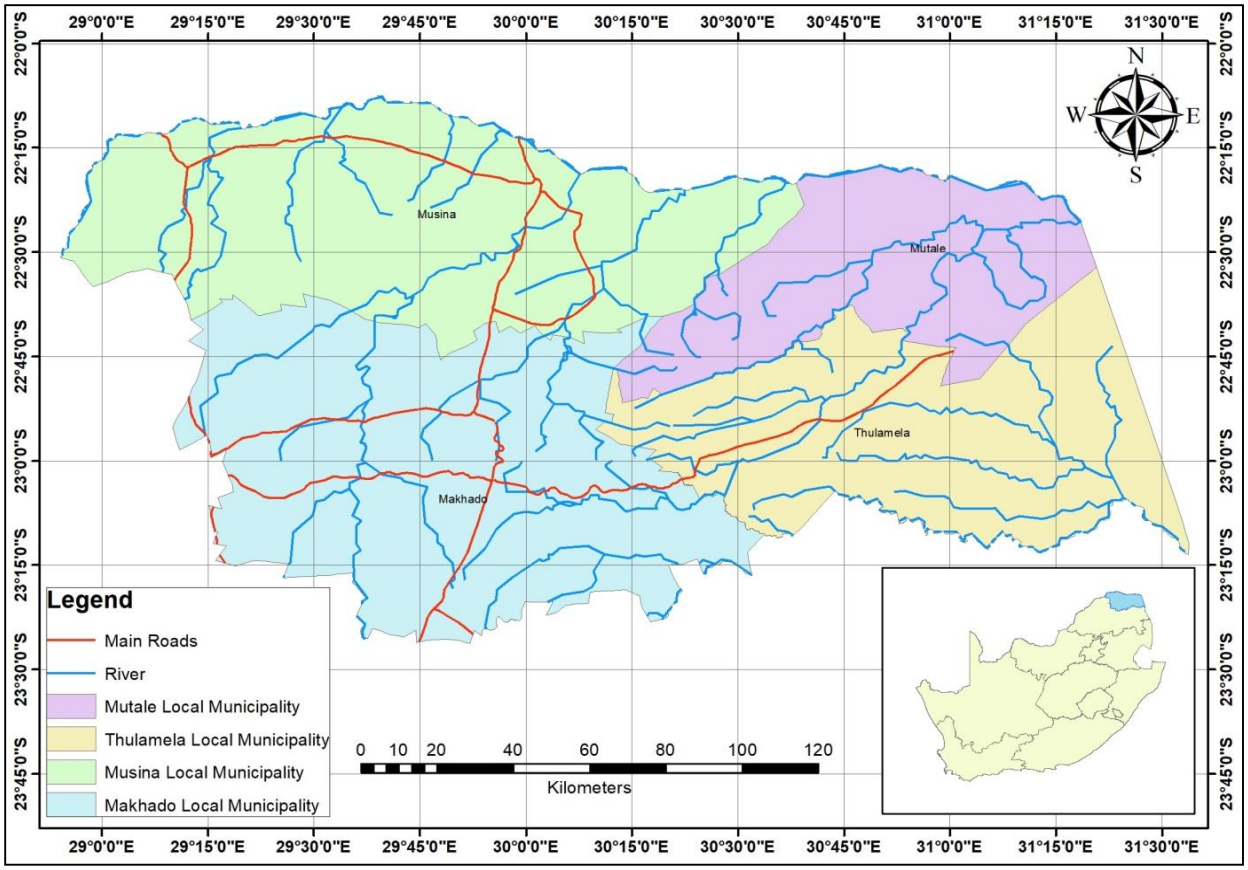

Figure 1.1: Geographical location map of the study area.

The topography of the study area is characterized by Soutpansberg mountain range. It is a major regional topographic feature and it extends in an east-west direction for approximately 130 km and this gives rise to prominent east-west striking mountains and valleys. The landform is moderately undulating and characterized by scattered outcrops of relatively small hills towards the East and the West. The access roads leading to the study area are good and easily navigated. The altitude at Thulamela and the environs ranges between 510 to 620m above the main sea level (Nemakundani, 2009).

According to Middleton and Bailey (2009), Limpopo River is the major river that drained the study area. However, six main river systems are tributaries to Limpopo River and have different sources. Luvuvhu, originating due east of Louis Trichardt; Mutale originating in Thathe Vondo; Mutamba originating on the farm Buelgum Poort; Nwanedzi originating near Mavhode; Nzhelele originating in Thathe vondo and Sandrivier originating between Potgietersrus and Pietersburg.

1.7.3. Land-use and vegetation

The anthropical activities that are common in the study area include agriculture, mining activities, pottery making trading and residential. Animal farming and plantain plantation are also part of the land-use activities practiced around the study area.

The study area falls within the Venda arid Mountain Bushveld and Mopani wooland, characterized by open grasslands with scattered trees and bushes. However, semi-deciduous forest prevails along the streams. Some types of trees that dominate the study area are Acacias and Baobab tree. At a relatively low proportion Poinciana (flamboyants), Jacandas, Frangipani and Bougainvillea flourish trees are also identified (Kleynhans *et al.,* 2005).

1.7.4. Climate of the area

The study area is situated in a dry savannah sub-region. The regional climate is strongly influenced by the east-west orientated mountain range which represents an effective barrier between the south- easterly maritime climate influences from the Indian Ocean and the continental climate influences (predominantly the Inter-Tropical Convergence Zone and the Congo Air Mass) coming from the north. The area experiences summer rainfall which occurs in the form of heavy thunderstorms or soft rain where the rainfall is in the order of 450 to 890 mm (Kleynhans *et al.,* 2005; Municipality, 2014). It is characterized as being hot and dry resulting in high evaporation rates. The area is characterized by cool, dry winters (May to August) and warm, wet summers (October to March), with April and September being transition months. Temperature ranges from 18°C to 39.9°C in elevated areas and whole region respectively while the area is generally frost free (Kabanda, 2003; Municipality, 2014).

1.7.5. Regional geology and geology of the study area

The Vhembe District falls within the geology of Soutpansberg Group of Sedimentary and Volcanic rocks (Krammers *et al.,* 2006). It is important to note that the Soutpansberg Group unconformably overlain the granitoid- greenstone terrains of both Kaapvaal and the Zimbabwe Cratons in the Limpopo mobile belt (Brandl, 1999). According to Brandl (2002), the Soutpansberg Group represents a volcano-sedimentary succession. The chronological succession of the Group from oldest to youngest are Tshifhufhu, Sibasa, Fundudzi, Wyllie's Poort, Nzhelele, Stayt and

Mabiligwe Formations as shown Figure 1.1. The mentioned figure illustrates the volcano-sedimentary succession of the Soutpansberg Group after Barker et al. (2006).

The study of Brandle (2000) recognized that the larger part of Vhembe District, which includes Makhado, Mutale, and Thulamela is underlain by the Fundudzi, Nzhelele and Sibasa Formations respectively while Phanerozoic Karoo Supergroup of sedimentary rock occurs locally in some part of Musina. Barker *et al.* (2006), indicated that Sibasa Formation (about 3000m thick) comprises pyroclastic lava with minor intercalation of sedimentary and tuffaceous rocks underlain the Thulamela Municipality. Similarly, Barker (1979) noted that the pyroclastics rocks of Sibasa Formation can reach estimated thickness of 200m in the Mutshindudi Natal House agglomerate north of Thohoyandou and best developed in the Kruger National Park.

Makhado Municipality is described to underlain by Fundudzi Formation which comprises mainly of arenaceous and argillaceous rocks with a few thin pyroclastic beds (Barker *et al.,* 2006). Previous studies of Barker (1984) and Brandl (1981) suggested that Fundudzi Formations with estimated thickness of 1900m are developed mainly in the eastern Soutpansberg and laterally wedges out in Mountain Inn Member in Makhado. The red argillaceous and arenite sediments with several layers of pyroclastic that constitute the Nzhelele Formation (about 600m thick) are observed to cover the Mutale Municipality (Brandl, 1981, 2000; Barker *et al.*, 2006).

According to Bumby (2000), the development of soutpansberg trough is connected to the Limpopo Orogeny of about 2.7 Ga which caused the uplifting of the Central Zone of Limpopo Mobile Belt. This uplift resulted in the isostatic creation of the Soutpansberg trough within the asymmetrical Northern Marginal Zone of Zimbabwe Craton and Southern Marginal Zone of Kaapvaal Craton. Although the much larger area is characterized by the formations of Soutpansberg (Kreissig *et al.,* 2000).

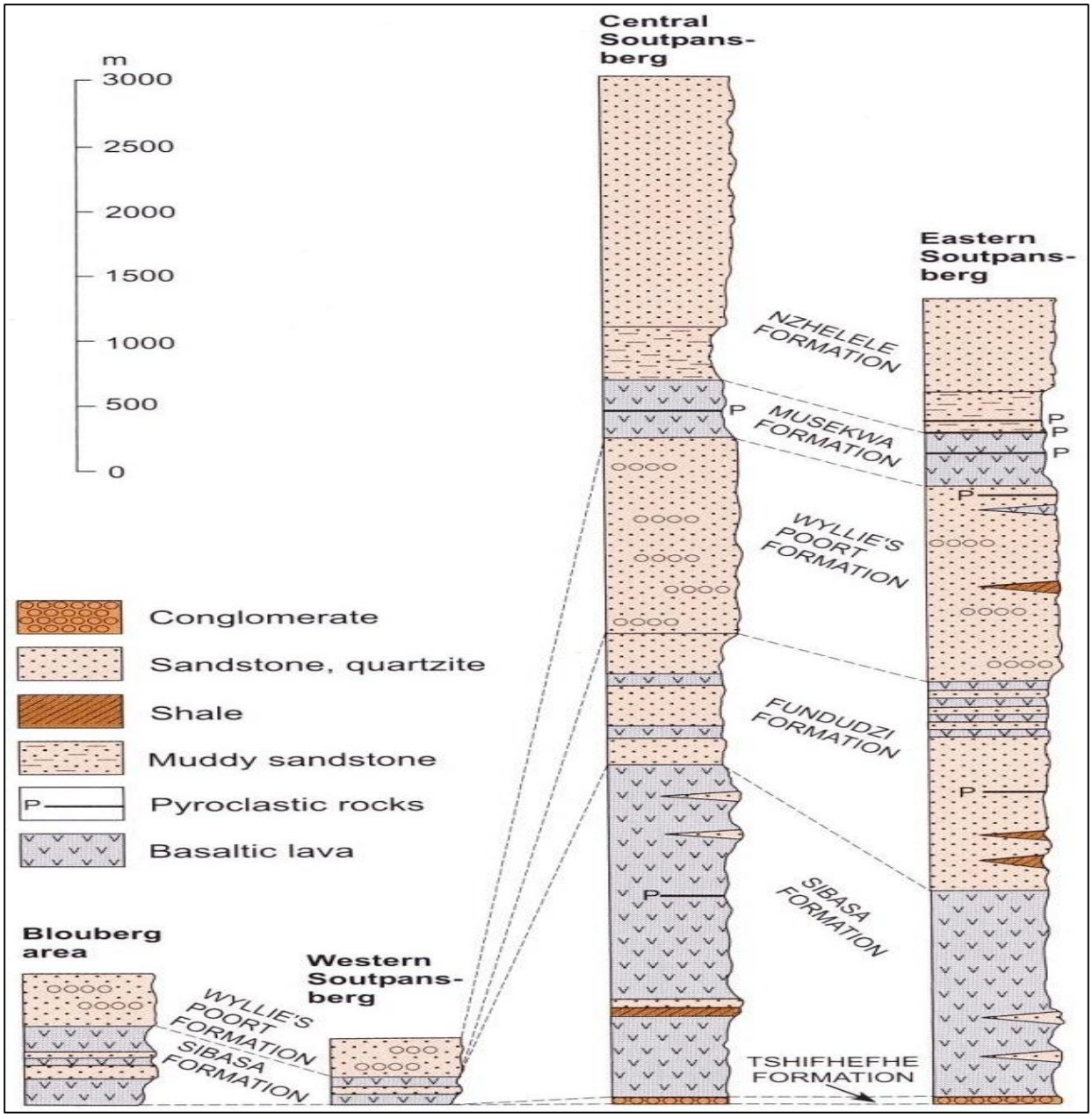

Figure 1.2: Stratigraphy of the Soutpansberg Group (After: Barker *et al.,* 2006)

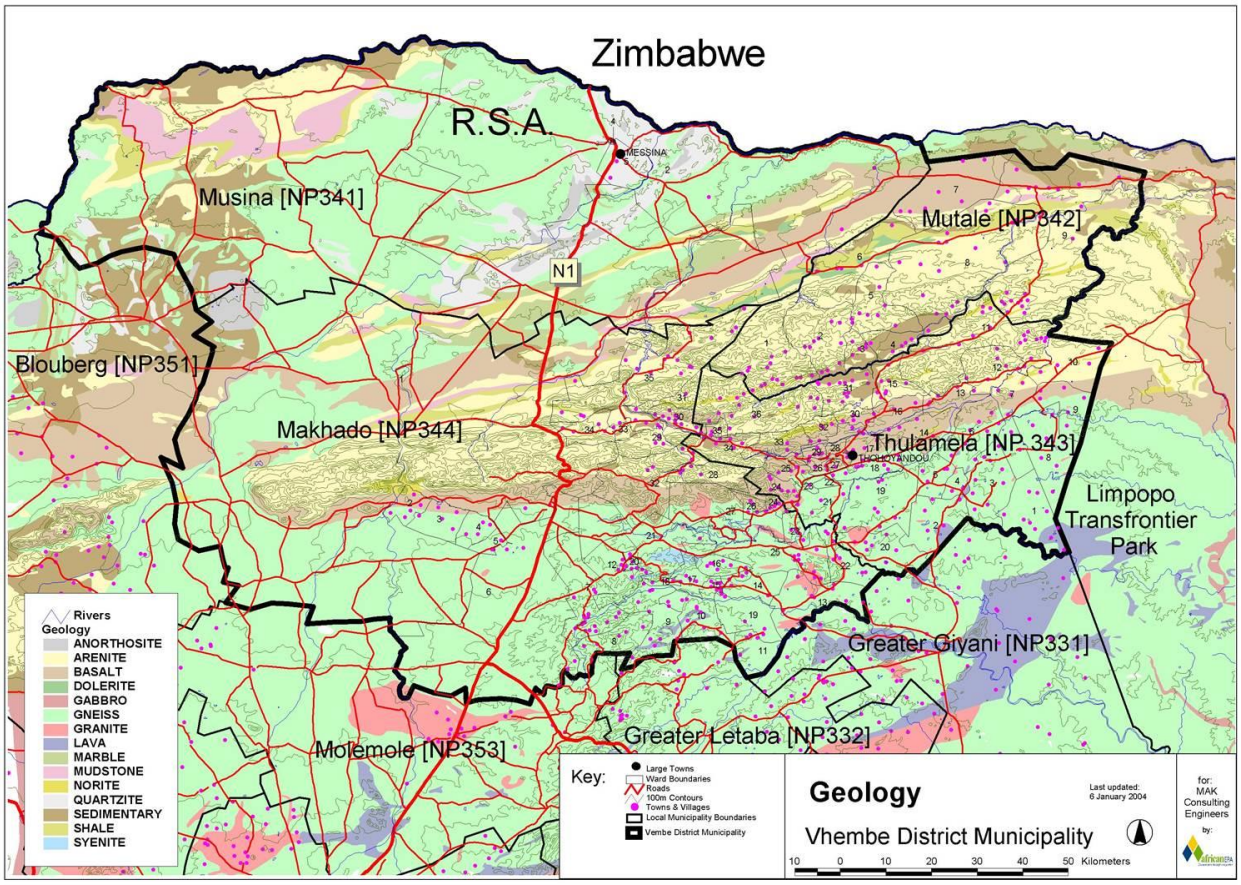

Figure 1.3: Geology map of Vhembe District Municipality.

1.8. Research Conceptualization

The mineralogy and chemical elemental composition of both studied rock and clay samples are determined to infer the petrogenesis of clay deposits in the study area. Mineral assemblages present in collected rock samples are identified when viewed under petrographic microscope after their thin sections with 25µm thickness have been prepared. The prepared rock samples were collected from country outcrops around the studied clay deposits. The clay deposits samples were characterized in terms of major and trace elemental composition using S2-Ranger X-ray fluorescence equipment. The relationship between progressive mobility of major elements such as Na, K, Ca, Mg and Si, and trace elements are investigated with respect to provenance of clay deposits using evaluated index indicators such as chemical index of alteration and weathering (CIA, CIW), weathering index of Parker, value ratio of chondrite normalization of K/Cs and SiO_2/ Al_2O_3which indicates the degree of desilicication and allitizaion.

It is important to note that the detail scientific understanding of the physico-chemical, mineralogical and thermal properties of clays are critical to the ultimate description of their industrial suitability uses. Consequently, in-depth understanding of physical properties of the studied clay samples such as tonality, cation exchange capacity, and pH are achieved using Munsell color chart, basic cation atomic absorption spectroscopy (AAS), pH meter respectively. Quantitative and qualitative mineral composition of studied clay and rocks samples were determined using a PANalytical X'Pert Pro powder diffractometer in θ–θ configurationwith an X'Celerator detector and variable divergence- and fixed receiving slits with Fe filtered Co-Kα radiation (λ=1.789Å). The phases were identified using X'Pert Highscore plus software. The degree of thermal and heat flow stability of the studied clay samples to increasing temperature was determined using Setaram apparatus with calcined Al_2O_3 reaching a maximum temperature of 1000^0C at heat rate of 25^0C/min serving as inert material. Engineering properties of the studied clay samples such as plasticity index, grain and pore sizes distributions were obtained using Casagrande apparatus, sieve and hydrometer tests and scanning electron microscope (SEM). The significance of the various characterizations is to understand the studied clay index properties to evaluate their suitability for different industrial purposes.

The suitability of the studied clay samples from Vhembe District for various industrial utilization Unified Soil Classification system (USCS), clay workability chart, Winkler's and direct inference from the studied properties. The USCS employs plasticity index parameter and grain size distribution as criteria for its standard. The Winkler's diagram assesses the technological allocation of clay for various domain field of application based on grain sizes classification. The domains application includes common bricks, vertically perforated bricks, roofing tiles, masonry and hollow bricks. While the clay workability chart uses plasticity parameter to determine domains of application of clay for pottery and brick.

1.9. Organization of the Dissertation

The dissertation is organized into seven chapters in which each section has distinct and separate information. Chapter One succinctly discusses the background on clay minerals and industrial applications in Vhembe District with the purpose of establishing their potential industrial uses. Chapter Two provides the literature review where current level of knowledge in relation to the general overview of the clay and the suitability properties of clay for industrial application are elaborately discussed. Chapter Three describes the procedural steps, tools, equipment used to locate the clay deposits, sample collections and research methodology. Chapter Four presents

the interpretation and discussion of the experimental results obtained from major and traces elemental composition of both clay and rock samples using X-ray fluorescence (XRF) and petrographic optical microscopy. It provides robust discussion on source rock indicators elements such as high field strength elements (HFSE), large ion lithophile elements (LILE) and rare earth elements (REE) which are pointers to provenance and paleo - tectonic setting of clastic deposits. Chapter Five presents interpretation and discussion of the results obtained from the physical, mechanical and thermal analyses of clay samples. Information about mass stability of studied clay samples over time as temperature increases were evaluated by the thermal analysis (TGA). The micro-pore analysis describes the microstructures and surface topography of the studied clays using scanning electron microscopy (SEM). Furthermore, information on the maximum temperature range beyond which the studied clays start to degrade was discussed. Chapter Six presents the summary of the dissertation and give some concluding and recommendation remarks.

CHAPTER TWO

LITERATURE REVIEW

The evaluation of clays as well as their potential industrial application requires comprehensive understanding of clay compositions and characteristics. This chapter provides the current level of knowledge in relation to the general overview of the clay definition, formation of clay minerals and deposits, classification of clay minerals and their structures, industrial application of clay, important clay properties for industrial application, assessment of industrial clays and the suitability properties of clay for industrial application.

2.1. An Overview of the Definition of Clay

The definition of clay had raised striking issue with respect to its constituents and “clay mineral” definition. According to Ekosse (2005), the word “clay” can be referenced to as a mineral term, rock term and range of particle sizes term. In the context of mineral term, clay is naturally occurring earthy substance composed of hydrous aluminum phyllosilicate with residual fragments of other minerals such as quartz, feldspars, iron, carbonates, oxides, hydroxides and non-crystalline associated clay phase such as colloidal matter, organic matter and iron hydroxide gels (Dacosta *et al*.,2013). Clay as rock term can be described as claystones and mudstones of sedimentary rock. Bentonite clay, for instance, is a rock term whose dominant clay mineral is montmorillonite while rocks that are rich in kaolinites are commonly described as kaolin (Murray, 2007). In terms of particle sizes, clays are fine-grained particles of unconsolidated sediments which are crystallite sizes and not aggregate (Walter, 2011).

According to Murray (2007), clay minerals are genetically insignificance and are rarely mono-mineralized. They can occur as residual weathering products, sedimentary deposits and hydrothermally altered products. According to Montes *et al*. (2016), the fact that sedimentary clays overlaid residual clays in the same deposit does not imply same genetic formation. However, it was suggested that clay formation could include hydrothermal or weathering processes. According to Veld (1992), the occurrences of clays in nature are usually in sediments and sedimentary rocks and hydrothermal deposit. Therefore, vivid understanding of clay genetic or formation process is important.

2.2. Formation of Clay Minerals and Deposits

Generally, clay deposits are formed from the transformation of silicate rocks such as granite or volcanic tuffs. They are formed where rocks are in contact with water, air or steam. However, the type of clay formed is principally controlled by the composition of the pre-existing rock mineralogy (Kabeto *et al.,* 2014). Other factors that influence clay formation include chemical composition, texture and structure of parent rock, climate conditions, time, vegetation pattern and topography (Obaje *et al.,* 2013). Montes *et al.* (2016), noted that topographic condition, rapid draining rate and well-drained environment favor the formation of kaolinites clay minerals from alkaline igneous rocks such as nepheline-syenite and phonolites. Geologic processes that give rise to clay formation are basically hydrothermal actions and weathering processes (Nyakairu *et al.,* 2002).

Hydrothermal actions play an important role in the formation of clay deposits. Hydrothermal solution enhances the removal of materials such as alumina, silica, alkali or alkaline earth elements and iron from basement rocks and become altered to form clay minerals (Yong *et al.,* 2012). According to Montes *et al*. (2016), hydrothermal solution gives rise to clay formation which originated from *in- situ* weathering of magmatic potassic (phonolites) and alkaline (syenite) rocks. The residual clay that is formed from this process has pegmatitic veins which are completely altered to clay material. This feature cross-cut different clay layers besides structural joints and fractures that are present in the parent rock.

Similar study was reported by Nyakairu *et al.* (2002) that gnessic and granitoid rocks of basement are leached, weathered and enriched in quartz. The clays were thought to have been formed from leaching of the deformed basement. These clays may be formed *in-situ* resulting to residual clay deposits, hydrothermal and/or mixed hydrothermal and residual clay (Prasad, 2005). Ekosse (2010), described such formation as primary clays from which primary kaolin can be formed. Furthermore, it was indicated that primary kaolin can be residually formed from the alteration of feldspar-rich, Al-rick rocks such as granite and rhyolites in which mica and feldspar are parent minerals.

Weathering processes are another way through which clay formation and deposition occur. This involves the chemical decomposition and mechanical disintegration of original rock forming minerals such as feldspars, quartz, mica, amphibole, alumina, mafic minerals to clay minerals (Parriaux, 2009). This process is not complete until weathered minerals are transported and deposited by agents such as river, streams, wind and glacier (Ekosse, 2010). This type of processes usually gives rise to sedimentary or secondary clay deposit. According to Prasad

(2005), the sedimentary clays display sedimentary structures such as bedded forms, banding, laminations and composition variations both vertically and laterally. The work of Montes *et al.* (2016), also supported the presence of stratification and material differential in color variation.

Prolonged and extensive weathering transforms the primary rock forming minerals such as the felsic and mafic minerals to clay minerals. Under favorable conditions, the process leads to the development of clay deposits of economic interest (Kabeto *et al.,* 2012). The economic value of sedimentary kaolin formed through weathering is higher compared to primary kaolin (Ekosse, 2000). According to Ekosse (2010), kaolin which plays significant role in the industry can be formed from weathering processes. Montmorillonite minerals that result to bentonite clay finds economic importance in oil and gas industry and ceramic industry (Kabeto *et al*., 2012).

According to Ekosse (2010), primary kaolin which could be residual or mixed residual and hydrothermal can be formed from alteration of feldspar-rick, Al-rick rocks such as granites and rhyolites. Similar study by Ekosse (2001) also indicated that secondary kaolinites can be formed from alteration of feldspathic arenites, such as arkose, through the activity of ground water. However, basic igneous rocks can also give rise to kaolinite formation if the magnesia is removed as soon as it is released at rapid leaching rate. On the other hand, smectite is form at less rapid rate. Its formation is favored by dry seasons alternating with less pronounced wet season, poorly drained environment as well as low-lying topography (Refaey *et al.,* 2015). This suggests the possibility of deposit containing smectite and kaolin to develop from the same parent rock. Similarly, deposit having same clay mineral type can result from different parent rocks depending on the weathering conditions (Refaey *et al.,* 2015).

According to Murray (2000), factors that control the formation of palygorskite are an arid to semi-arid and strongly seasonal climate, an impeded drainage accompanied by water logging, an adequate supply of Mg and Si, and low Al activity, high prevailing ground water and soil pH conditions and host rock or ground water enriched in divalent elements.

2.3. Classification of Clay Minerals

Classification of clay minerals had been based on different parameters such as swelling property, structure and compositions, utilities, grain sizes, texture, origin and formations. According to Murray (2000), clay minerals can be broadly classified based on their swelling properties as well as non-swelling properties. Based on origin and formation, clay minerals can be classified as residual or primary deposit, hydrothermal and sedimentary or secondary deposit (Veld, 1992).

Clay can also be classified as crystalline or amorphous. The amorphous clays include the allophane group which is characterized by poorly crystalline clay mineraloid with random structural arrangement of silicon in the tetrahedral coordination and metallic ions in octahedral coordination without symmetry (Ekosse 2005). Another important classification can be based on their chemical composition, structure and size of which four groups of clay minerals are recognized namely kalolinite, smectite, illite and chlorite (Kabeto *et al.,* 2012). The work of Murray (2000) indicated that, based on industrial application, kaolinite, smectite and palygorskite and sepiolite are among the world's most important and useful ones.

Kaolinite is the commonest clay mineral member of the kaolin group. Structurally, kaolin group consist of one tetrahedral and octahedral sheet arranged in layers as shown in Figure 2.1a. Substitution in the lattice layers is very little with minimal layer charge and Base Exchange capacity. Other members include nacrite, dickite and halloysite. Halloysite has water molecule between tetrahedral and octahedral structural layer units. It is rarely found as weathering product of sedimentary origin but present in hydrothermal and residual deposits (Murray, 2007; Ekosse, 2010). Dickite and nacrite are usually found in hydrothermal deposits (Murray and Keller, 1993; Ekosse, 2010).

The smectites group of clay minerals consists of several clay minerals but the two most important industrially are sodium and calcium montmorillonites (Elzea and Murray, 1994). Their importance stems from their many faceted industrial applications. Bentonite is the whole rock term in which its dominant clay mineral is smectite and the most common smectite is calcium montmorillonite (Murray, 2000). Structurally, smectite is composed of one octahedral sheet sandwiched between two tetrahedral sheets layers (see Figure 2.1b). Silica is substituted by alumina in the tetrahedral layer and iron and magnesium substitute for aluminium in the octahedral layer. The resulted net positive charge deficiency is compensated by exchangeable cations absorbed into the interlayers. Whilst sodium montmorillonite forms when the dominant exchangeable cation is sodium, calcium montmorillonite resulted if it is predominantly calcium. Other clay minerals in this group are hectorites, saponites, nontronites and beidellite (Murray, 2005).

The illite group is formed by the decomposition of some clay-sized micas and feldspar. It can be found in hydrothermal alteration zone of muscovite where hot springs or metalliferous veins occurs (Ekosse, 2005). According to Ferrari and Gualtieri (2006), illite can be referred to as aluminium-potassium mica-like, non-expanding dioctahedral mineral present in clay sizes. Unlike mica minerals, illite is described to be depleted in potassium oxide and contain more silica and

water than the true mica minerals. Other mineral in this group includes hydrous micas, phengite, celadonite, brammalite and glauconite (green clay sand). Structurally, the octahedral sheet is sandwiched between two silica tetrahedral sheets as shown in Figure 2.1c (Murray, 2007).

Palygorskite - sepiolite clay minerals series is a hydrous magnesium aluminium silicate which is characterized by two laterally continuous sheets displaying regular inversion of the tetrahedral and a centrally located, discontinuous octahedral later (Figure 2.1d) (Cryssikos *et al.*, 2009). The palygorskite contains magnesium and aluminium in approximately equal proportions while magnesium has replaced most of the aluminium cations in the sepiolite (Suarez and Garcia-Romero, 2010). The frequent partial replacement of magnesium and aluminum by iron (Fe) in the octahedral layer produces a moderately high layer charge which in turn with the high surface area give palygorskite an intermediate cation exchange capacity. The high layer charge, high surface, the inverted structure facilitates the absorption and adsorption of elements and molecules onto the clays. Sepiolite differs from palygorskite in terms of slightly larger unit though both are structurally and chemically identical (Post and Heaney, 2008).

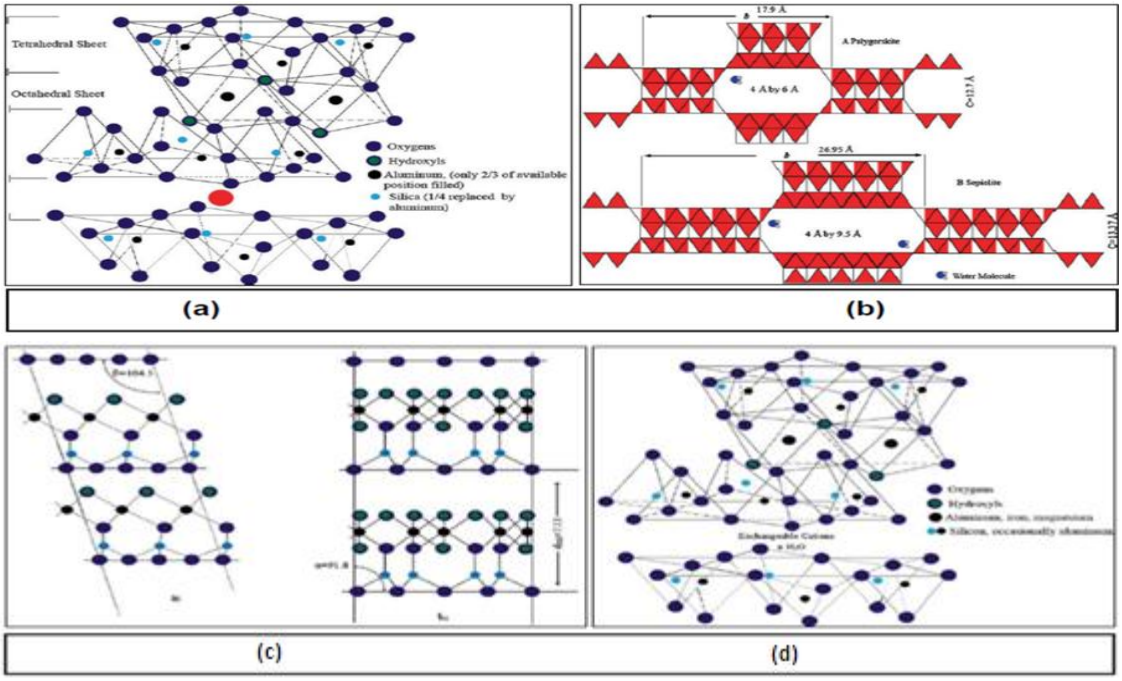

Figure 2.1: Structural illustration of different clay minerals (a) kaolin (b) smectite (c) illite (d) palygorskite and sepiolite (after Murray, 2007)

2.4. Industrial Application of Clay

According to Murray (2000), some of the more important common industrial application of clay include fiberglass formulator, plastic filler, paint extender, paper coating, ceramic ingredient, drilling fluids, cement, chemical carriers, foundary boundants, liquid barriers, decolorizations and catalysis. Kaolinite, smectite and palygorskite and sepiolite are described among the World's most important due to their wide application.

According to Ekosse (2010), the industrial application of kaolin in Africa is economically significant. It was indicated that kaolin is used in the production of paint, paper, plastics and rubbers. Other application includes pharmaceutical, polymer filler and reinforcement, cosmetics, chemicals, fertilizers. Bricks and tiles making, pottery, sanitary, tableware porcelain, ink extender, adhesives are also major consumers of kaolin (Murray, 2000).

According to Murray (2000), the smectite's properties such as high Base Exchange capacity, high absorption capacity, high surface area, high layer charge and high viscosity are related to its industrial application. Bentonite clay which belongs to smectite group of phyllosilicate minerals has a characteristic swelling property. Bentonite, primarily composed of montmorillonite, and is used as light-drilling mud in oil and gas industry (Kabeto, 2012). Appropriate quality of smectite can be used in production of ceramics, pottery and water filters (Dacosta *et al.,* 2013). They are also used as absorbents and adsorption, foundries and stabilizing emulsions (Obaje *et al.,* 2013).Illite has been considered as a major component of clays used in traditional ceramics for production of cooking pots, plates, tiles and bricks (Ferrari and Gualtieri, 2006).

In the same work of Murray (2000), it was indicated that the high absorption capacity and elongated habit of palygorskite-sepiolite makes the clay useful in many industrial applications. The industrial use of fuller's earth clay as bleaching agent and adsorptive agent is due to the presence of palygorskite and calcium montmorillonite minerals. Palygorskite-sepiolite is used in drilling mud for oil and gas and geothermal wells. Other growing use for these clays are as fertilizer suspension, floor absorbents, reinforcing fillers in rubber, adhesives, agricultural carriers, paint, cat box absorbents, tape joint compounds and anti-caking agent (Obaje *et al.,* 2013).

2.5. Important Clay Properties for Industrial Application

This section describes some of the important properties of clay for industrial application. These parameters include colour, cation exchange capacity and pH of clay, thermal capacity, plasticity and compressibility and water absorption properties.

2.5.1. Colour of clay

Colour is considered as an important property of clays that are used as fillers such as kaolins and white bentonite (Pruett and Pickering, 2006). Although, application of clay as fillers require white color, this can be affected by differences in mineralogical and chemical characteristics, particle size and shape (Christidis *et al.,* 2004). The varying colour of light gray to dark reddish-brown kaolin was attributed to the presence of goethite and hematite (Iron oxide minerals) (Ekosse, 2000). However, it is important to note that the natural red color of raw clay material does not confirm the presence of iron oxides but until the mineralogical analysis show its presence in much-crystalline form (Traore *et al.,* 2000). The colour is essentially a result of reactions of the mineralogical component present in a clay blend, when fired at high temperatures (Karaman *et al.,* 2006). It provides important information about constituents of the raw clay material.

The marketability of some clay products is based on several factors of which colour are one of the most important factor (Khan, 2000). The selection of a clay product; such as clay-brick, is often based on its color besides its resistance to stress. Colour is one of the most important properties of bricks in commercial aspect due to the common belief that the red colour is an indicator of a better quality for bricks (karaman *et al.,* 2006). According to Ekosse (2000), the poor colour of kaolin indicated very low brightness thus needed to be beneficiated. Natural colours of clay products range from reds and burgundies to yellowish brown, whites and buffs. There are several chemical constituents found in clays, but iron oxides probably have the greatest effect on colour formation.

2.5.2. Cation exchange capacity and pH of clay

The cation exchange capacity (CEC) of clay refers to the amount of negative charges in soil existing on the surfaces of clay and organic matters (Sidi *et al.,* 2015). According to Cui *et al* (2011), the cation exchange capacity of soil is as higher as the amount of montmorillonite in bentonite. It was noted that the exchangeable cations such as Mg^{2+} and Ca^{2+} have greater affinity for the negatively charge ions thus resulting in clay with more negative charges. Although CEC is

a good indicator of clay quality and productivity especially as fertilizer carriers, other measure of fertility such as pH is important as well. Ross and Kettering (1967) reported that a soil with a higher CEC may not necessarily be more fertile because it can be occupied by acidic cation such as Al^{3+} and H^{+}. The CEC value may be better at near-neutral pH than the acidic. The use of clay as fillers on road construction is widely acknowledged and the CEC capacity of clay can significantly affect it application as subgrade material. Wei *et al.* (2014) reported that decrease in strength of stabilizer used in construction is attributable to high CEC values. It was indicated that the concentration of main ions can create pores owing to exchange of cations.

2.5.3. Thermal capacity of clay

The thermal behavior of clay materials has been related to mass changes that occur due to kinetics analysis of volatiles present in the clay as temperature rises (Ptacek *et al.,* 2011). According to shriver *et al*. (2006), introduction of heat to different clay materials causes changes in mass due to process such as dehydration, decomposition, desorption and oxidation. As a result of heating, substantive mass loss has occurred in kaolin at temperature around 601-1020^{0}C which correspond to its dehydroxylation and mullitizaton processes (Haurine *et al.*, 2016). However, kaolin which finds utilization in refractory and ceramics is indicated to possess mullitization (i.e. crystal formation) temperature of 1200^{0}C or more (Ptacek *et al.,* 2011). Illite clay which can be used for structural clay products is observed to reach mullite phase close to that of kaolin (Araujo *et al.,* 2004).

During heating, soil rich in smectite and palygorskite clay which tend to possess high water absorption capacity showed low mutilization temperature (Murray, 2007). The onset of their thermal decomposition which is reflected by easy cracking at increasing temperature showed excessive mass loss during dehydration process. According to Karaman *et al.* (2006), thermal stability is an important factor that affects the resistance to stress property of clay products. Presence of chemical composition such as alumina and silica has been observed to improve thermal expansion of natural clay during heating (Pana *et al*., 2016). At rising temperature, liquid phase with high viscosity may form glassy fluid, *i.e.* vitrification, and fill the voids within clay particles thereby preventing dehydration process.

2.5.4. Plasticity and compressibility of clay

Plasticity has been described as the characteristic property that enables clay to be deformed under stress and retain the new shape after stress is removed (Horm and Strydom, 1998; Mueller *et al.,* 2007). According to Ince and Ozdemir (2010), plasticity which is a measure of cohesion possessed by soil when wet tends to reflect the mineral compositions present in the oil. Furthermore, clay minerals as well as colloidal particles i.e. associated phase, have been suggested to impart plasticity on soils besides the influence from range of particle sizes-associated minerals (Manoharan *et al.,* 2012). In terms of range of particle size, glauconite-sand which contain less fines tends to increase plasticity of soil while associated phase of chlorite species has been described to either improve or reduce the plasticity of soil (Guggenheim and Martin, 1995; Das*,* 2013). Plasticity property can thus be imparted on soils by one or combination of the chemical composition, associated phases and associated minerals. Low plasticity in clay has been ascribed to presence of high content of quartz and absence of expandable clay minerals (Mahmoudi *et al.,* 2008).

2.5.5. Water absorption

The existence of minute pores confers marked capillary properties on raw clay material (Wieffering and Fourie, 2009). High absorption capacity of clay minerals such as montmorillonite and palygorskite can be related to their fine particle size, high layer charge and large surface area (Murray, 2000). This imparts excellent absorbent and swelling properties on the clay which makes the useful as drilling mud in oil and gas, foundries, dam and irrigation industries (Murray, 2000). Water absorption is also an important property use in brick manufacturing. It indicates the durability and quality of bricks (Narayanan and Sirajuddin, 2013). According to Nyakairu *et al* (2002), clay that has high percentage of water absorption can exhibit marked shrinkage and cracking during firing. As result, low quality of clay products for pottery-making is evaluated. Clay materials with pores that allow liquid to pass through its surface would change its weight and thus affect the durability and strength of the material (Mukhopadhyaya *et al.*, 2002). According to Larbi (2004), durability of fired clay bricks can be adversely affected by several inhomogeneity voids on a micro-level. Porosity and particle size distribution are parameters considered by Elert *et al* (2003) to influence water absorption of fired bricks rather than degree of vitrification.

2.6. Suitability Properties of Clay for Industrial Application

This section discusses the suitability of clay materials for specific industrial applications. The key properties required for specific clay product are identified and compared with standards quality

control or similar clay products available for the same application. Suitable properties that enable the use of clay as refractories, white wares, sanitary wares, fired clay bricks, water filter and agriculture enhancer are discussed.

2.6.1. Suitability of clay for refractories application

Refractory refers to material which can withstand high temperature without deformation. Chemical and thermal stability as well as high mechanical strength have been recognized as prioritizing properties necessary for clay materials to be suitable for refractories application (Omotoyinbo and Oluwole, 2008). The study indicated that alumina and silica are major chemical constituents that make clay suitable for refractory material at temperature above 1050^0C. According to Mark (2010), alumina and silica tend to form glassy substance at very high temperature in the presence of low content of alkaline minerals like oxide of calcium and potassium thereby making such clay to withstand very high temperature. It was noted that clay materials with high content of magnesia, dolomites can exhibit resistance to iron oxides and basic slags associated with steel-making.

Based on mineralogy composition, clay materials with high content of kaolinite have been considered suitable for refractory products (Aramide *et al.,* 2014). Besides the ability of clay material to resist chemical attacks from corrosive molten materials or gases at high temperature, mechanically stability is important as requirement for use as refractories material (Aye and Oyetunji, 2013). This can enable such clay materials to resist thermal shock and shrinkage, deformation or spalling under high temperature change (Djangang *et al.,* 2008). These essential parameters enable clay materials to be useful in metallurgical, electrical, ceramics and foundries industries.

2.6.2 Suitability of clay for ceramic products

The type and quality of ceramic products such as pottery and white-wares depend on properties imparted by raw clay and the specification for that product. However, plasticity and compressibility properties have been identified asone of most important property when considering a material for ceramic purpose (Dies, 2003). This is due to fact that plasticity ensures that different shapes of products are retained before and after firing or drying. Bennour *et al.* (2015) reported that plastic or expandable clay such as smectite and vermiculite can be suitable for ceramic production when the liquid limit varies between 30-52%. Furthermore, clay whose plasticity index ranges from 39 to 56% can be suitable for manufacture of ceramic tiles (Mahmoudi *et al.,* 2016).

Key properties for production of white wares such as sanitary wares and table wares are described to be plasticity and light colour when fired (Kogel *et al.*, 2006). According to the British Geological Survey (2011), plasticity property makes it easy for the products to be moulded while the light color facilitates the marketability of the white ware. Similarly, Reeves *et al.* (2006) have indicated that rheological property of clay materials is the key criteria in the production of sanitary wares. Rheological property of casting slip exhibits plasticity when the concentrate suspension is increased thereby making plasticity to have a direct relationship with rheological behavior (Collyer, 2012).

2.6.3. Suitability of clay for fired bricks

Several properties have been suggested by various researchers to be suitable for fired bricks (Baiden *et al.,* 2014; Munov *et al.,* 2015; Fadil-Djenabou *et al.,* 2015; Mahmoudi *et al.,* 2017). The key properties mentioned in their studies include compressive strength, water absorption and thermal stability. The America Society for Testing and Materials (AC62) has considered the minimum required quality indexes for compressive strength and water absorption of fired clay bricks to be 20.7MPa and 17% respectively where weather condition is severe.

In case of negligible weather condition compressive strength can be above 10.3MPA while water absorption is not limited. According to South African National Standard (SANS 2001-CM1:2007), the requirement for acceptance limits and quality control for compressive strength and water absorption of fired clay bricks are specified as 2.4MPa and 1.5-3% respectively for individual brick used in single-storey construction. Whilst in double-storey construction, a minimum compressive strength of 5.6MPa and water absorption ranges between 4-7% are specified, high-rise building employs engineering fired clay brick with a minimum compressive strength of 70MPa.

The firing temperatures that ranged from 900^{o}C and above have been reported by many studies. According to Fadil-Djenabou et al. (2015), common and perforated bricks could be fabricated from clastic clays whose firing temperature ranges from 900^{o}C to 1100^{o}C. Their water absorption can vary from 12.7% to 20.7% while flexural strength also varies from 0.60 to 2.07MPa. In case of ceramic tiles and bricks production, raw clay which vitrifies or form glassy substance at temperature from 900^{o}C to 1150^{o}C was reported (Mahmoudi *et al.,* 2016).

2.6.4. Suitability of clay for water filters

The relevant properties of raw clay that determines its suitability for making water filter has been demonstrated to include porosity, plasticity and thermal shock (Annan *et al.,* 2006). Despite ceramic water filter depends on the small pore sizes of ceramic materials to filter dirt, debris and bacteria out of the water, plasticity and thermal stability are important criteria as well (Mikelonis *et al.,* 2016). The study of Kava (2006) has indicated that intermittent cooling and heating during firing of clay product could result in shrinkage thus leading to presence of cracks, mega fracture and opening. Obviously, water filter with mega opening tends to act as funnel rather than a filter. Water filters with micro and nano pores can be made from plastic clays and combustible materials such as sawdust and husks which burns out during firing process thus leaving a porous structure (Rayner *et al.,* 2013). However, the volume fraction of the combustible materials can also determine the sizes of pores opening presence in the clay ceramic ware while plasticity tends to ease molding process of the desired shape (Plappally *et al.,* 2011).

2.6.5. Suitability of clay for suspension fertilizers

Clay can function as suspension stabilizer or agent during the production of suspension fertilizers. Suspension fertilizers are supersaturated fluids in which the undissolved solute or fertilizer material such as phosphorus and potassium are prevented from settling out by addition of argillaceous clay. According to Murray 2000, the particle size and shape of clay are important properties considered in production of suspension fertilizer due to ease of re-dispersion with mild agitation to become viscous enough and thus uniformly applied to the soil. The role of clay fraction is significant not only in fertilizer particle retention but also in the release of essential nutrient elements to soil and plants (Saidi, 2012). The cation exchange capacity (CEC) and surface area properties of clay determine its adsorption and ability to hold certain compound which influences the size, shape and structure distribution of soils (Straaten, 2002; Obaje *et al.,* 2013).

2.7. The Geochemistry of Clay Deposits

The utilization of clay deposit in different industries have been primarily attributed to their varying mineralogical and chemical property which, in turn, depends on many geological processes (Mahmoudi *et al.,* 2017; Boussen *et al.,* 2016; Montes *et al.,* 2016). Geological processes such as diagenesis, weathering and metamorphism have significantly influenced the composition of clastic or clay sediments. A common diagenetic process in clays involves the gradual breakdown of smectite to illite and is a well-known occurrence in sedimentary basins (Casey, 2014). Chemical weathering uses chemical reaction such as hydrolysis, dissolution, ion exchange to redistribute,

remobilize and transform primary minerals and elements in parent material into secondary minerals or elements. According to Galan *et al.* (2017), weathering or chemical alteration of rock-forming minerals such as feldspars and muscovites to clay minerals are transported to depositional environment and it critically suggest the functional properties of resultant clay minerals.

In clay sediment, mobility of major elements such as K, Na, Ca, Mg and Si are progressively removed from parent materials due to high reactivity and solubility properties at surface temperature while Al, Fe, and Ti will be relatively enriched in the weathered material (Nesbitt *et al.,* 1980; Qui *et al.,* 2014). The relationship between the parent, country or distant rocks and weathered materials have been widely investigated with respect to provenance using certain indices such as chemical index of alteration and weathering (CIA, CIW), ratio of K/Cs,SiO_2/ Al_2O_3, Al_2O_3/TiO_2 and weathering index of Parker (Parker, 1970; Mosheni *et al.*, 2017; Qui *et al.,* 2014).The chemical index of alteration and weathering (CIA, CIW) are often used to estimate weathering-related alteration (Nesbitt and Young, 1982; Goldberg and Humayun, 2010).

In highly weathered rocks the ratios of K/Cs can be used to measure the role played by chemical weathering in the production of clay sediments while SiO_2/ Al_2O_3 suggest the degree of desilicication and allitizaion (McLennan 2006). Furthermore, several studies which include McLennan et al. 1990, 1993, 2006; Staden *et al.,* 2014, Blanco and Abre, 2014 have considered high field strength elements (HFSE), large ion lithophile elements (LILE) or rare earth elements (REE) and transition elements as a robust source rock indicator which can be employed to infer the provenance and paleotectonic setting of clastic sediments. The HFSE are usually highly immobile elements and tend to resist metasomatic, metamorphic, diagenetic and hydrothermal alteration. As a result, their content is possibly representative of the source rock. Contribution of detrital mineral or chemical inputs from different or local source rock can equally be examined using A-CN-K and Ti/Al ratio plots (Akanish and El-Gohary, 2008). Conversely, LILE or REE are fluid-mobile which provide information about the altered mineral composition and modified major element content. Many previous work have successfully used the ratios of highly immobile elements Zr/Ti vs. Nb/Y to estimate the average source rock composition for clastic sediments (Bertolino *et al.,* 2007; Lacassie *et al.,* 2006).

2.8. Physical Properties of Clay and Its Application

Physical properties of clay deposits such as color, cation exchange capacity and soil pH differs from one soil to another and thus requires detail characterization. Basic insight about mineral composition and depositional processes of clayey soils can be invariably obtained from soil colors. Although the presence of some minerals such as hematite and goethite have been widely attributed to reddish to yellowish coloration in clays, significant amount of magnesium oxide (MnO_2) and titanium oxide (TiO_2) are contributors to the tonality of clays as well (Schwertmann, 1993; Kreimeyer, 1987; Boussen *et al.,* 2016).

Clay that exhibits pale yellow to gray colour suggests reducing depositional environment due to leachable Fe resulting from hydromorphic condition while reddish to very pale brown indicates oxidizing zones where Fe is enriched in the clay deposits (Montes *et al*., 2016). Clay mineral and organic matter component of soil have negatively charged sites on their surfaces which adsorb and hold positively charged ion by electrostatic force (Mckenzie *et al.,* 2004). In general, clay property to adsorb base cations such Ca^{2+}, Mg^{2+}, Na^{+}, and K^{+}, which is referred to as Cation Exchange Capacity (CEC), tend to influencethe soil pH, structure and fertilizer carriers (Hazleton and Murphy, 2007).

2.9. Mechanical Properties of Clay Deposits

Mechanical analyses involve the determination of size ranges of particles which constitute the soil mass and its cohesive properties using sieving, hydrometer and Casagrande methods respectively. Particle sizes larger than 0.075mm in diameter are determined using sieving analysis while the hydrometer analysis determined particle sizes smaller than 0.075mm in diameter. Although many classification organization and profession described clay size as particles smaller than 0.002mm in diameter, Unified Soil Classification System (USCS) mechanically recognized both clay and silt as particle sizes smaller than 0.075mm in diameter which is also adopted by American Society for Testing and Materials (ASTM) as indicated by Das, 2007. It is important to note that clay minerals differ from clay-sized particles. Several studies such as Murray (2007), Horm and Strydom (1998) Mueller *et al.* (2007), Ince and Ozdemir (2010), Das (2013) have indicated that clay minerals such as smectite impart plasticity property on soil while clay-sizes which ranges from below 0.002 to 0.075mm in diameter may or not. The plasticity determines the molding and cohesive properties which makes the clay to retain its shape after molding, firing or hardening.

The particle size distribution analysis quantifies the textural classes of soil into gravel, sand, silt and clay whose size diameter ranges from >2mm, 2 to 0.05mm, 0.05 to 0.002mm and <0.002mm respectively (Fadil-Djenabou *et al.,* 2015; Mahmoudi *et al.,* 2016). However, the USCS and ASTM classify clay and silt as fines whose grain sizes is below 0.075mm. Particle size distribution analysis determines particles size ranges but not clay type minerals. Meanwhile, particle size distribution represents a rather stable soil characteristic and exerts an influence on many soil physical and chemical activities (Das, 2014). Therefore, clay surface activity is a function of both grain size which determines total specific surface area while clay type determines relative surface reactivity.

The particle size distribution analysis result is therefore expressed in terms of the percentage of total weight of soil that passed through different sieves and equivalent sphere that settled at the same rate as a soil particle in hydrometer sedimentation test. Results from the hydrometer and sieve analysis are hence presented on semi logarithm plot which is regarded as particle size distribution curve. Important engineering parameters such as effective size$(D10)$, coefficient of uniformity$(C_{u)}$, gradation$(C_{c)}$, and sorting were determined. This determination was achieved by estimating values corresponding to D_{10}, D_{30}, D_{60} and D_{75} respectively on the percent finer axis of the particle size distribution curve (Figure 5.2).

2.10. Thermal, Microstructural Properties and Clay Deposits

Various clay minerals such as smectites, kaolin, illites, chlorites with varied chemical components can used for different industrial products. The use of illitic clay whose silica, alumina, iron oxide contents are moderate are indicated suitable for production of glazed red stoneware, whiteware, cottoforte, and monoporosa at temperature range of 1100-1150^{o}C, 1000-1050^{o}C and below 950^{o}C respectively (Mahmoudi *et al.,* 2017).The suitability of clay materials for ceramic products such as refractory, white and sanitary wares, water filter, tiles and bricks are primarily determined by their thermal properties aside other properties like chemical stability (Aye and Oyetunji, 2013). Although,clay materials which can withstand very high temperature (> 1200^{o}C) without significant mass loss or shrinkage are indicated to be suitablefor refractory applications, clay with temperature above 1000^{o}C are suggested suitable for other application mentioned above as well (Aye and Oyetunji, 2013; Aramide *et al.,* 2014; Djangang et al., 2008). This important property enables clay materials to resist thermal shrinkage, deformation or spalling under high temperature change and thereby useful in metallurgical, electrical, ceramics and foundries industries (Dacosta *et al.,* 2013; Bennour *et al.,* 2015).

The distribution of micropore structures present in clay material are related to the density and strength of the clay products. The homogeneity and heterogeneity structure of pore determines the vitrification extent as temperature increases (Ekosse, 2008; Diko *et al.,* 2011). As temperature rises above 1000^{o}C, fluxing oxides such as K_2O, Na_2O, CaO and MgO begin to vitrify and crystallize as viscous flow. This flow eventually saturates the micropore structure which act as a capillary system to reduce or close all open pores. It has been noted that the crystallization of new phase like mullite and crystobalite, contribute to higher densification and strength of clayey materials.

CHAPTER THREE

RESEARCH METHODOLOGY

This chapter describes specific steps and procedures that were followed to achieve the objectives of this research. The research was systematically approached by locating the clay deposits during reconnaissance and field surveys. In the field, clay samples and rock outcrops within the study area were collected, labeled and taken to the laboratory for various analyses. Several analytical methods were used to characterize the samples in terms of physical, chemical, mineralogical and mechanical properties as shown in Figure 3.1. Experimental results that were obtained from the characterizations were evaluated for possible industrial application using different empirical charts and diagrams.

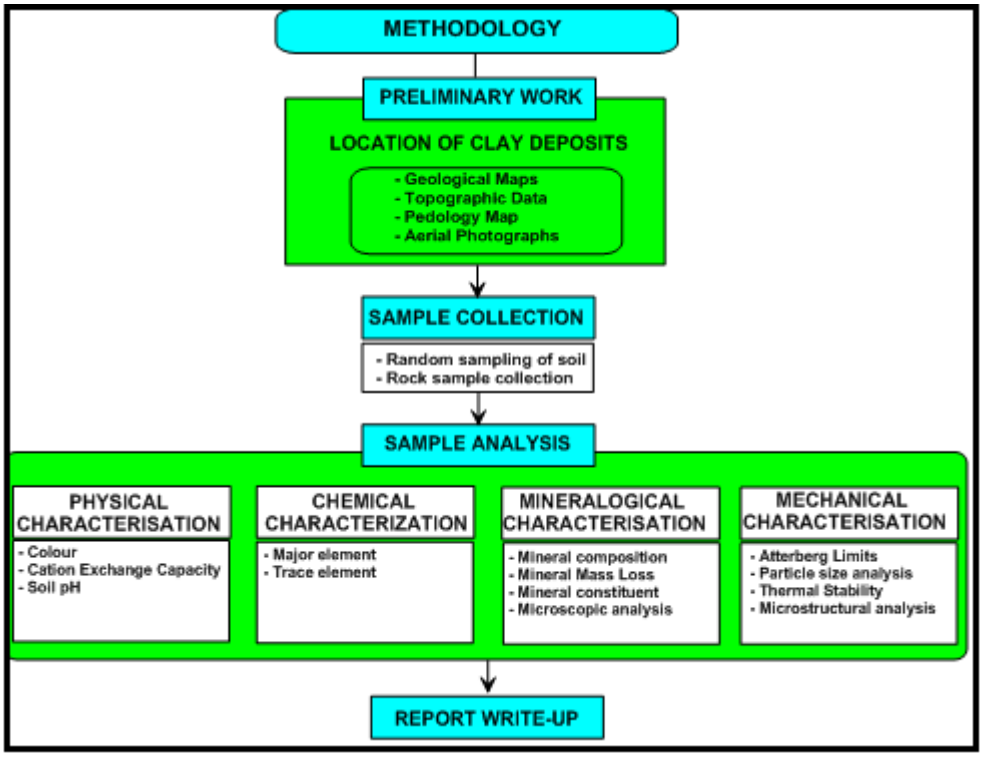

Figure 3.1: Flowchart of the research methodology

3.1. Location of Potential Clayey Deposits

This section provides information about the preliminary study which was undertaken to locate the potential clayey deposits in Vhembe District. It involved superimposition of shelf-file database from geology, topography and pedology maps of the Vhembe District using Arc GIS 10.2 tool. The geodatabases such as rock and soil types, slopes, and geometric networks were imputed and geocoded as rasters using datasets such as numeric format. The Arc GIS tool was used to geoprocess the data after appropriate query language had been created. The output of this task was a modeled schematic map that depicts geodatabases such as clay, lithology with their geographic location coordinate as shown in Figure 3.2.

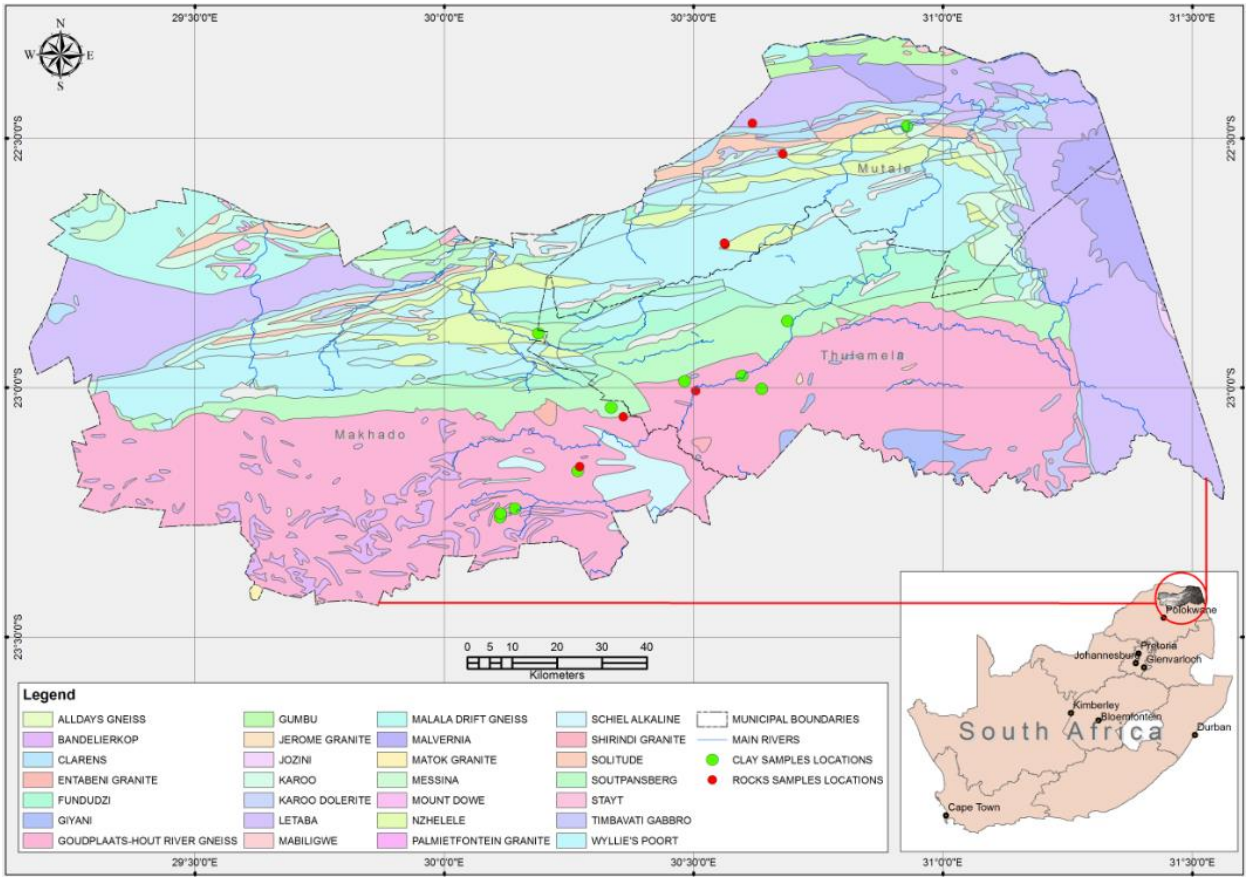

Figure 3.2: The map for the identified location of clay deposits and rock outcrops

It is significant to emphasize that the identification of locations with potential clayey deposits in the Vhembe District was complemented with the use of high spatial resolution of 5m pixel aerial photography of the study area. The purpose was to obtain a wide coverage and high resolution that enhances key structural features of clayey deposit and rock exposure. It was achieved

byanalyzing the high-resolution stereo-pair under stereoscopic examination using key elements to delineate polygon boundaries. Key elements such as tone or colour, shape, size, pattern, texture, shadow, vertical exaggeration was used to classify polygons and thus delineate surficial clayey deposits and rock outcrops.

The surficial clayey deposits reflect dark tones which suggest poor-drainage and high organic matter content while reddish clayey deposit appears darker on high resolution aerial photographs. Furthermore, reflected tones of light colour from the photograph are usually indicative of well-drained material such as sand or gravel. Soil profile of well-drained deposit has a granular texture due to aggregation of clay particles into lumps. Fine-grained material is usually less resistance to erosion thus display fine texture drainage on the high-resolution photographs. Lithology and stratigraphic thickness of sediments are delineated by vertical exaggeration using the structure contoured. This involves calculating separate homogeneous and variant textural layers based on the gray-level co-occurrence matrix. Edge-detection techniques were used to identify fine-scale features and distinctive shapes such as faults, folds, joints and roads from high-resolution photographs.

3.2. Preliminary sampling Technique

Based on the map that was generated, preliminary field tests were conducted prior to samples collection. The importance of this task was to verify the actual information about clay deposits and rock outcrop in the schematic map. The tests which were conducted to provide the first-hand insight on clay properties include rolling, smearing and ball tests.

The rolling test gave an insight about the plasticity nature of the material. While conducting this test a handful quantity of soil was grabbed from potential clay location initially identified on the schematic map. An appropriate water quantity was added until a paste not slurry was obtained. This soil paste was placed in between the hand palms and rolled into ellipsoidal shape. The soils that retain this ellipsoidal shape without scattering were seemly considered as clayey soils or materials.

Furthermore, the smearing test was carried out on the potential clays located on the schematic map to feel their texture. It was assumed that clayey soils have finer texture compared to sandy or gravelly soils. An appreciable amount of water was added to lose dry soil until it is wet. A pinch of the wet soil was taken and smeared on the thumb with the index finger to feel the degree of fine or coarseness of the soil.

The ball test was finally conducted to provide insight about the portions of sands and clays present in the identified soil. A handful amount of soil was wet with appropriate quantity of water until a ball was molded. The deformation shape of the ball was observed as it hit the ground when dropped from the level of shoulder height. Balls that flattens out upon hitting the ground are likely to have more sand compared to balls that retain their shapes though may have small deformation upon impact with the ground.

In addition to the various tests conducted on clayey soils that were earlier identified in the map, petrological structures and features of rock outcrop and lithology were identified. The clayey lithology depicted variation in sediment pattern, texture and color and features such as lineation and mud cracks since they are markers and pointers to clayey deposit which were used to locate clayey material in the field. Illustrations of these properties of clayey soils identified in the study area were shown in Figure 3.3.

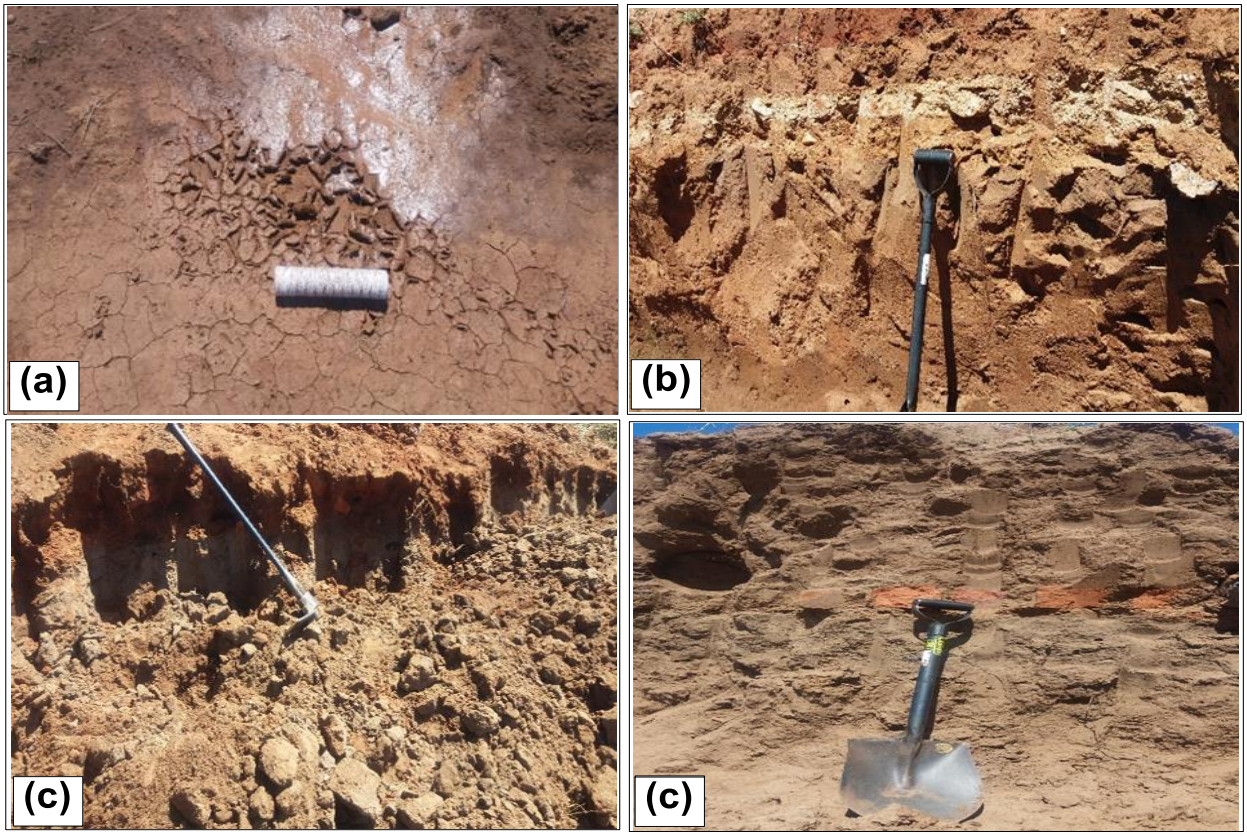

Figure 3.3: Structural feature and markers of clayey deposit (a) mud cracks (b) lineation (c) strata variation (d) lateral deposit.

3.3. Clay and Rock Samples Collection

This section explains the stepwise procedures used to collect clayey soil and rock samples in the study area. Based on the generated map and preliminary sampling technique conducted, thirteen (13) different locations of clayey deposits were identified for this research as shown in Table 3.1. The identified locations fall within the Vhembe District Municipality which of comprises Makhado, Thulamela, Mutale and Musina local municipalities. The sampling nomenclatures and codes are based on locality name where the clayey soils were found.

Collection of clay samples

Prior to collection of samples, the vegetation cover was cleared and samples were collected up to about two (2m) metres deep with shovel and hand auger. Sometimes, a pick axe was used to dig locations where soil was highly compacted and indurated as shown in Figure 3.4b. The position of each sampling point was obtained using a geographical position system device following such exercise, samples were collected and stored in plastic sampling bags and labeled accordingly with permanent marker (Figure 3.4a). The samples were then taken to the laboratory. The representative samples for further analyses were obtained when the samples (10) collected from each location were thoroughly mixed until homogeneity was achieved and then quartered.

Table 3.1: Geographical location of clayey soils sampling points.

Location	Code	Municipality	Sample Code	Longitude (E)	Latitude (S)	Elevation (m)
Mukondeni	Muk	Makhado	L1	30°˚ 06' 42.14"	23°15' 35.22"	525
Mashamba1	Mas1	Makhado	L2	30°˚ 08' 30.14"	23° 14' 33.64"	511
Mashamba2	Mas2	Makhado	L3	30°˚ 06' 45.11"	23° 15' 08.36"	547
Mashamba3	Mas3	Makhado	L4	30°˚ 55' 39.81"	22° 28' 35.65"	477
Doli	Doli	Makhado	L5	30° 16' 03.35"	23° 10' 03.18"	515
Lwamondo	Lwa	Thulamela	L6	30° 20' 04.46"	23° 02' 23.73"	519
Matsika	Mat	Thulamela	L7	30° 41' 15.70"	22° 51' 59.95"	437
Mavambe	Mav	Thulamela	L8	30° 38' 11.69"	23° 00' 09.45"	523
Nandoni	Nan	Thulamela	L9	30° 35' 49.29"	22° 58' 34.79"	481
Manini	Man	Thulamela	L10	30° [28]' 54.06"	22° 59' 15.10"	564
Siloam	Sil	Mutale	L11	30°11' 18.77"	22° 53' 29.99"	463
Tshipise	Tsh	Mesina	L12	30°40' 43.30"	22° 31' 55.48"	482
Thengwe	Thn	Mutale	L13	30° 33' 46.55"	22° 42' 46.55"	598

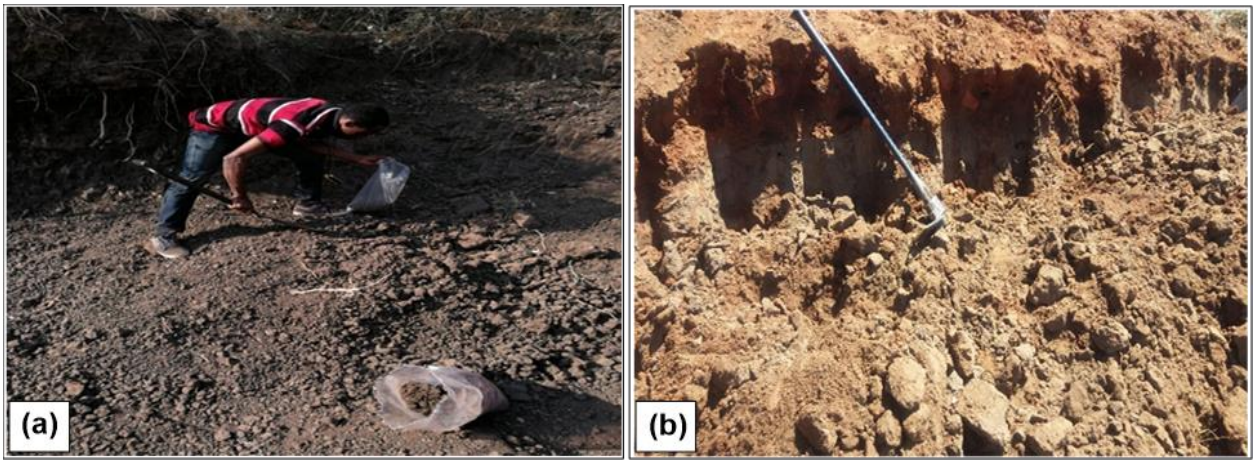

Figure 3.4: Sampling based on observed variations in soil colour and texture.

Collection of rock samples

The purpose of this was to establish the possible relationship between the clayey deposits and the surrounding rocks. The dominant rock types encountered during geological investigation within the clayey deposits of Mavambe, Matsika, Siloam, Tshipise and Thengwe were quartzitic sandstone and granodiorite (Figure 3.5a). In location such as Nandoni, Manini and Lwamondo, the granite gneisses were dominant as major rock types. The gneissic texture such as banded foliation of mafic and felsic minerals was observed in the outcrop as shown in Figure 3.5b. Other rock types encountered in locations such as Mukondeni, Mashamba-1, Mashamba-2, Mashamba-2 and Doli include basalt and quartzite. The basalts have an aphanitic texture while the colour was melanocratic. The quartzite was leucocratic in color and generally interspersed with iron oxide minerals but hard to break with hammer owing to hardness gained during metamorphism process. Fresh samples were collected with the aid of geological hammer and chisel and labeled appropriately with permanent marker. Table 3.2 showed the sampling points for rock samples.

Table 3.2: Geographical location of rock sampling points

Location	Latitude	Longitude	Location	Latitude	Longitude
Mukondeni	30° 05' 32.14"	23° 16' 32.21"	Mashamba1	30° 07' 30.14"	23° 13' 42.47"
Mashamba2	30° 06' 10.01"	23° 14' 09.57"	Lwamondo	30° 21' 05.46"	23° 02' 32.53"
Nandoni	23° 58' 23.97"	30° 34' 13.53"	Mashamba3	30° 56' 24.18"	22° 28' 43.25"
Mavambe	23° 00' 32.19"	30° 38' 17.86"	Thengwe	22° 42' 37.21"	30° 33' 41.39"
Siloam	22° 52' 32.56"	30° 11' 31.01"	Tshipise	22° 28' 12.59"	30°37' 44.12"

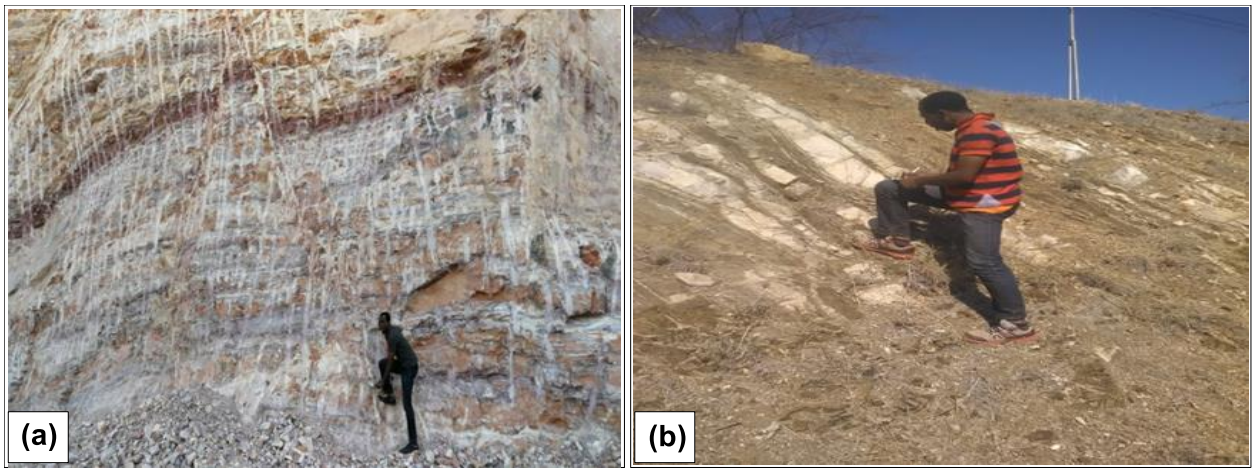

Figure 3.5: Source of the rock samples present in the study area (a) is the ferruginised quartzitic sandstone and (b) is the gneissic features.

3.3. Analysis of Clay and Rock Samples

This section discusses the various procedures, equipment and methods that were used to analysis the clay and rock samples to achieve the set objectives. The clay samples were subjected to physical, chemical, mineralogical, mechanical and thermal analyses while the rock samples were analyzed in terms of chemical, mineralogical and petrographical characterization. The aim of these characterizations was to determine and evaluate the suitability of the properties for industrial utilization.

The section below presents physical characterization of clay samples which involved determination of clay sample colour, pH and their Cation Exchange Capacity (CEC). This was followed by the geochemical and mineralogical analysis of clay and rock samples as well as the optical microscopic analysis of rock. Furthermore, the particle size distribution and Atterberg limits of the clay samples were determined. Finally, the thermal stability and microstructural analyses were conducted on the collected clay samples.

3.3.1. Physical characterization of clay samples

The physical properties of clay sample such as colour, pH and Cation Exchange Capacity (CEC) were determined using the Munsell chart, pH meter and CEC technique respectively. These physical properties were selected for analyses because they provide important information about

the composition of raw clay and their industrial use. For example, the use of clay as fillers requires gray color which, in turn, can be influenced by the composition of the raw clay.

Colour Test

The colour of raw clayey samples was determined using the Munsell colour chart. The chart consists of standard colours in different hue, value and chroma. With the aid of spatula, oven-dried clay samples were mounted on white sheet which serves as a plate holder. The colour of soil sample on the white sheet was compared and correlated with the standard colour of Munsell chart to determine its hues, value and chroma. The colour test provides information about colour stability and mineral composition of clays from Vhembe District when subjected to engineering and mineralogical tests.

Cation Exchange Capacity (CEC) of Clay Samples

The CEC of clay sample was determined using exchangeable cation extraction and atomic absorption spectrometer as shown in Figure 3.6. About 25g of the sample was initially oven dried at 110^{o}C for 6 hours until constant weight was achieved. The sample pH was later adjusted to 7.0 when diluted with 1L of NH_4OH inside a 500 mL conical flask. The near-neutral solution was then thoroughly mixed with 125 mL of 1M NH_4O_{AC} for 12 hours using a mechanical shaker. With the aid of suction machine, the solution was poured into a funnel lined with filter paper. The filtrate was refiltered until the solution is clear by pouring 25 mL of 1M NH_4O_{AC} into the suction clay solution. The cleared filtrate was then poured into a beaker for determination of exchangeable cation such as Na^+, K^+, Ca^{2+} and Mg^{2+} using atomic absorption spectrometer as shown in Figure 3.6. The results of detected cations were displayed on the computer screen connected to the spectrometer and given ml/g although converted to meq/100g using:

(a) $\text{Total solution (ml)} = \text{final tube weight (g)} - \text{tube tare weight (g)} - 2\text{g(weight of soil used)}$

(b) $\text{Mg in solution, not on CEC (meq)} = \text{Total solution(mls)} \times 0.003\ (1.5\text{mM MgSO4 has } 0.003\text{meq.l}$

(c) $\text{Total Mg added (meq)} = 0.1\text{meq(meq in 10mls of 5mM MgSO4)} + \text{meq added in } 0.1\text{M MgSO4}$

(d) $\text{CEC}\left(\frac{\text{meq}}{100\text{g}}\right) = (\text{c} - \text{b}) \times 50\text{(total Mg added} - \text{Mg in final solution)}$

Figure 3.6: Exchangeable cations determination using Atomic absorption spectrometer

Soil pH

To determine the pH of the soil about 100ml of de-ionized water was added to 100 g of pulverized clay samples placed in a 100ml beaker. The clay solution was stirred continuously for an hour using stirring rod until a homogeneous solution was achieved. This was to allow the pH of the soil slurry to stabilize. The pH meter was calibrated with buffer solutions of pH 4.00 and 7.00 to standardize the acid-base condition. The thermometer was used to measure the temperature after which the pH meter electrodes were inserted into the soil slurry. After 2 minutes, the displayed value was read and recorded.

3.3.2. Chemical and mineralogical characterization of samples

The clayey and rock samples were analyzed to determine their chemical and mineral compositions using the X-ray fluorescence (XRF) and X-ray diffraction (XRD) respectively. The rock samples were also subjected to microscopic analysis when their thin sections were examined under petrologic microscope. The information about the rock forming minerals present in rock and clay samples were identified and characterized.

Major and trace element geochemical analyses of the fine bulk clay and rock samples were quantitatively estimated using S2-ranger X-Ray Fluorescence (XRF) spectrometer shown in Figure 3.7a. Rock samples were crushed and milled to a fine powder with an agate disc milling machine shown in Figure 3.6b. Furthermore, the samples were pulverized to obtain <32µm fractions and then calcined at 1000 ^{0}C for minimum period of 3hours to oxidize iron (ii) oxide (Fe^{2+}) and sulphur (S).

Pressed powder pellets for XRF analyses were prepared using 6g of sample powder and 12g of boric acid as a binder. The mixture was fused into a steel cup and pressed at a pressure of 30tons in hydraulic set. The XRF instrument equipped with a 4 KW Rhodium (Rh) tube was used to analyze major oxides by inserting a glass disks containing 1g calcined sample, 8g flux composed of 35% alkali borate ($LiBO_2$) and 64.71% lithium tetra borate ($Li_2B_4O_7$) as oxidant at 1050 ^{0}C into the XRF equipment. Trace elements were determined by mixture of 3g Hoechst wax and 12g milled sample.

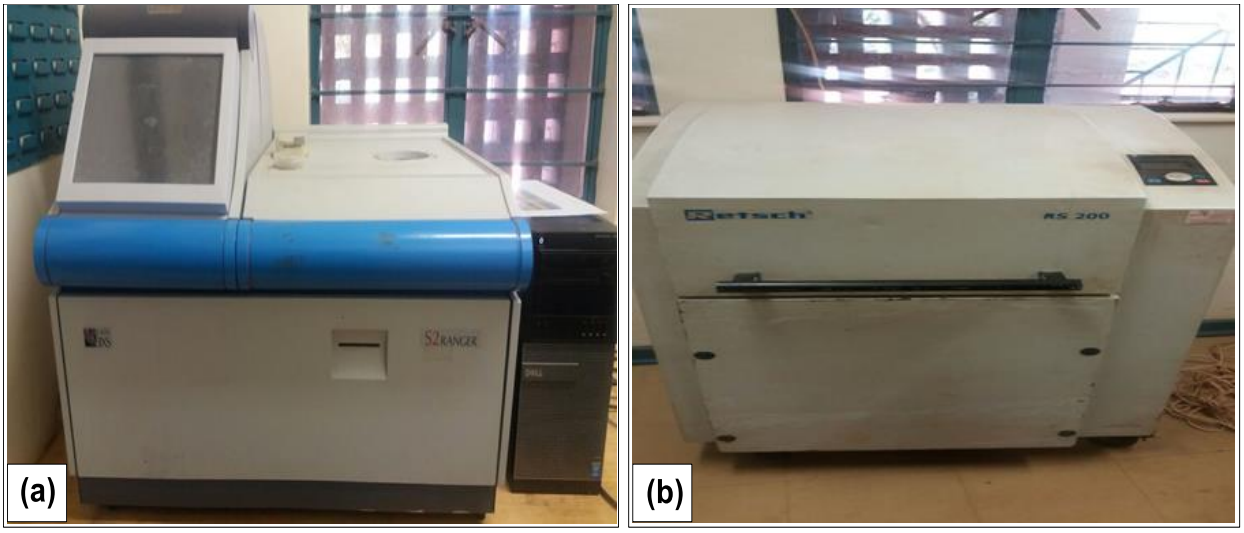

Figure 3.7:(a) X-ray fluorescence (XRF) analysis using S2-ranger spectrometer (b) Retsch-RS 200 milling machine used to pulverised the clay samples

Mineralogical characterization of the samples

The mineral composition of fine powders of the clay fractions and rock samples were semi-quantitatively determined using X-ray Diffraction (XRD) spectrometer. This analytical technique revealed the crystallinity and concentrated clay mineral phases present in samples. The powder of finely ground homogenous clay fractions <2µm and pulverized rock were obtained by timed sedimentation. After glycolation and oven-drying the samples at 300^{o}C for 1 hour, it was tightly

mounted on oriented sample holder with very little pressure using black loading preparation technique for XRD analysis. The analysis was done using PANalytical X'Pert Pro powder diffractometer equipped with X'Celerator detector coupled with receiving slits, variable divergence and Fe- filtered Cu-Kα radiation. Whilst the receiving slit is positioned at 0.040^0, counting area was from 5 to 70^0 on a 2θ scale at 1.5s. The clay phases were identified using X'PertHighscore plus software. Rietveld refinement (Autoquan Program) employed a least-square matching algorithm based on sample parameters and instrumental parameters to estimate relative phase amounts. A quantitative analysis of the different mineral phases was estimated by measuring the areas of the main representative peaks. Peaks which are characteristics of the presence or absence of minerals are measured from the general background while amorphous phases, if present were not taken into consideration in the quantification.

Optical Microscopic analysis of rock samples

Prior to microscopic examination of the mineral assemblages in rock samples, petrographic thin-sections of the samples were prepared. Essentially, the thin-sections were 30µm thick in diameter but translucent and highly polished. The purpose of the analysis was to provide a better understanding of mineral present in the rock samples. Suitable size slabs from piece of rock samples were cut using diamond saw shown in Figure 3.8a.

The slabs were labeled on one side while the other side were lapped and smoothen on a cast-iron lap with grit carborundum as abrasive. It was then mounted and finished on a glass plate. The glass slide was glued to the lapped face of slab with epoxy resin after drying on a hot plate. The slab was cut-off close to the slide using a thin section saw shown in Figure 3.8b while the thickness was further reduced on the thin section grinder. The surface ground flat on the thin section grinder to further reduce its thickness and then finished to a thin section (Figure 3.8c). Suitable finished thickness of 30µm was achieved by lapping the thin section on glass plate with grit carborundum as abrasives. The prepared thin sections were viewed and analyzed under petrologic microscope for minerals identification and characterization.

3.3.3. Mechanical characterization of clayey soil

This section discusses the mechanical tests conducted on the clayey samples collected from the study area. The test involved determination of particle size distribution of the soil using sieves and hydrometer analysis and performing Atterberg limits tests using a Casangrande apparatus. This

provided better understanding of the different engineering and industrial properties such as coefficient of uniformity, gradation, sorting, effective sizes and plasticity. The particle sizes, plasticity and compressibility properties are among the key parameter required for ceramic and refractory use of clay

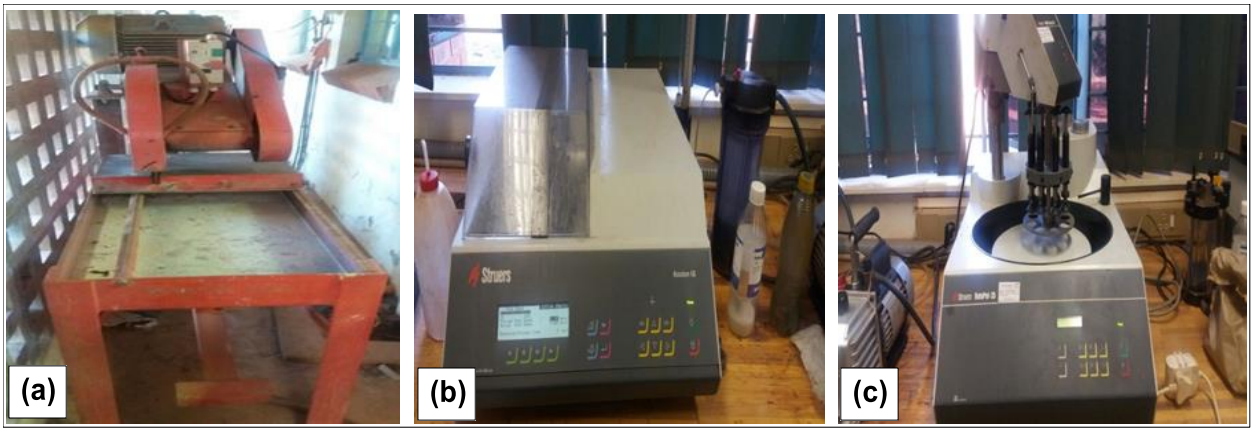

Figure 3.8: Preparation of thin-sections during (a) rock cutting (b) slab grinding (c) thin section polishing

Sieve size analysis

The distribution of particle sizes within soil sample helps to classify the soil and better understand its physical properties for industrial purposes. The particle sizes larger than 75µm were obtained by No 200 sieve while the less than 75µm sized fractions were determined by sedimentation process using hydrometer test. The stack of sieves, the hydrometer test set up and the stirrer that were used during the textural characterization of the clayey soils are shown in Figure 3.9.

The collected samples were first air-dried until constant mass was achieved and 500g of weighed soil samples were shaken through a stack of sieves with openings of decreasing size from top to bottom using mechanical shaker. The mass of soil retained and passing each sieve was weighed and recorded after the soil was shaken on mechanical shaker. The percent finer on each sieve size was determined using equation 3.1.

$$F = \frac{\sum M - (M_1 + M_2 + \cdots M_i)}{\sum M} \quad (3.1)$$

Where: $\sum M$ is the Summation of the cumulative mass retained in each sieve, $\sum M - (M_1 + M_2 + \cdots M_i)$ is the cumulative mass of soil retained above each sieve, and F is the percent finer on each sieve size

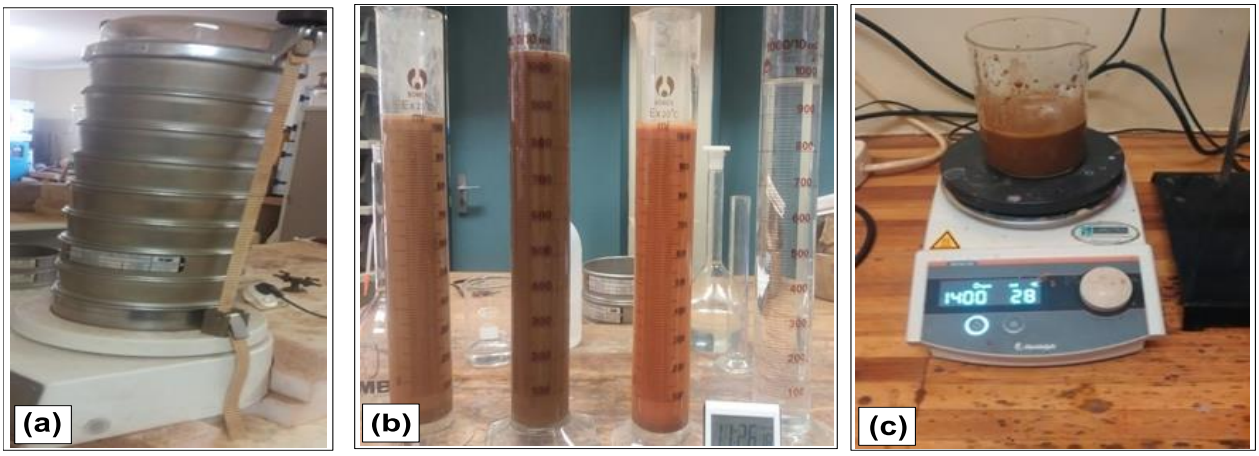

Figure 3.9: (a) Sieving analysis for grain sizes (b) hydrometer tests for clay size fractions (c) stirring of clay sample.

About 50g of soil which passed through No 200 sieve or <75µm fractions were treated with hydrogen peroxide (H_2O_2) solution in order to oxidize organic material. The resultant slurry was mixed with 125ml of 4% sodium hexametaphosphate ($NaPO_3$) solution which act as the deflocculating agent. The mixture was transferred to high speed stirrer to allow homogenous dispersion for about a minute.

After mixing, contents of the dispersion cup were carefully poured into graduated sedimentation cylinder. Distilled water in plastic squeeze bottle was used to rinse any soil in the dispersion cup into the sedimentation cylinder. Prior to agitation of sedimentation cylinder, it was filled with distilled water to 1000ml mark and cap with rubber stopper. Agitation was achieved by turning the sedimentation cylinder upside down and back 60 turns for a period of one minute and later placed beside the control cylinder filled with distilled water. The 152H hydrometer bulb is removed from the control cylinder and inserted in the sedimentation cylinder to measure the density of solids in solution. Measurement of sedimentation started at time-t, as the hydrometer and thermometer were inserted into the soil suspension.

The sieve and hydrometer data were combined and graphed on semi-logarithmic plot to give a visual representation of the total particle size analysis. The percent finer values were represented on the y-axis while diameter sizes on the x-axis. The diameter of soil particles and percent finer in suspension were calculated using equation 3.2 and 3.3 respectively.

$$D\ (mm)\ = K\sqrt{(L/t)} \tag{3.2}$$

Where: K is a constant value that varies with temperature and specific gravity of soil, L is the distance from the surface of the suspension to the level at which the density of the suspension was measured or effective depth and T is the time interval from the beginning of sedimentation to the reading in minutes. The percent of soil by weight finer than a given diameter was calculated knowing the amount of soil in suspension (L) and (t) using equation 3.3.

$$\text{Finer}\ (\%) = \frac{\text{AxR}_{\text{cp}}}{\text{W}_\text{s}}\text{X}\ 100 \tag{3.3}$$

Where: A is a constant value of 1, R_{cp} is hydrometer reading and W_s is the sample weight.

Important engineering parameters such as effective size(D_{10}) coefficient of uniformity(C_u), curvature(C_c) and gradation(C_g), were determined using equation 3.4, 3.5 and 3.6 respectively. The percentages of gravel and sand were obtained from the gradational curves produced from the results.

$$\text{C}_\text{u}\ = \frac{\text{D}_{60}}{\text{D}_{10}} \tag{3.4}$$

$$\text{C}_\text{c}\ = \frac{\text{D}_{30}}{\text{D}_{60} \times \text{D}_{10}} \tag{3.5}$$

$$\text{C}_\text{g}\ = \frac{\text{D}_{30^2}}{\text{D}_{60} \times \text{D}_{10}} \tag{3.6}$$

The effective size (D_{10}) refers to diameters of grains that correspond to 10% finer on the particle distribution curve. This parameter is an important measure of porosity and transmitability of fluid through the soil. The coefficient of uniformity (C_u), curvature(C_c) and gradation (C_g)of the soil is a measure of uniformity, gap discontinuity and gradingrespectively.

Atterberg Limits Tests

The clay samples were subjected to Atterberg limits tests which revealed information on liquid limit, plastic limit and plastic index properties. The test was significant because much empirical evaluations for industrial utilization required these properties. The liquid limit (LL) test was

conducted using the Casagrande apparatus as shown in Figure 3.10. Prior to commencement of the procedure for liquid limit the apparatus was properly adjusted to the consistency height of 10mm. Correctness of calibration was confirmed by vibrated sound when the crank struck the cam follower.

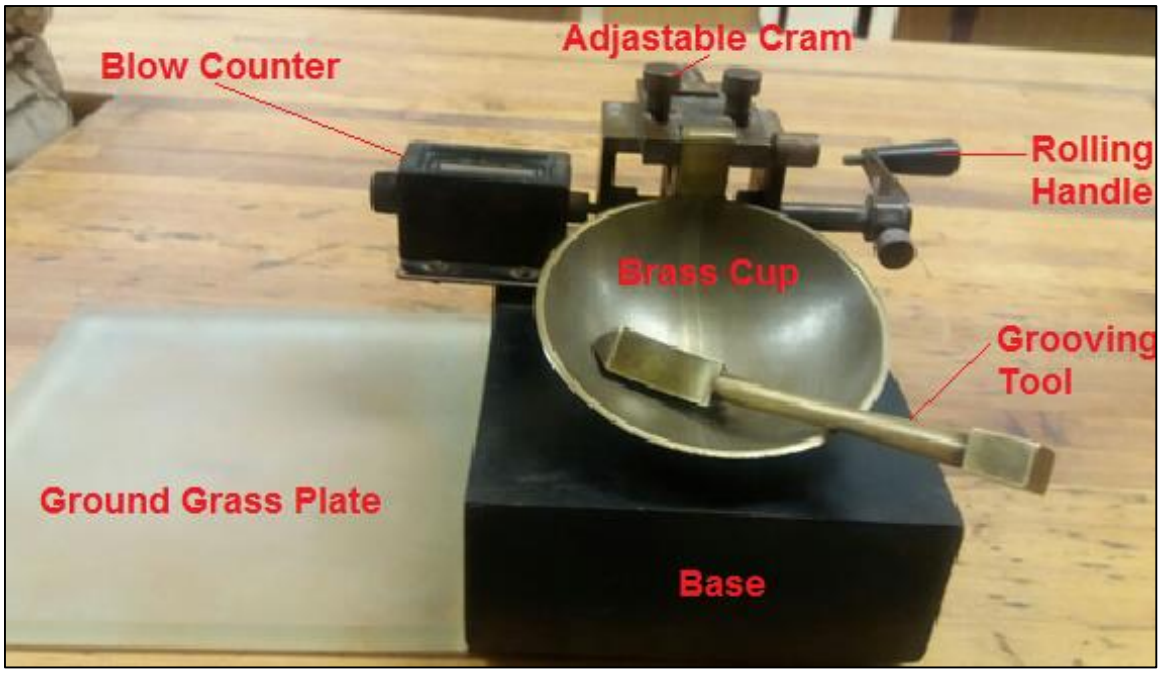

Figure 3.1: Casangrande apparatus for Atterberg limit tests.

De-ionised water wasadded to the dried sample placed in an evaporating dish with repeated stirring, cutting and kneading with the spatula. The moist sample wasplaced in the brass cup stroked to the maximum depth of 8mm. A groove of 2mm wide at the bottom was cut at center line of the soil pat placed in cup using the grooving tool and the device will be cranked at two revolutions per second until the two halves of the soil pat come into clear contact of about 13mm long at the bottom of the groove. The number of drops of the cup (or blows) that caused the closure of the groove was recorded. The sample in the pat was collected and weighed together with the can after which it was dried in oven at 110^0C for more than 5 hours and weighed again. Subsequent trials were repeated producing successive number of blows to close the grooves. The number of blows (N), as the ordinates on the logarithmic scale, was plotted against the moisture contents as the abscissae on the arithmetic scale using semi-logarithmic graph paper. The flow curve was a straight line of best-fit drawn as nearly as possible through the plotted points to determine the moisture content at 25 blows.

The plastic limit (PL) of a soil is the moisture content at which a soil will just begin to crumble when rolled into thread of about 3mm in diameter using a ground glass plate. The plastic limit property test of the clay samples was determined using a 3mm diameter rod, surface glass plate, evaporating dish, spatula, pulverizing apparatus, watering bottle, oven and balance. The procedure started by squeezing water on clay sample of about 8g until it was wet and then rolled into ellipsoidal shaped mass using hand palm and the glass plate. A calibrated plastic limit device (can rod) with diameter opening 3.18mm was used during the rolling until the soil crumbles. The crumbled portion was collected and weighed on a weighing balance. It was later dried in oven and weighed again to determine the moisture differences. The mass of the can and wet soil was recorded separately while the mass of the can was predetermined. The trial was conducted repeatedly for different moisture content to determine the plastic limit. For both plastic limit and liquid limit tests, equation (3.7) was used to determine the percentage of moisture content $W(\%)$in the clay samples.

$$\mathrm{W}(\%) = \left(\frac{\mathrm{w}_{2-}\ \mathrm{w}_3}{\mathrm{w}_{3-\mathrm{w}_1}}\right) \tag{3.7}$$

Where: W_1 is the mass of the can, W_2 is mass of Can + wet soil and W_3 is the mass of can + Dry soil.

Plasticity index is considered as a measure of the cohesion possessed by a soil. It gives the range in moisture at which soil is in a plastic state. Generally, the numerical difference between the liquid limit and plastic limit is taken as the plasticity index of the soil. Equation (3.8) was used to determine the plasticity index (PI) of the clay samples.

$$\mathrm{PI} = \mathrm{LL} - \mathrm{PL} \tag{3.8}$$

Scanning Electron Microscopy

A Ziess EVO MA15 scanning electron microscope (SEM) equipped with a tungsten filament and a Bruker energy dispersive X-ray spectrometer was used for the morphological analysis of the clays (Figure 3.11a). The system was operated under high vacuum of approximately 2.15 e-006mbars. The electron beam was generated with an accelerating voltage of 20KV and probe current of approximately 2nA.

The clay sample was sprinkled onto a carbon tape substrate and carbon coated prior to being loaded into the SEM machine shown in Figure 3.11b. A secondary electron detector was used to produce images at 300X, 600X and 900X magnifications. Some of these particles are out of focus

owing to the three-dimensional depth loss of information. Focusing one-part results in the other being out of focus on some of the images particularly at the high magnification.

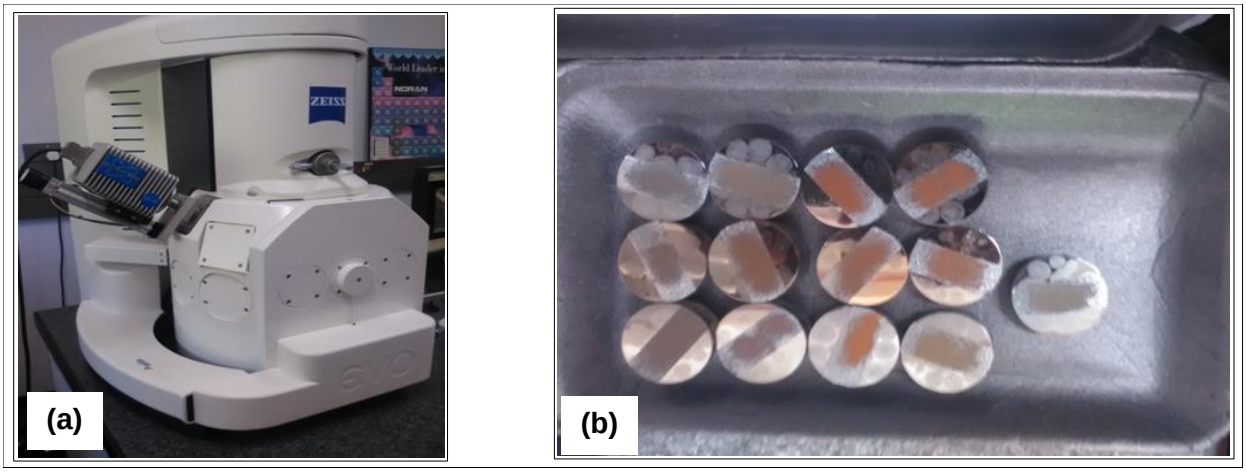

Figure 3.2:(a) Scanning Electron Microscopy analysis of clay samples (b) Carbon coated of samples.

3.3.4. Thermal analysis of clay samples (DTA)

The thermal analysis was conducted to determine the thermal stability of samples and to provide information regarding mass changes in mineralogy of the clay samples as the temperature increases. The differential thermal (DTA) and thermogravimetry (TGA) analyses were conducted using Setaram apparatus which was calcined inert substance (Al_2O_3). Samples were obtained based on principles of stokes law of sedimentation of clay and placed in sample holder of the furnace. The sample holder was a piped block with two small holes for the sample and inert substance. Differential thermocouple junction wire was inserted into the sample and inert substance holder while the heat source was powered.

The maximum temperature attained was 1000^0C at heat rate of 25^0C/min owing to the heat capacity which the inert substance can withstand. The temperature difference between sample and calcined inert substance (Al_2O_3) was recorded after undergoing identical thermal cycles. The differential temperature was then plotted against time as DTA curve. The degree of structural stability was evaluated from both the dehydroxylation temperature and asymmetry of the endothermic peak. Slope ratio was also obtained by calculating the ratio of the limiting gradients of the exothermic and endothermic material in a liquid medium.

CHAPTER FOUR

LITHOGEOCHEMICAL AND PETROGRAPHIC PROPERTIES OF SOIL AND ROCK

This chapter presents and discusses the results obtained from the geochemical, mineralogical and petrographic analyses of clay and rock samples collected from Vhembe District. The major and trace elements was analyzed using X-ray fluorescence instrument (XRF) while the mineralogical composition of both clay and rock samples were determined with the aid of X-ray diffractometry (XRD) machine. Furthermore, thin-sections of rocks were prepared, examined and analyzed under petrographic microscope. The microscopic analysis provides better understanding of mineral assemblages present in the studied rock sample.

The chapter placed emphasis on geochemical and mineralogical characteristics of clay and rock samples. The first section presents the geochemical composition of clay and rock samples particularly on major and trace elements. The geochemical relationship between the clay and rock within the study area was established in respect to geologic events such as weathering, transportation, deposition and diagenesis. The later part of the section presents mineral compositions of the clay as well of the rock samples which were systemically elucidated by analyzing their mineral constituents. Finally, the chapter discusses the distribution of clay deposits within the Vhembe District Municipality.

4.1. Geochemical compositions of the studied clay and rock samples

This section discusses the major and trace element results obtained from XRF analysis. The geochemical plots such as Al_2O_3 /TiO_2, discriminate functions were used to interpret the major element in relations to degree of clay and rock weathering as well as their relationship. In addition, the trace elements distributions were analyzed and discussed in order to provide composite information with the major elements results.

4.1.1. Major element geochemistry

The geochemical results for both studied bulk clay and representative rock samples collected in different parts of the Vhembe District showed the presence of major element such as Si, Al, Na, K, Mg, Ca, Ti, Fe and Mn in their oxide forms (see Appendix B). The results showed varying

amount of silica (34.1-59.5%), alumina (13.1-22.4%), sodium oxide (0-1.3%), potassium oxide (0.4-3.5%), magnesia (0.09-4.4%) and calcium oxide (0.07-2.1%) in clays (see Figure 4.1a). Similarly, the rock samples were found to composed of SiO_2 (42.0-91.2%), Al_2O_3 (3.21-12.72%), Na_2O (0-3.25%), K_2O (0.02-3.87%), MgO (0.09-10.13%) and CaO (0.05-13.52%) as shown in Figure 4.1b. All clay and rock samples had high SiO_2 content that was above 42% and high Al_2O_3content that was below 20% but with a notable exception of Lwamondo clay sample which had the lowest SiO_2 content (34%) and highest Al_2O_3 content (22.4%). The Lwa sample which was characterized by relatively higher Al_2O_3content suggested the abundance of phyllosilicates that had undergone chemical weathering (Figure 4.1a). The enrichment of high SiO_2 (average 52%) and Al_2O_3 (average 15%) content in both clay and rock samples suggest some relative low concentrations of all other major elements (average <15%) as shown in Figure 4.1b.

The average abundance of the fluxing oxides (FO) such as K_2O, N_2O, CaO, MgO, MnO and P_2O_5 present in the clay sample ranged from 0.06% to 1.78% (see Appendix B). Despite all other samples showed similarity in FO contents, Lwamondo clay sample had the lowest concentration of K_2O (0.46%), N_2O (0%), CaO (0.07%), MgO (0.09%) but highest in MnO (0.155%) and P_2O_5 (0.151%).

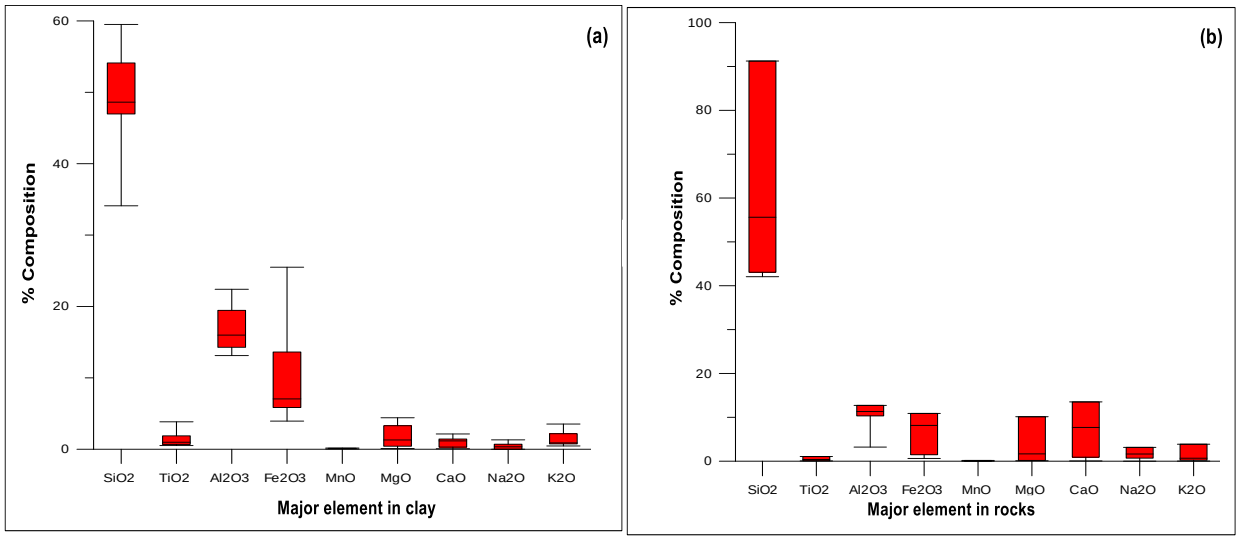

Figure 4.1: Plots showing major elements distribution for (a) clay samples (b) rock samples.

The Fe_2O_3 and TiO_2 content in all samples averages at 9.2% and 1.3% respectively with Lwamondo sample showing unusual iron content above 25% while other samples contain less than 15% iron. It also showed the highest TiO_2 content (3.8%) relative to other samples. Meanwhile, clay samples from Matsika (14.59%), Tshipise (13.62%) and Siloam (11.14%)

showedto be having an iron content that was above 11% compared to others sample that had relatively lower concentrations (< 9%).

The chemical index of alteration (CIA) value of clay samples was found to be homogenous and relatively high (73-94) compared to the rock samples values (42-98) which were widely varied. The elevated CIA values in all clay samples were related to the increased Al_2O_3 content and low amount of CaO contents. The degree of desilicication and allitizaion (shown by SiO_2 /Al_2O_3 ratio) was > 1 for all samples. In comparison to the clay samples with SiO_2 / Al_2O_3 ratio value between 1.5 and 4.4, the rock samples showed exceptional high ratio value that ranged between 3.4 and 28.4. This does not only indicate an ongoing process of desilicication and allitization but that the parent rock diversity had some effect on the SiO_2 /Al_2O_3ratio of clay samples. In comparison with the upper continental crust (UCC) values, K/Cs value of 6200 reflects the typical ratio for unweathered materials (McLennan *et al.,* 1990; 2006). The studies have noted that low weathering processes are connected to K/Cs value above 6500 while samples having K/Cs values less than 6200 are characterized by high degree of weathering. Apart from clay samples from Siloam which showed K/Cs value >6500, all other clay samples ranged from 851-5629 hence showing to be characterized by high degree of weathering. Meanwhile, the K/Cs values of the rock samples varied with one sample having value of 7166 while others ranged from 37-1257. The high and low K/Cs value for rock samples was consistence with their variable CIA values. The values of Al_2O_3 and TiO_2 are considered as a good indicator of sediment provenance during weathering, diagenesis and metamorphism (Gatench, 2000; Hayashi *et al.,* 1997; Paikaray *et al.,* 2008; Mosheni *et al.,* 2017).

The plot of TiO_2 versus Al_2O_3 suggested that the Lwamondo clay had nearly basaltic source whereas Matsika and Tshipise samples showed granodiortic to basaltic tendency (see Figure 4.2). The remaining clay samples plotted in the granite domain suggested that their provenance was granitic in origin prior to weathering events. This interpretation seemed plausible when compared with the discriminate function plot shown in Figure 4.3. The plot suggested that the Lwamondo, Matsika and Tshipise clay deposits have mafic igneous provenance domain while the remaining samples as felsic igneous and quartzose sedimentary provenance.

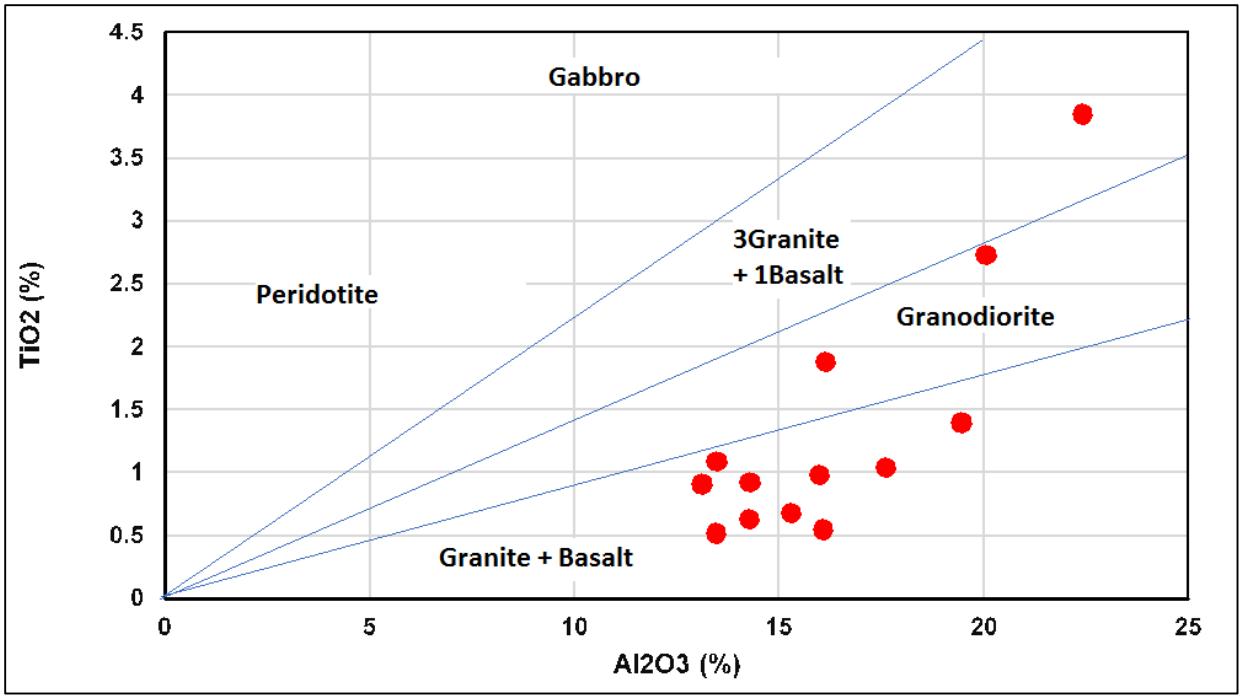

Figure 4.2: Plot of Al_2O_3 versus TiO_2 studied clay samples suggesting basalt, granodiorite and granite provenance tendency.

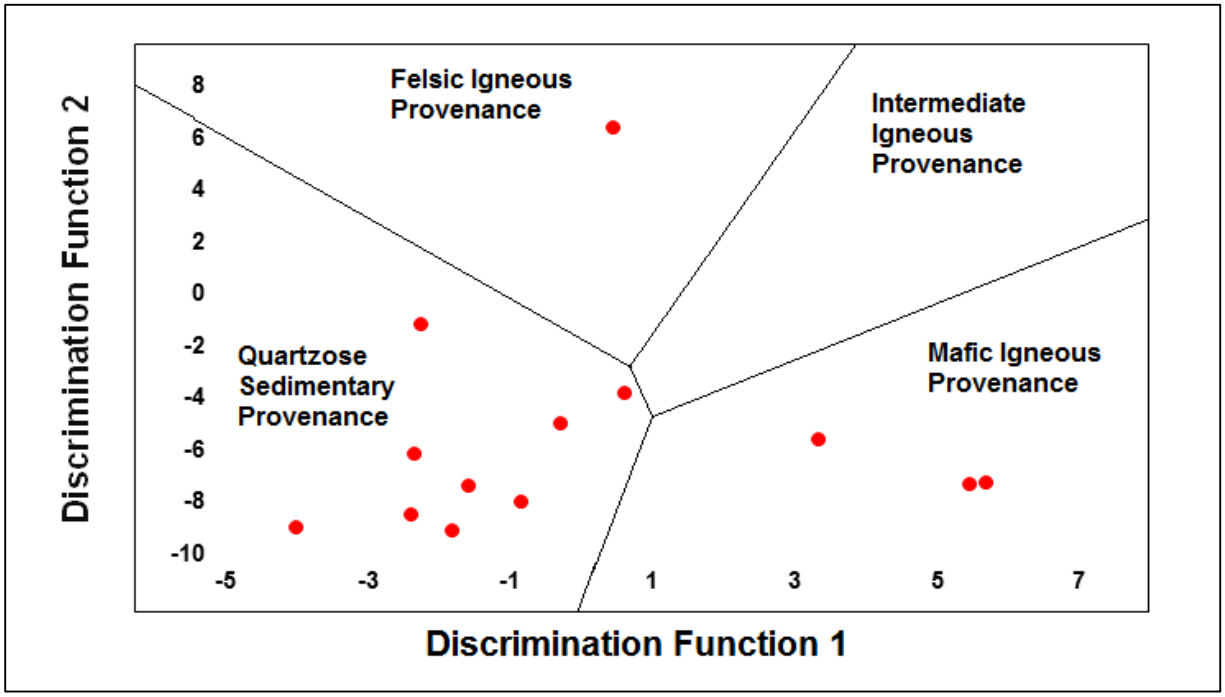

Figure 4.3: Plot of Discrimination function using major elements suggesting felsic and mafic provenance and quartzose sedimentary provenace. (**Note:** Discrimination Function 1: - 1.733 TiO_2 + 0.607 Al_2O_3 +0.76 Fe_2O_3 (t) - 1.5 MgO + 0.616 CaO + 0.509 Na_2O - 1.224K_2O -0.909. Discrimination Function 2: 0.445 TiO_2 + 0.07 Al_2O_3 - 0.25Fe_2O_3 (t) - 1.142 MgO + 0.438 CaO + 1.475 Na_2O + 1.426K_2O - 6.861).

The predominance of Al_2O_3 and TiO_2contents in clay (13-22%) and rock samples (3-12%) suggested a positive relationship. This positive proportionality indicated some input of detrital minerals from surrounding rock suites. Although the value of SiO_2 content in rock samples are exceptionally higher when compared with clay samples, the ratio of SiO_2 / Al_2O_3in rock samples (9.2%) give higher value than clay samples (3.1%) thereby suggesting an ongoing desilicication and allitization processes.

4.1.2 Trace element geochemistry

The trace element distribution plot shown in Figure 4.4 revealed that the detected large ion lithophile element (LILE such as K, Rb, Sr, and Ba), high field strength element (HFSE such as Hf, Th, Ta, Nb, U, Zr) and Rare Earth element (REE from La-Lu, Y, Sc) are relatively enriched in clay samples than in rock samples from the study area.

The enrichment in both clay and rock samples followed a decreasing sequence from LILE>REE>HFSE (see Figure 4.4). The higher value of LILE enrichment relative to other elements proposed a provenance with subduction zone geochemical domain which is consistent with study conducted by Crow and Condie (1990). The mentioned work indicated that Soutpanberg Formations are characterized with enriched LILE over other elements. LILE and HFSE generally show incompatible behavior during mantle melting processes though respond differently to post magmatic processes such as weathering, hydrothermal and metamorphic alteration hence useful for predicting the source of any sediment or magma.

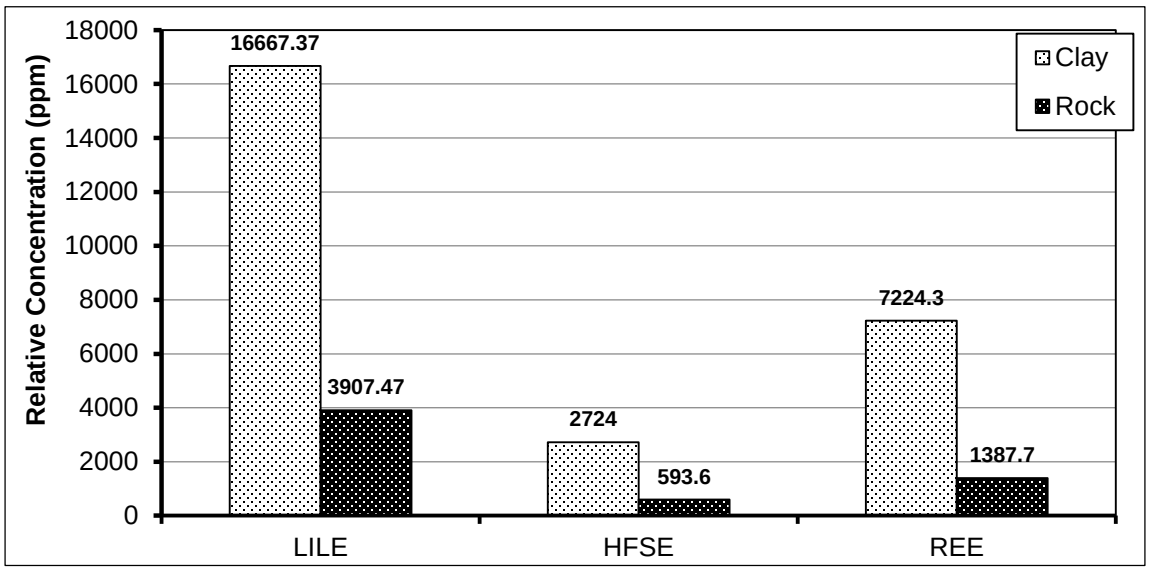

Figure 4.4: Plot of trace element distribution in clay and rock samples.

The chondrite normalization showed higher concentration and abundance of Rare Earth Elements (REE) in clay samples when compared with the rock samples (see Figure 4.5 and Figure 4.6). The normalized REE values for clay samples were enriched at concentration slightly above 1000ppm up to 3000ppm while rock samples values concentrated from 1ppm to less than 1000ppm.

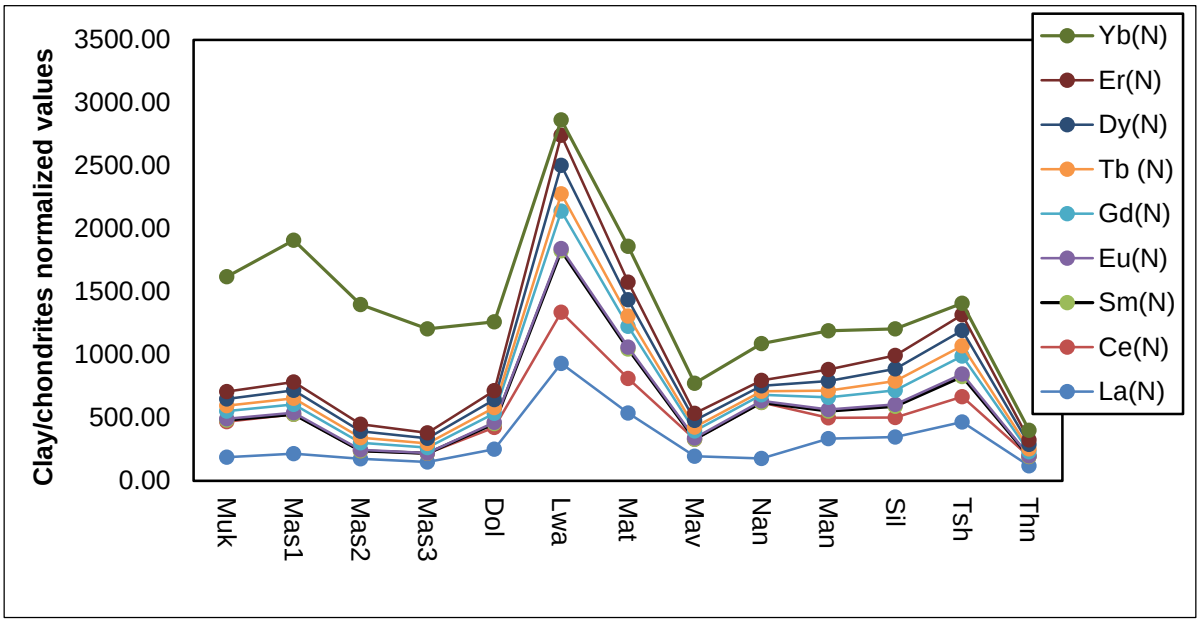

Figure 4.5: Plot of chondrites normalized REE concentration of clay samples

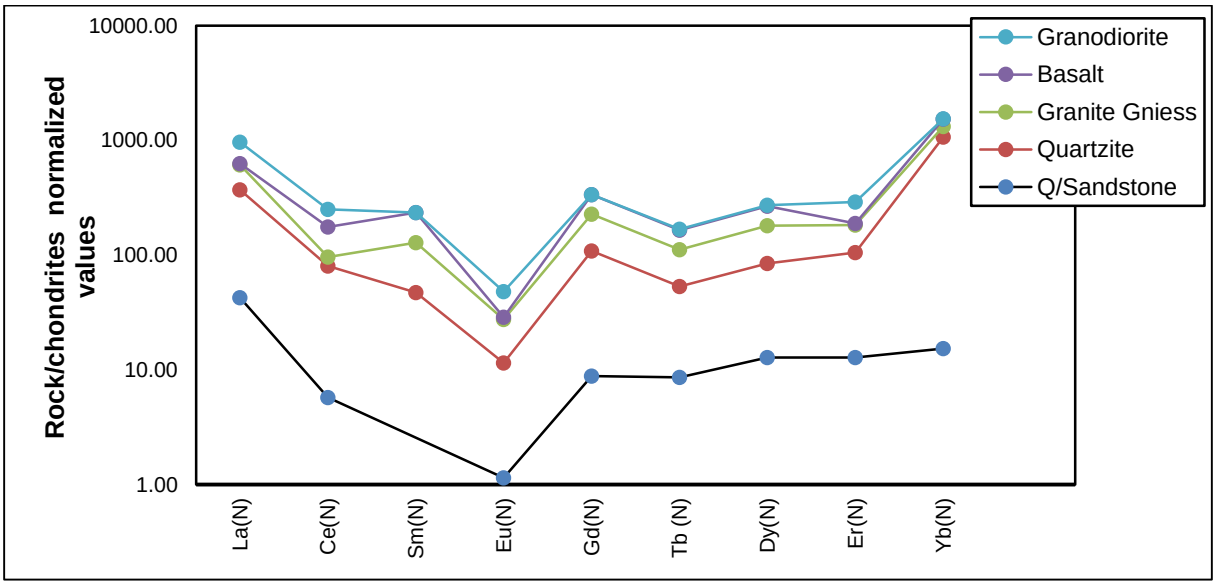

Figure 4.6: Plot of chondrites normalized REE concentration of rock samples

The distribution of Heavy Rare Earth Elements (HREE) was enriched both in clay and rock samples following Yb>Dy>Gd>Er>Y>Tb decreasing order. It also showed a slight depletion in Light Rare Earth Element (LREE) following Ce>La>Sm>Eu>Sc sequence for clay samples while La>Ce>Sm>Eu>Sc sequence for rock samples. The slight depletion in the LREE was reflected both in low La_N/ Yb_N values (LREE<6) and proportionality-function plot in Figure 4.7a and b which show upward abundance in HREE values towards clay samples and downward depletion in LREE values towards rock samples.

Anomalous Ce* value which is less or greater than 1 are used to indicate anoxic and oxidizing environments respectively (Patten *et al.,* 2005; Calvert and Padersen, 1993; Staden *et al.,* 2014). The concentration of this element in studied rock samples ranged from 0.2 to 3.2 which suggest both anoxic and oxidizing environments. This variation in Ce* enrichment was suggestive of unreworked upper continental crust. Furthermore, all the clay samples have Ce* values above 1 indicating anoxic and oxidizing depositional environments. This explained the argillaceous deposits found in the study area and it is consistent with the work of Barker *et al* (2006). Both clay and rock samples were found to be having low Eu* anomalies which were generally below 0.6 (see Appendix B). The Eu* anomalous value <0.6 has been proposed to represent mainly felsic composition with relatively scarcity of plagioclase occurrence. The compositional trends of highly immobile elements (Zr/Ti, Nb/Y) present in the studied clays depict ryholitic and alkaline trends which alluded to a more felsic nature than mafic (see Figure 4.8). In addition, all samples plotted above the upper continental crust (UCC) values, marked by the black star in Figure 4.9. The clay samples are more enriched in Th element compared to rock sample thus the latter plotted at lower part of UCC.

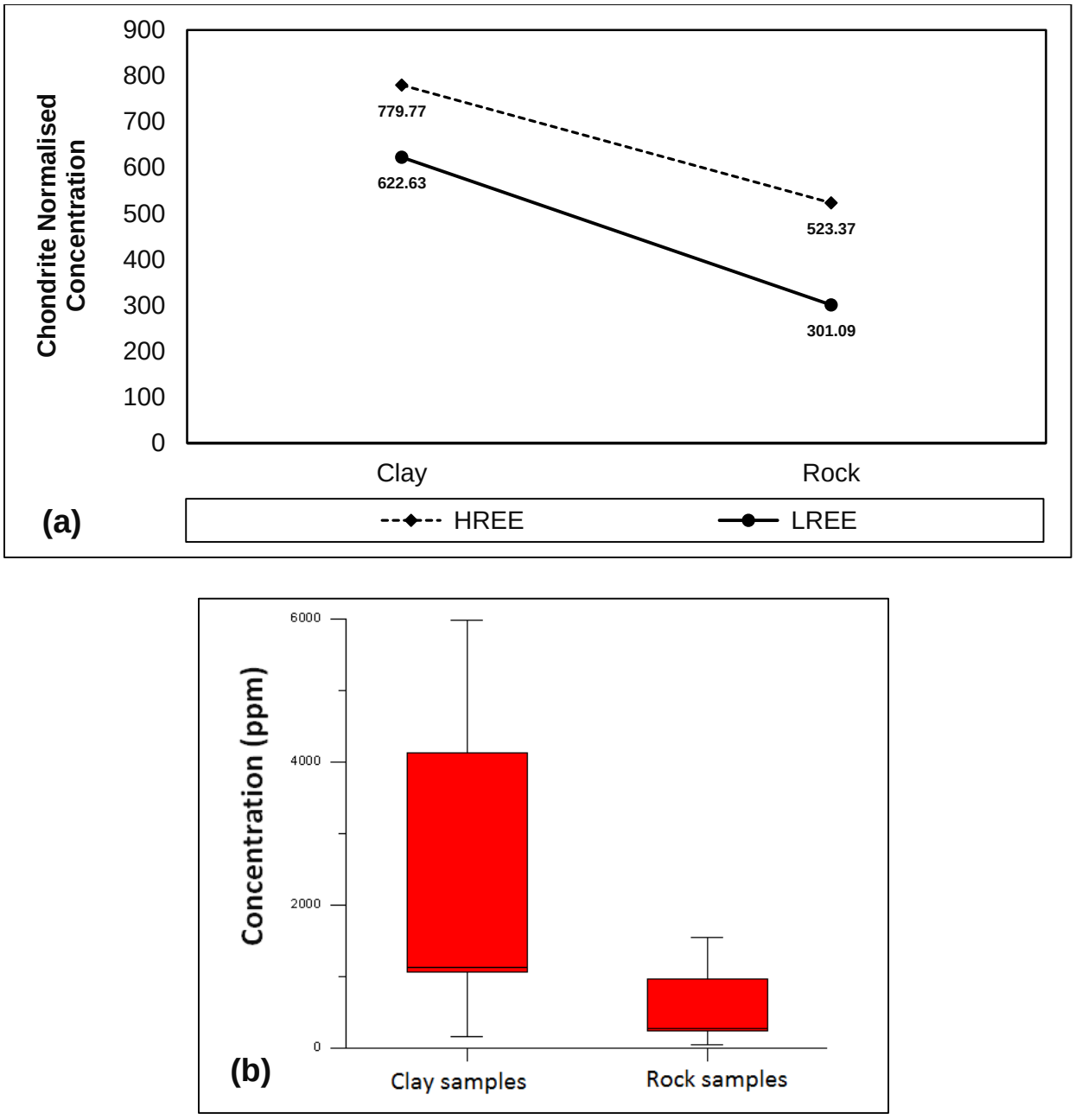

Figure 4.7: (a) Plot of HREE and LREE concentration in clay and rock samples (b) relative LREE concentration clay and rock samples.

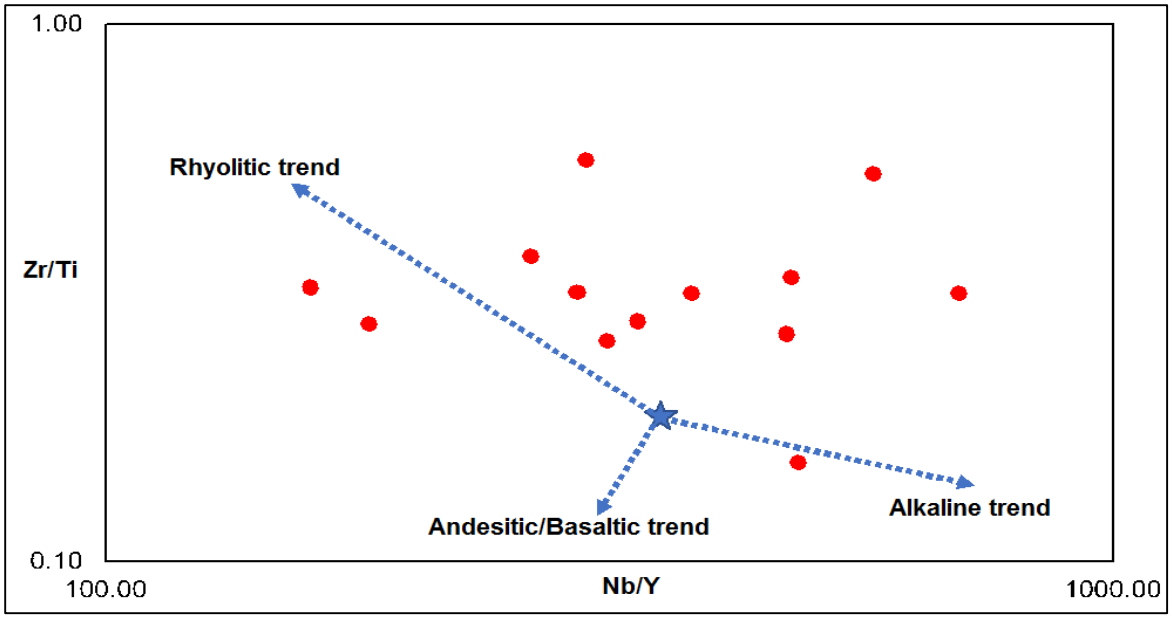

Figure 4.8: Plot of Zr/Ti versus Nb/Y of immobile elements in clay samples.

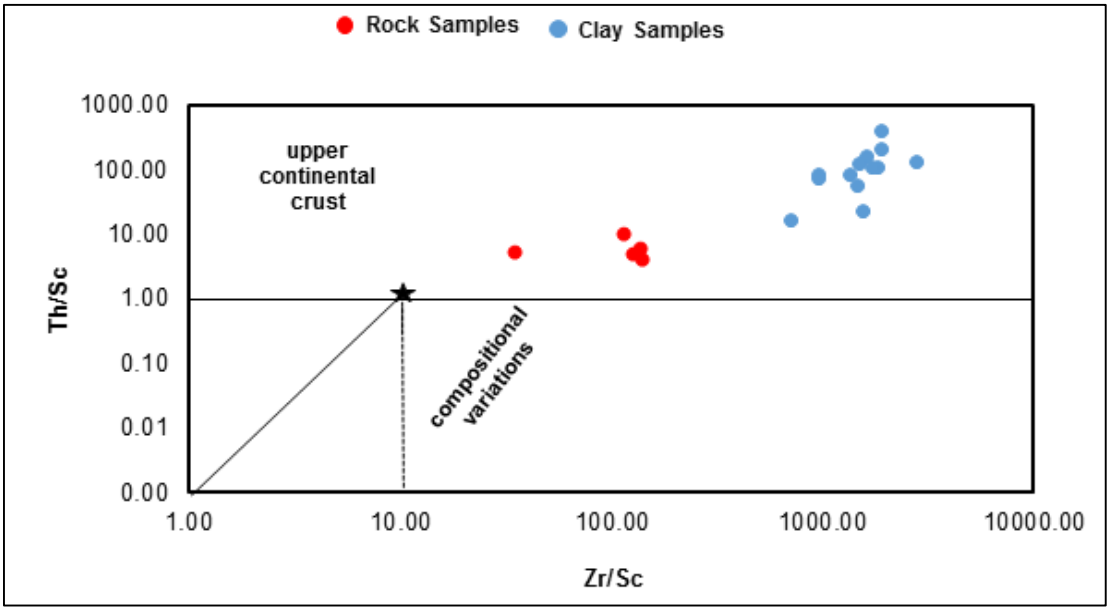

Figure 4.9: Plot of Th/Sc versus Zr/Sc in clay and rock samples.

4.2. Mineralogical compositions of clay and rock samples

This section presents and discusses the result of mineral compositions for both clay and rock samples based on the XRD and microscopic analyses. The thin-sections of the rock samples were prepared, viewed and analyzed under petrologic microscope to obtain better understanding of the composition of rock samples.

4.2.1. Mineral composition of clay samples

The quantitative result of clay samples using X- ray diffraction was presented in Table 4.1 while their qualitative descriptions were shown in Figure 4.10 a and b. In all clay samples presented in Table 4.1, smectite content showed predominance values which ranged from 8.25% to 29.32%. It showed the highest and most symmetrical peak in samples collected from Mashamba1 (29.32%) followed by Mukondeni (15.92%), Mashamba-3 (11.37%), Mashamba-2 (10.28%) and Siloam (8.25%) although kaolin and chlorite were present as well. The kaolin content had a relatively higher value in samples collected from Mashamba2 (17.24%) compared to Mashamba-1 (15.36%) and Mashamba-3 (14.91%) but absent in Mukondeni sample. The chlorite content of the mentioned locations ranged from 5.94% to 12.785 showing highest and lowest values in samples collected from Mukondeni and Mashamba-1 respectively. Besides the moderate values of kaolin content in samples collected from Mashamba-1, Mashamba-2 and Mashamba-3, it showed the highert value in studied sample of Lwamondo (59.26%) followed by Tshipise (25.13%), Manini (22.80%), Matsika (22.19%), Doli (20.46%) but lowest in Thengwe (4.60%). The relative high content of kaolin suggests a secondary deposition due to intense weathering and transportation of minerals such as microcline, plagioclase, and muscovite as indicated by their CIA values. Samples collected from Siloam indicate the predominance of chlorite content (16.54%) compared to all other studied samples which ranged from 5.94% in Mashamba sample to 12.78% in Mukondeni. Among the non-clay minerals present quartz and plagioclase contents have a relatively high value which range from 20.50% - 91.37% and 14.69% - 38.16% respectively compared to other minerals.

Table 4.1: Mineralogical composition of the studied clay samples.

Samples	Sm	Ka	Ch	Qz	Pl	Mi	He	Hor	Mu	Tal	Ana	Geo
Mukondeni	15.92	-	12.78	26.63	30.28	2.97	-	4.74	-	6.68	-	-
Mashamba1	29.32	15.36	10.38	20.50	14.69	2.07	-	0.95	-	6.75	-	-
Mashamba2	10.28	17.24	5.94	36.06	20.53	2.21	-	1.95	-	5.79	-	-
Mashamba2	11.37	14.91	6.43	35.36	16.16	4.44	-	4.91	-	6.94	-	-
Doli	-	20.46	-	29.11	18.58	12.23	-	-	-	13.35		-
Lwamondo	-	59.26	-	22.81	-	-	9.23	-	-	-	8.70	-
Matsika	-	22.19	-	59.48	-	-	5.06	-	-	-	4.85	8.4
Mavambe	-	-	8.03	42.02	38.16	7.53	-	4.26	-	-	-	-
Nandoni	-	-	8.83	37.39	33.09	16.35	-	4.34	-	-	-	-
Manini	-	22.80	9.07	34.88	24.82	4.66	-	-	-	-	-	-
Siloam	8.25	-	16.54	33.69	-	-	6.47	-	35.05	-	-	-
Tshipise	-	25.13	-	58.42	-	-	5.59	-		-	3.90	6.9
Thengwe	-	4.60	-	91.37	-	-	1.57	-	2.46	-	-	-

Note: Sm - smectite; ka- kaolin; ch - chlorite; Qz- Quartz; Pl- Plagioclase; Mi -Microcline; He - Hematite; Hor - Hornblend; Mu -Muscovite; Tal - Talc; Ana - Anatase; Geo– Geothite

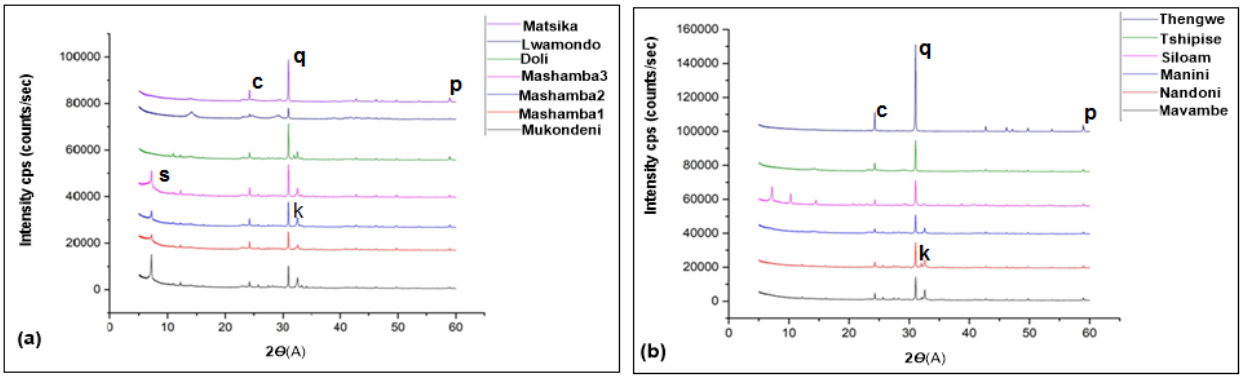

Figure 4.10: X-ray diffractograms for studied clay samples (Note: Q-quartz; P-plagioclase; S-smectite; K-kaolin; C-chlorite

4.2.2 Mineral composition of rock samples

Based on field observation and the results of the thin-sections examinations under microscope, the rock samples collected from the vicinity of the clay deposits were classified into three general groups. Granodiorite (G1) and consolidated ferruginized quartzitic sandstone(G4) dominated the rock types distributed around the clay samples collected in Thengwe, Tshipise, Siloam, Matsika and Mavambe. The granite gneisses (G2) were mainly observed to be dominating the clay samples from Nandoni, Manini and Lwamondo. Clay samples collected from Mukondeni, Mashamba1, Mashamba2, Mashamba3 and Doli were mainly developed around repetitive sequence of grabboic-texture basalt (G3) which is interspersed with resistant quartzite rocks (G3).

Quartzitic sandstone rock units

Quartzite is metamorphosed sandstone whose original precursor mineral is at least 95% quartz and less than 15% of the finer fractions (Tucker, 2001; Pedergnana *et al.,* 2017). In this study, macroscopic visual screening revealed brownish grey to yellowish grey tone of the quartzite samples in G3. It displayed conchoidal fracture when broken with geological hammer and exhibited aphanitic granular texture. The colour which ranged from brownish grey to yellowish grey could be attributed to be due to the presence of hematite and muscovite minerals.

The muscovite was distinguished by its bird eye's orientation extinction angle of 2^{o}as well as pleochroic in plane polarized light since colour becomes darker. The hematite mineral was opaque both under plane and crossed polarized light and this can be due to high content of iron or mafic elements present. The quartz mineral showed lack of visible twinning, cleavage and

colour but exhibited low relief when viewed under plane and cross polarized light. However, fine lamellae sweep across quartz grain in an irregular manner as the stage is rotated clockwise between 4-7^{o} and this could be adduced to strain and/or metamorphic pressure or deformation. . Figure 4.11 showed the photomicrograph of the quartzitic sandstone whereby quartz mineral essentially dominated the quartzite composition. This mineral composition was observed in both photomicrograph and XRD results shown in Table 4.2.

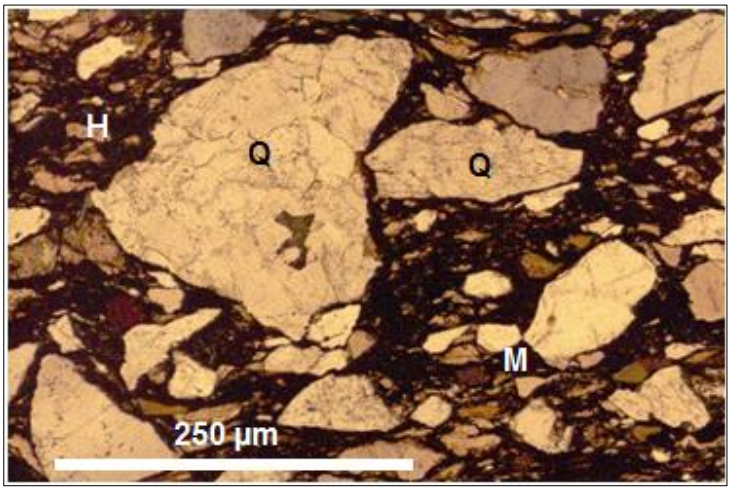

Figure 4.11: Photomicrograph of quartzitic sandstone. Q-quartz, M-muscovie, H-hematite.

Table 3.2: Percentage composition of minerals present in the quartzitic sandstone

Mineral	**Quartz**	**Muscovite**	**Hematite**
Composition (%)	95.59	4.14	1.27

Basalt rock units

The studied basalt samples found in G3 are generally both black to greyish black in colour with no identifiable mineral in hand specimen when viewed with naked eyes but differ in felsic content. In contrast to dark green, epidotised, amygdaloidal basalt which are present in Sibasa Formation (Barker, 1979, Barker *et al.,* 2006), the studied basalt of G3 exhibited medium grained gabbroic texture which is relatively coarse. Microscopic and mineralogical analyses of this rock unit revealed the average composition of mafic minerals such as enstatite (17.77%), forsterite (4.34%), diopside (23.84%) and plagioclase (35.82) with accessory minerals which include muscovite and quartz in the groundmass. Unlike the enstatite mineral which showed weak green pleochroism when the stage was rotated, the diopside mineral was observed to be with no

pleochroism but exhibited extinction angle of 39°. In comparison with basalt from the Sibasa Formation (Barker *et al.,* 2006), the average quartz content of G3 basalt is lower although contain a higher amount of plagioclase as revealed by their carlsbad twining (see Figure 4.12). This mineral composition was observed in both photomicrograph and XRD results shown in Table 4.3.

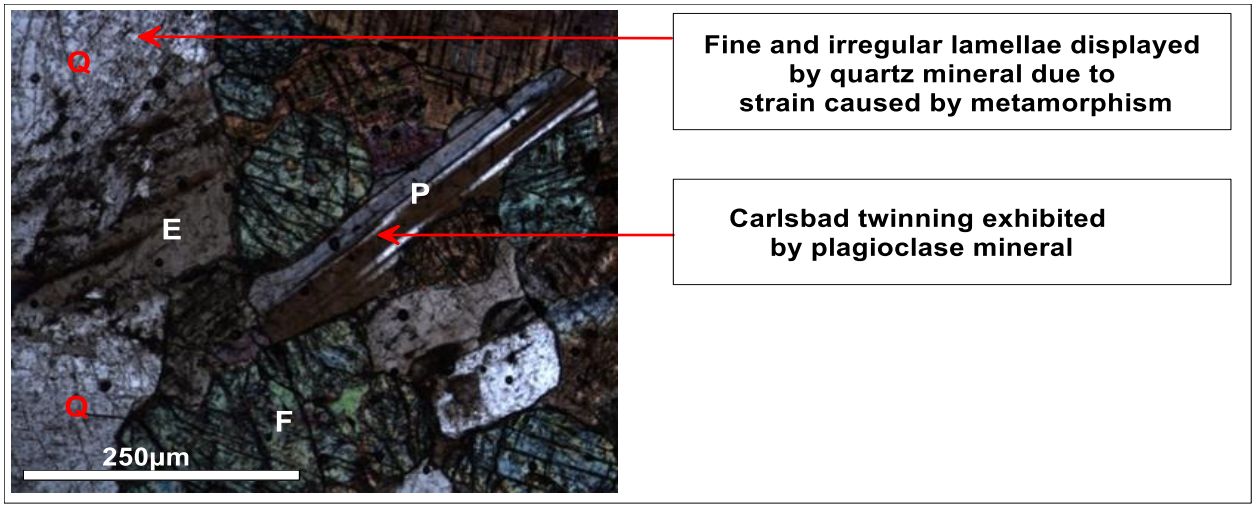

Figure 4.12: Photomicrograph of basalt rock. Q-quartz, P-plagioclase, E-enstatite, F-forsterite, Mu-muscovite.

Table 4.3: Percentage composition of mineral present in the basalt rock units.

Mineral	Quartz	Plagioclase	Diopside	Enstatite	Forsterite	Chlorite	Talc	Actinolite
Comp (%)	8.59	35.61	23.84	17.77	4.34	2.5	3.24	4.11

Granite gneiss rock units

The studied rock samples from G2 showed gneissic structure due to the mafic and felsic minerals which aligned in preferred orientation and separate bands. Generally, they had the color which can be mesocratic. This indicated a blend of both melanocratic and leucocratic minerals (see Figure 4.13). Table 6 showed quartz (31.6%) and chlorite (6.48%) as the primary light-colored minerals while epidote and augite constitute the dark minerals. The presence of the metamorphic minerals such as augite (1.4%) and epidote (60.52%) suggest the high temperature and pressure that separate the mafic and felsic magma melts into preferred orientations.

Table 4.4: Percentage composition of minerals present in the Granite gneiss

Mineral	Quartz	Chlorite	Augite	Epidote
Composition (%)	31.6	6.48	1.4	60.52

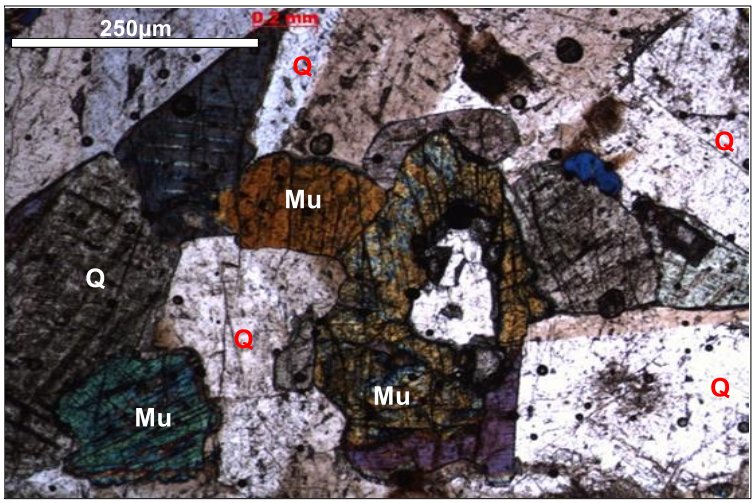

Figure 4.13: Photomicrograph of granite gneiss rock. Q-quartz, Mu-Muscovite, A-augite

Quartzo-feldspathic gneiss rock units

In contrast to G3 gneissic rock, the felsic minerals which dominate the G1 quartzo-feldspathic gneiss rock samples include quartz (39.41%), plagioclase (30.46%), microcline (24.54%) and chlorite (3.24%) as against the 2.35% mafic hematite mineral (see Table 4.5). The textural framework is not only generally phaneritic whereby grains or minerals are easily identifiable in hand specimen but easily disintegrate when broken with hammer. This fragile nature could be adduced to probable small amount of cementing matrix such as hematite (2.35%). The shape of grains and minerals ranged from angular, sub angular to round. Whilst microcline exhibited cross-hatched twinning under cross polar light the plagioclase showed Carlsbad twinning (Figure 4.14).

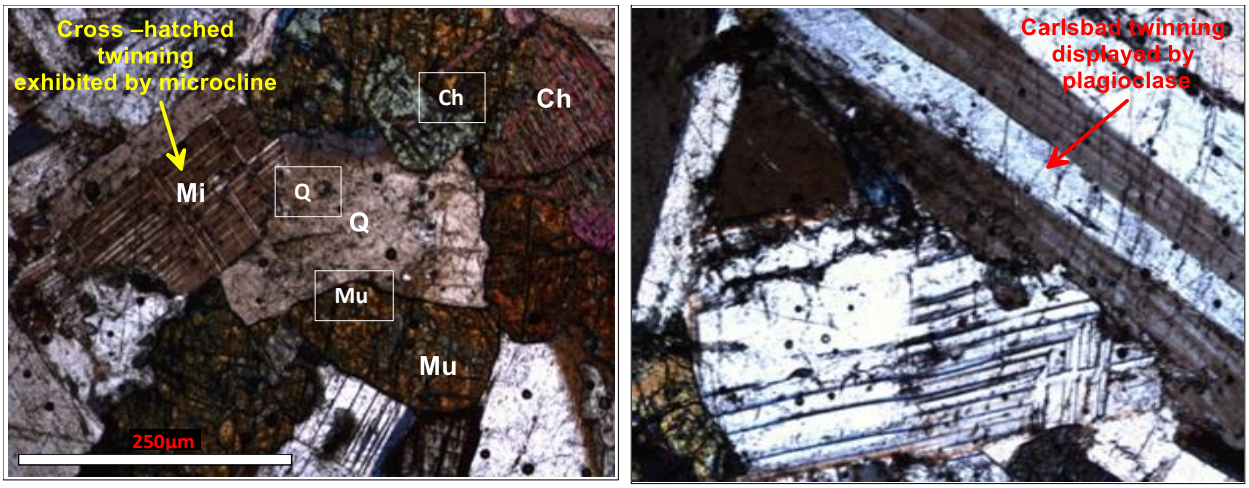

Figure 4.14: Photomicrograph of gneissic rock. Mi-microcline, Mu-muscovite, ch-chlorite, Q-quartz

Table 4.5: Percentage composition of minerals present in Quartzo-feldspathic gneiss rock units

Mineral	Quartz	Plagioclase	Microcline	Chlorite	Hematite
Composition (%)	39.41	30.46	24.54	3.24	2.35

CHAPTER FIVE

PHYSICAL, MECHANICAL AND THERMAL PROPERTIES OF CLAY

This chapter presents and discusses the results obtained from the physical, mechanical and thermal analyses of the studied clay samples. The physical tests result provided information on the colour, cation exchange capacity (CEC) and pH of the clay samples collected from Vhembe District using Munsell colour chart, atomic absorption spectrometry and pH meter respectively. Mechanical details on the particle size distribution (PSD) and Atterberg limit of studied samples were presented and discussed as well. The PSD and plasticity tests were achieved using sieve and hydrometer analyses and Casagrande method respectively. Information about mass stability of clay samples over time as temperature increased was evaluated by the thermal analysis (TGA-TGA) while the micro-pore properties describes the microstructures and surface topography of the studied clays using scanning electron microscopy (SEM).

5.1 Physical Properties of Clay

This section discusses the physical properties of clay deposits which include color, cation exchange capacity (CEC) and soil pH differs from one clay sample to another and thus required detailed characterization. Basic insight about mineral composition and depositional processes of clayey soils were deduced from these properties.

The raw clays varied in hue/value/chroma with their corresponding tonality shades (refer to Table 4.6). Their hue/value/chroma ranged from 2.5YR/5/8 to 10YR/5/1 with corresponding tonality of red and gray. Clay that exhibited pale yellow to gray colour suggested reducing depositional environment due to leachable Fe resulting from hydromorphic conditions. The reddish to very pale brown clay indicated that they formed or deposited under oxidizing zones where Fe was enriched in the study area such as Doli, Lwamondo, Matsika, Siloam and Tshipise. Clay samples of Mukondeni, Mashamba-1, Mashamba-2 and Mashamba-3, Doli, Lwamondo,Manini, Siloam and Tshipise whose Fe content is relatively high (above 5%) exhibited a deep tonality (Figure 5.1).

Table 8presents the results of both CEC and soil pH. Although the CEC values of studied samples widely varied from 15.37 to 83.16 meq/100g, soil pH exhibited similar near-neutral-pH values ranging from 6.13 to 7.50. Samples from Mukondeni, Mashamba1, Mashamba2 and Mashamba3 have relatively high CEC values above 60meq/100g compared to all other samples in which their CEC values ranged between 15 and 44 meq/100g. Figure 5.2 indicated that the pH of the samples

were near neutral and favored the CEC value above 15meq/100g which is consistent with the report of Mckenzie *et al*. (2004).

Table 4.6: Summary of Physical Properties of studied clay samples

Location	Hue/value/chroma	Colour	Soil pH	CEC (Meq/100g)
Muk	5YR/5/2	Reddish gray	7.28	75.24
Mas 1	10YR/5/1	Gray	7.09	64.58
Mas 2	10YR/6/4	Light yellowish brown	7.15	71.68
Mas 3	7.5YY/6/1	Gray	7.35	83.16
Dol	2.5YR/5/6	Red	6.75	44.06
Lwa	5YR/5/8	Yellowish red	6.13	20.69
Mat	7.5YR/4/6	Strong brown	6.99	27.86
Mav	7.5YR/5/8	Strong brown	7.5	37.05
Nan	7.5YR/5/4	brown	7.02	17.60
Man	2.5YR/5/8	Red	6.78	42.73
Sil	5R/5/3	Weak reddish grey	7.13	33.28
Tsh	2.5YR/5/8	Red	6.77	15.37
Thn	2.5YR/6/6	Light yellowish brown	6.25	34.90

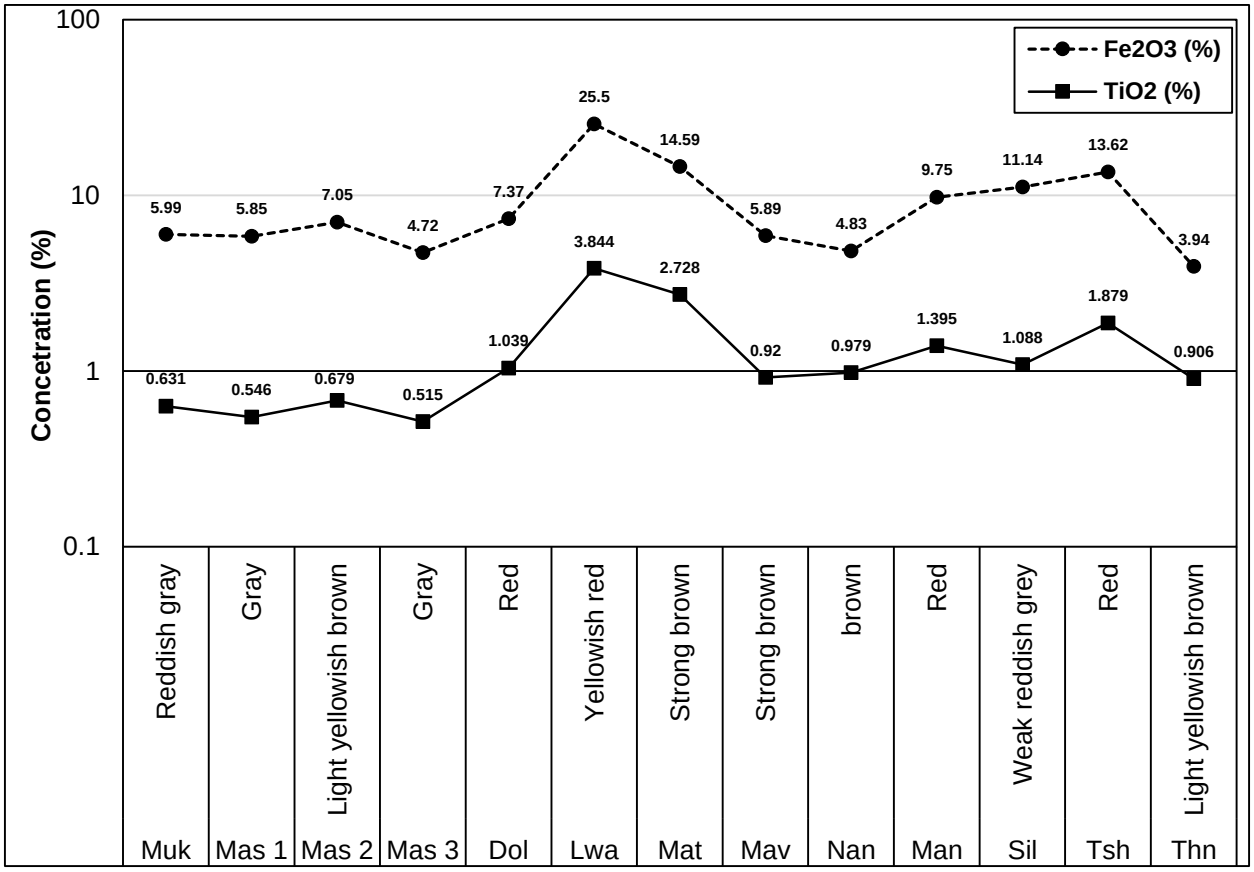

Figure 5.1: Plot of tonality Vs Iron and Titanium oxide.

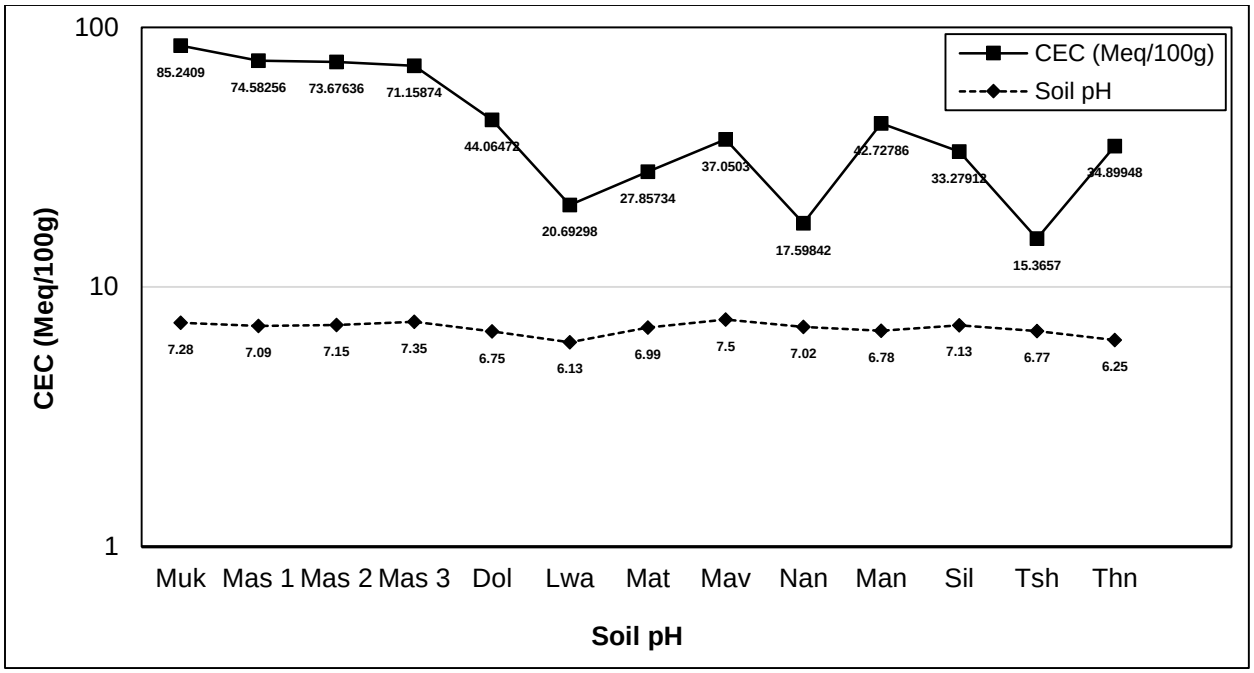

Figure 5.2: Plot of CEC Vs Soil pH of studied samples.

5.2. Mechanical Characteristics of Clayey Samples

The section explains the plasticity and compressibility properties of the different clay deposits as well as their textural classification. Engineering parameters such coefficient of uniformity, gradation and sorting were evaluated owing to variation of the parameters in different clay materials. Based on the mechanical properties, the potential industrial application for the clay deposits were deduced using various empirical charts and graphs.

5.2.1. Plasticity and compressibility properties of clay

The plasticity properties of the clay deposits exhibited heterogeneous behaviors as revealed in plastic limit (PL), liquid limit (LL) and plastic index (PI) values presented in Table 4.7. The studied samples from Mukondeni and Mashamba-1 have both LL and PI values that are above 50 and 30 respectively thus plotted above A-line of plasticity chart shown in Figure 5.4. This A-line separated the inorganic clay above the line from the inorganic silts below the line. Hence, the Mukondeni and Mashamba-1 samples indicate inorganic clays with high plasticity properties due to their location above the A-line in plasticity chart.

Similarly, the studied samples from Lwamondo, Mashamba-2 and Mashamba-3 were found to be having LL values that are greater than 50 but lower PI value than 30 when compare with

Mukondeni and Mashamba-1 clay samples. Therefore, it implied that these soils are inorganic silts with high compressibility and organic clays properties since it plotted below the A-line of plasticity chart.

The samples that were found to be having medium plasticity properties whose LL values ranged from 30 to 50 includes Doli, Mavambe, Thengwe and Siloam samples. These samples plotted above the A-line of plasticity chart with intermediate PI value between 15 and 21 as shown in Table 4.7. Comparatively, samples collected from Nandoni, Matsika and Manini have similar LL values between 30 and 50 but lower intermediate PI values between 10 and 20 thus located below the A-line of plasticity chart. These samples indicate silt clay of medium compressibility properties with the presence of organic clay. In contrast to all other studied samples from the study area, only sample collected from Tshipise varied widely with lowest liquid limit (25) and Plastic index (5) values.

Table 4.7: The results of the plasticity properties of the clay

Sample Location	S/N	PL	LL	PI	PLASTICITY PROPERTIES DESCRIPTION
Mukondeni	L1	11.62	73.62	62.00	Inorganic clays of high plasticity
Mashamba-1	L2	18.62	51.39	32.77	Inorganic clays of high plasticity
Mashamba-2	L3	22.92	51.46	28.54	Inorganic silts of high compressibility and organic clays
Mashamba-3	L4	24.15	67.15	43.00	Inorganic clays of high plasticity
Doli	L5	15.05	30.17	15.12	Inorganic clay of medium plasticity
Lwamondo	L6	55.93	65.43	9.50	Inorganic silts of high compressibility and organic clays
Matsika	L7	23.36	44.22	20.86	Inorganic clay of medium compressibility and organic silts
Mavambe	L8	14.06	31.34	17.28	Inorganic clay of medium plasticity
Nandoni	L9	21.77	32.39	10.62	Inorganic clay of medium compressibility and organic silts
Manini	L10	22.56	44.21	21.65	Inorganic clay of medium compressibility and organic silts
Siloam	L11	18.90	40.25	21.35	Inorganic clay of medium plasticity
Tshipise	L12	19.73	25.56	5.83	Inorganic clay of low plasticity
Thengwe	L13	10.67	30.69	20.02	Inorganic clay of medium plasticity

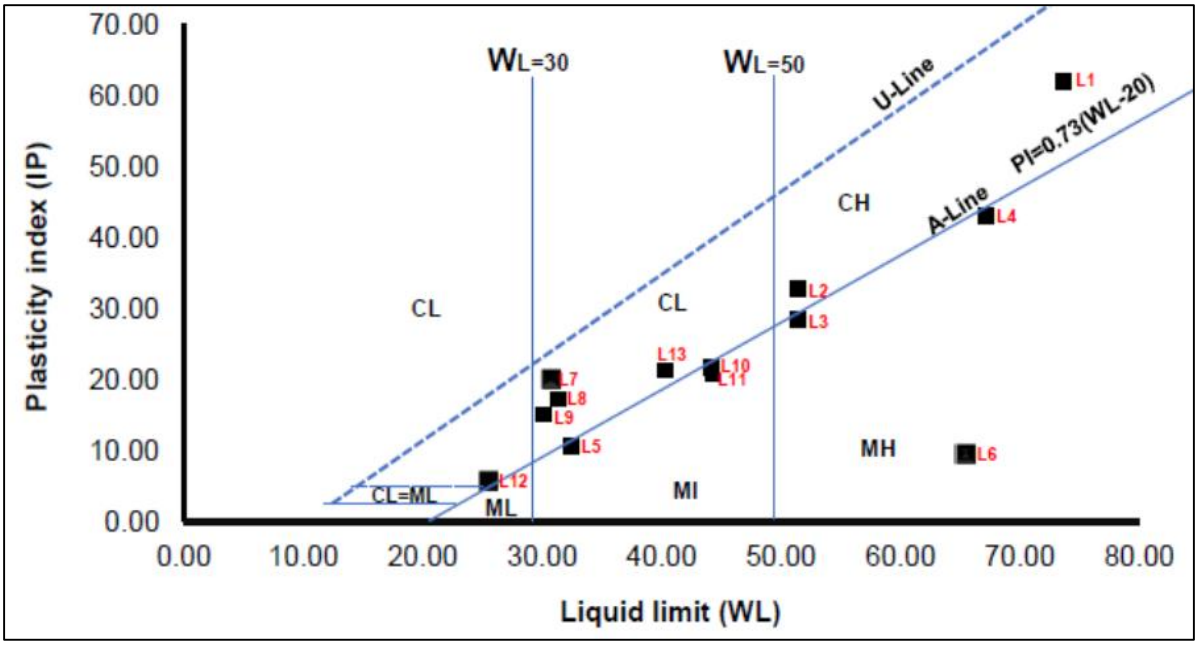

Figure 5.3: Plasticity chart showing degree of plasticity and compressibility of studied clays.

5.2.2. Textural properties of clay

The results of the particle size distribution analysis for the bulk samples collected from the study area were presented in semi-logarithm plots known as gradational curves (see Figure 5.4). All samples showed homogeneous distribution of sand size fractions (2 to 0.05mm) with compositional values ranging from 86.98-98.66%. This abundance followed a decreasing order from Mavambe > Nandoni > Manini > Matsika > Lwamondo > Thengwe > Doli > Mashamba2 > Mashamba3 > Siloam > Mashamba1 > Tshipise > Mukondeni samples.Similarly, the fines sizes whose size diameter rangedfrom 2µm to 0.05mm showed heterogeneous abundance with average value greater 10%.

However, the gradational curves shown in Figure 5.4a depicted that all the soils collected from Mukondeni, Mashamba-1, Mashamba-2, Mashamba-3 and Doli showed a similar pattern with exception of soils from Doli area. This could be due to the presence of relative higher abundance of sand size fractions and lowest fines sizes compared to others. Figure 5.4b likewise indicated that the soils collected from Lwamondo showed the relative highest content of fines compared to those found in Nandoni. Other soils in this group showed similar curves progression owing to similar grain sizes distributions. Figure 5.4c showed a gap in particles between 0.3 and 1.2mm diameter of soils collected Siloam thereby differing in gradational pattern compared to Tshipise and Thengwe soils.

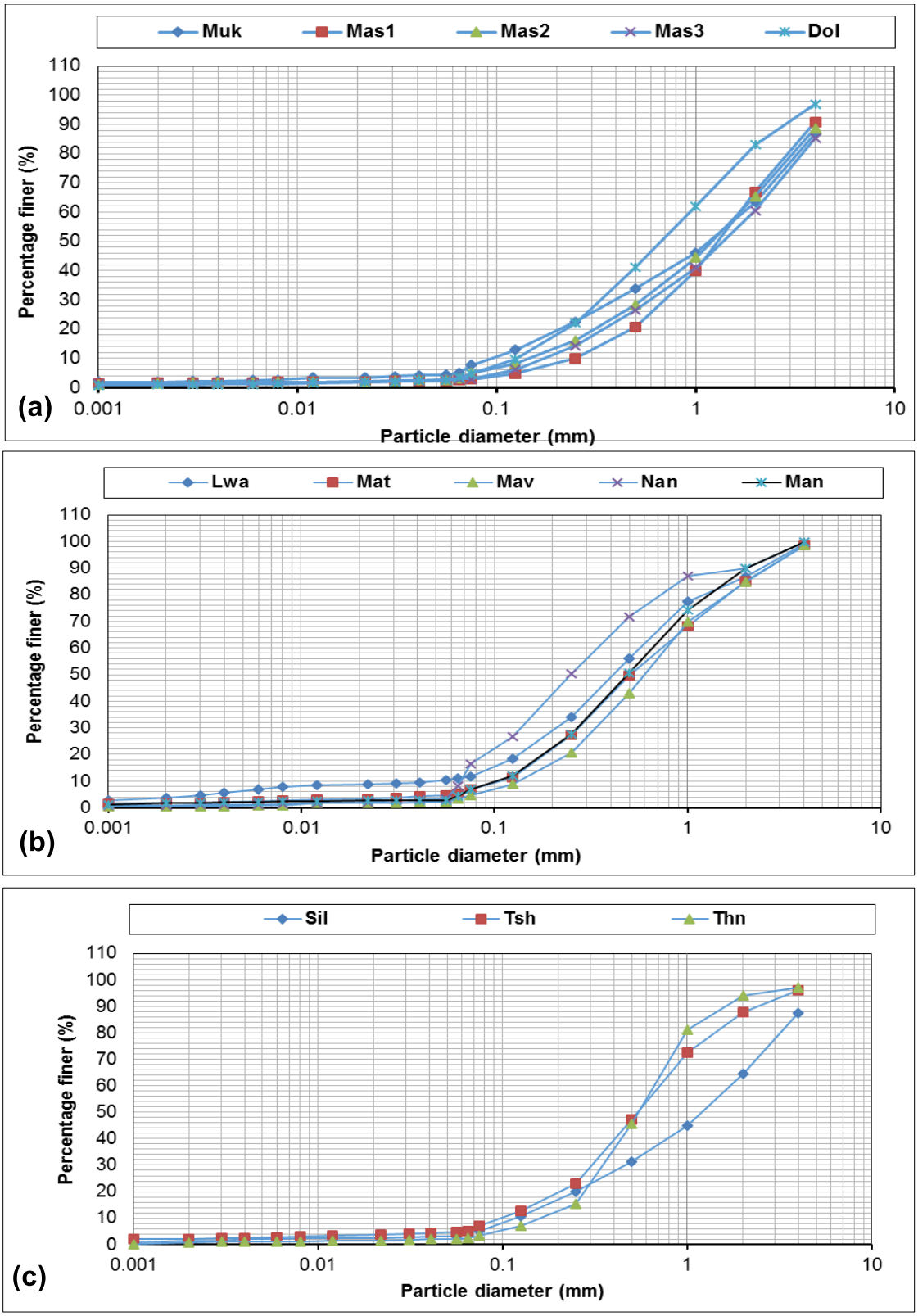

Figure 5.4: Gradational curves for particle size distribution in the mentioned studied area.

From the gradational curves, particle distribution of the studied samples showed an effective (D_{10}) sizes value that ranged from 0.06 to 1.00%. The coefficient of uniformity (C_u) showed heterogeneous variation in all samples from 0.70 to 18.00 however, soils collected from Matsika, Mavambe, Nandoni, Manini, Tshipise and Thengwe had value less than 6.00. The coefficient of gradation (C_c) for soil samples generally showed low values less than 2. There was also similarity in the degree of sorting (S_o) as all samples have values ranging from 1.83 to 3.41 (see Table 4.8).The S_o indicated that the studied soils have particle sizes that are widely distributed.

According to the Unified Soil Classification System, soils from Mukondeni, Mashamba-1, Mashamba-2, Mashamba-3 are considered as inorganic fat clay (CH) since they have coefficient of uniformity (C_u) less than 3 and have more than 50% liquid limit values which plotted above the "A" line. Soils from Lwamondo showed similar properties with the mentioned soils but plotted below the "A" line and thus classified as elastic silt (MH). Soils collected from Manini, Mavambe, Siloam and Thengwe have fine grains whose liquid limit values are less than 50 but plotted on above the "A" line and classified as inorganic lean clay (CL) while soils from Nandoni, Doli, and Matsika plotted below the line and considered as inorganic silt (ML). Soils from Tshipise was considered to be clayey sand since it consists more than 12% of fines fractions and have both liquid limit and plastic index to be less than 30 and 7 respectively.

Table 4.8: The results of the textural properties of studied soils.

	Grain sizes composition(%)							Engineering parameters			
Location	**Sand**	**Silt**	**Clay**	**D_{10}**	**D_{30}**	**D_{60}**	**D_{75}**	**C_u**	**C_c**	**S_o**	**USCS**
Muk	86.98	10.41	2.67	0.10	0.40	1.80	2.90	18.00	0.89	3.41	CH
Mas1	88.43	9.06	2.54	0.25	0.70	1.90	2.50	7.60	1.03	2.04	CH
Mas2	89.88	7.91	2.15	0.15	0.40	1.90	2.50	12.67	0.56	2.53	CH
Mas3	89.54	8.11	2.40	0.13	0.60	2.00	3.00	15.38	1.38	2.58	CH
Dol	93.34	5.83	0.79	0.14	0.34	1.00	1.50	7.14	0.83	2.24	ML
Lwa	94.39	3.43	2.21	0.07	0.22	0.55	0.80	7.86	1.26	2.11	MH
Mat	96.41	1.99	1.68	0.12	0.25	0.70	1.50	5.83	0.74	2.67	ML
Mav	98.66	0.78	0.62	0.15	0.35	0.75	1.00	5.00	1.09	1.83	CL
Nan	98.56	0.80	0.62	0.06	0.15	0.35	0.50	6.36	1.17	2.04	ML
Man	96.67	1.94	1.36	0.12	0.28	0.62	0.88	5.17	1.05	2.00	CL
Sil	88.75	10.13	1.07	0.13	0.48	1.80	2.50	13.85	0.98	2.67	CL
Tsh	87.98	10.53	1.45	1.00	0.34	0.70	0.90	0.70	0.17	2.37	SC
Thn	94.27	5.04	0.73	0.14	0.25	0.65	0.78	4.64	0.69	1.84	CL

Note: CH-Fat clay; MH-Elastic silt; CL-Lean clay; SC-Clayey sand; ML-inorganic silt

5.3. Differential Thermal, Thermogravimetric and Microstructural Characteristics of Clay Samples

This section presents the interpretation and discussion of the experimental results obtained from thermal characterizations and microanalyses of the studied clay samples. Information about mass stability of studied clay samples over time as temperature increases is evaluated by the thermal analysis (TGA) whereas the micro-pore analysis describes the microstructures and surface topography of the studied clays using scanning electron microscopy (SEM). Furthermore, information on the maximum temperature range beyond which the studied clays start to degrade was discussed. This analysis is critical to investigating the thermal strength of studied clays for their suitability for potential ceramic and other industrial utilization.

5.3.1. Interpretation of differential thermal and thermogravimetry analyses

The results of the differential thermal (DTA) and thermogravimetric analyses (TGA) of the studied clay samples are presented in Appendix-E. Different endothermic and exothermic peaks characterize various clay mineral types present in the studied samples. There are two conspicuous endothermic and exothermic peaks which characterizes studied clay from Mukodeni as shown in Appendix-E. The endothermic reaction occurred at 200^{o}C and 610^{o}C while the exothermic event conspicuously peaked at 100^{o}C and 450^{o}C. The first endothermic reaction was attributable to the expulsion of weakly bond and adsorbed water which corresponds to mass loss of about 1.2% as indicated by the TG curve. The second endothermic reaction occurred at temperature range from 500^{o}C to 650^{o}C. Similarly, the first exothermic expansion was noted near 100^{o}C due to expulsion of surface water from the Mukondeni sample while the second exothermic peak occurred near 450^{o}C. The temperature corresponds to decomposition of organic matters. At this TG temperature where the total mass loss was 3.8%, polymorphic transformation of α-quartz to β-quartz is suggested to have occurred as observed by dehydroxylation reaction.

In comparison with samples collected from Mukondeni, similar endothermic and exothermic peaks and reactions were observed in thermograms of Mashamba-2, Doli, Lwamondo and Matsika apart from exothermic reaction trend near 900^{o}C. At this temperature, a total mass loss of 6.6% (Dol), 7.2% (Lwa), 8.4% (Mat), 6.2% (Tsh) and 2% (Thn) which correspond to complete destruction of the clay minerals and decarbonacious reaction were observed and thus consistent with the work of Boussen *et al.* (2016). As temperature rise above 900^{o}C, samples collected from Mukondeni, Mashamba2, Thengwe and Doli show progressive increase until 1000^{o}C while samples from

Mashamba1 and Manini terminate at 800^{o}C. This temperature suggests that the threshold of new crystallization processes has been reached. It was indicated that new mineral such spinel is usually accompanied by rapid shrinkage during the process (Mahmoudi *et al.,* 2017). Whilst samples collected from Siloam showed endothermic peak near 1000^{o}C, Nandoni samples showed exothermic reaction at same temperature and both reactions indicate the onset of glass phase formation processes

5.3.2. Micro structural properties

Figure 5.5 presents the scanning electron photomicrographs of all the studied samples. The surface topography of all studied samples varies from coarse to fine texture. Variation in the topography can be adduced to different particle sizes present in samples and coarse topography suggests the presence of resistance minerals to weathering such quartz. The fine texture indicates the mineral that are susceptible to weathering such plagioclase and microcline. The platy shaped grained tends to form aggregated particles. This implied the presence of clay minerals as well as their plasticity properties. Tiny pore and stroma were present in all samples although differ in sizes and volume from one sample to another (see Figure 5.5). The voids constituted a capillary system in which molten minerals such as mullite, spinel and crystobalites that usually formed at higher temperature can saturate.

The thermal behavior of studied samples from Mukondeni, Mashamba-1, Mashamba-2 and Mashamba-3 indicated shrinkage above 9% as shown in Figure 5.6. The high shrinkage percentage could be owing to preponderance of smectite mineral. The expansion of smectite mineral rapidly shrinked when heated at temperature above 450°C due to expulsion of interlayer and surface water and the entrapped CO_2 gas that resulted from decomposition of carbonates. Other samples which were rich in kaolinite and chlorite minerals exhibited low shrinkage (<2%). The drying trends of the studied clay suggest their suitability for fast drying processes like refractory and ceramics.

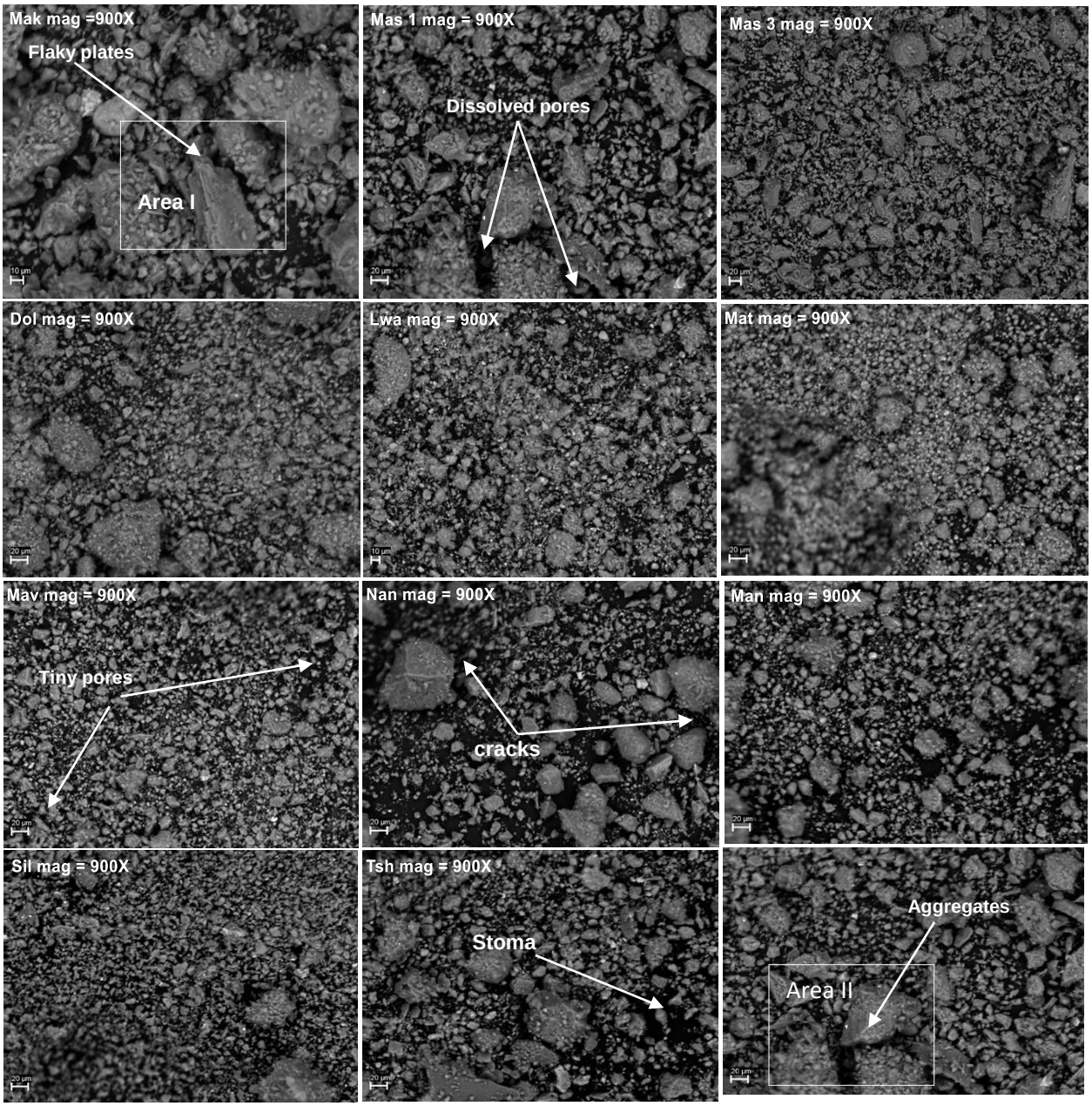

Figure 5.5: SEM Photomicrographs of the studied clays showing topography, pores and texture

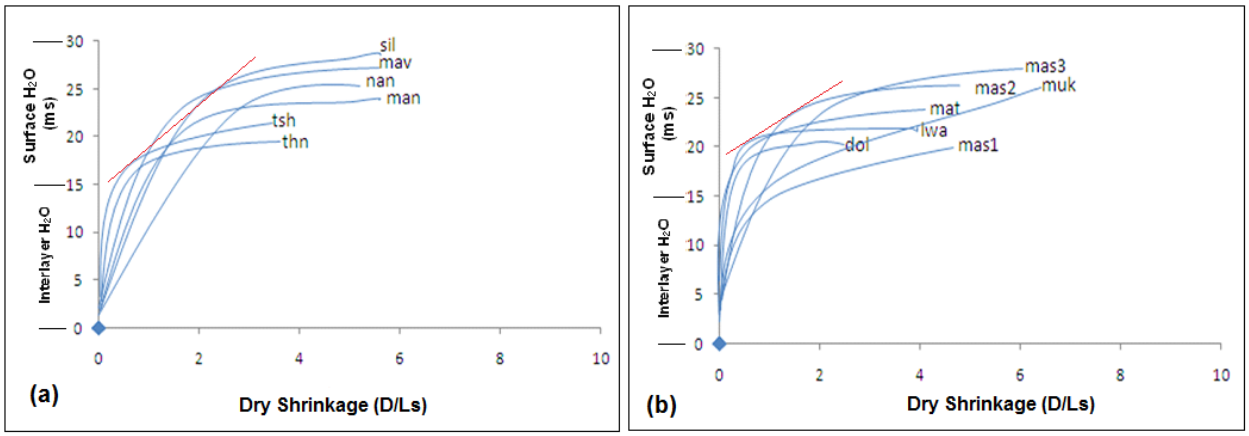

Figure 5.6: Bigot curves of the studied clay samples.

5.4. Distribution of Clay Minerals in Vhembe District

The clay minerals in Vhembe district are most commonly composed of smectite-kaolinite-chlorite series. Clay deposits that are rich in smectite mineral and present in different proportion are found in Makhado municipality around Mukondeni, Mashamba, and Thandoni as shown in Figure 5.7. Clay materials from this region exhibit high plasticity and compressibility properties with cation exchange capacity (CEC) that ranged from 64 to 83 meq/100g. Although the enrichment of smectite mineral in the clay deposits decreases around Doli in Makhado region, the kaolinite content increases towards Thulamela region as depicted in Figure 5.7.

The clay materials which are investigated in Thohoyandou are found to be rich either in kaolinite and/or chlorite minerals. Clay samples collected from Lwamondo and Matsika show the presence of kaolinite mineral as the only clay mineral although other non-clay minerals are present. In same region, clay materials from Mavambe, Nandoni are solely enriched with chlorite mineral while Manini clay material contain higher amount of kaolinite compared to chlorite content. Clay materials from this region show medium plasticity and compressibility with CEC ranging from 20 to 42.

Furthermore, kaolinite mineral solely characterized clay materials from Tshipise in Musina and Thengwe in Mutale regions. Low plasticity and CEC value are associated with clays from Tshipise while Thengwe clays exhibit medium plasticity with relatively higher CEC value. In all the studied clay deposits, non-clay minerals such as quartz, plagioclase, microcline, talc, anatase and goethite are present.

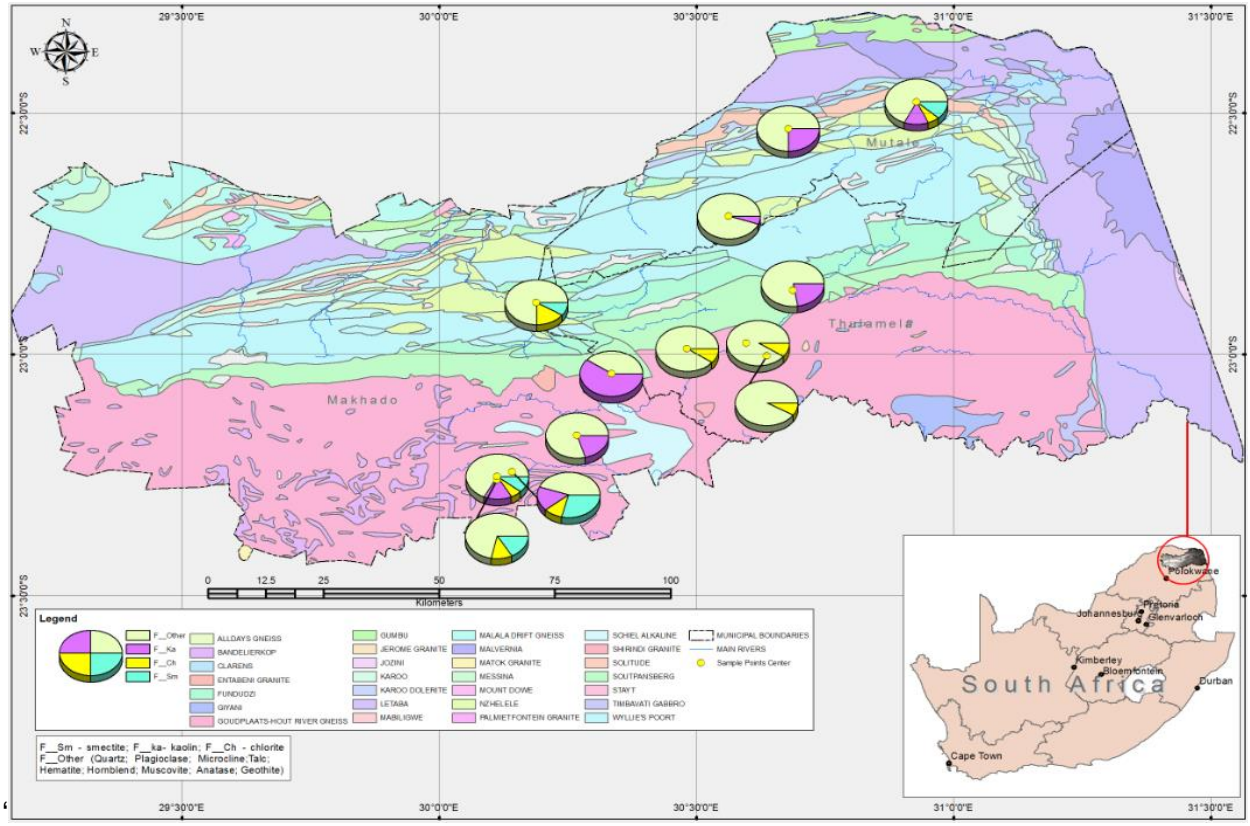

Figure 5.7: The map showing the clay deposits distribution in Vhembe District.

5.5. Potential Industrial Utilization of Vhembe Clays

The particle size and plasticity properties were used to infer the possible industrial use of the studied samples from Vhembe District. The Winkler's diagram and workability chart were empirically used to assess their industrial application of studied clay. It was observed that a clay material can be in one or more purposes. The samples collected from Mukondi, Mashamba-1, Mashamba-2, Mashamba-3, Siloam, Manini and Matsika show their possible suitability for pottery as shown in Figure 5.8. The samples showed high plasticity and compressibility with high sticky consistency. This result is consistent with the work of Dacosta *et al.* (2013) which indicated that the clays from Mukondeni can be suitable for pottery. Similarly, samples collected from Lwamondo, Doli, Nandoni and Thengwe possess relatively less plasticity property but show potential application for vertical perforated bricks as shown in Figure 5.9. Furthermore, samples collected from Mashamba-2, Matsika, Mavambe can be suitable for roofing tiles and light blocks

whereas Mashamba-1, Mashamba-3, Nandoni and Manini can be employed in production of thin-walled hollow bricks and blocks.

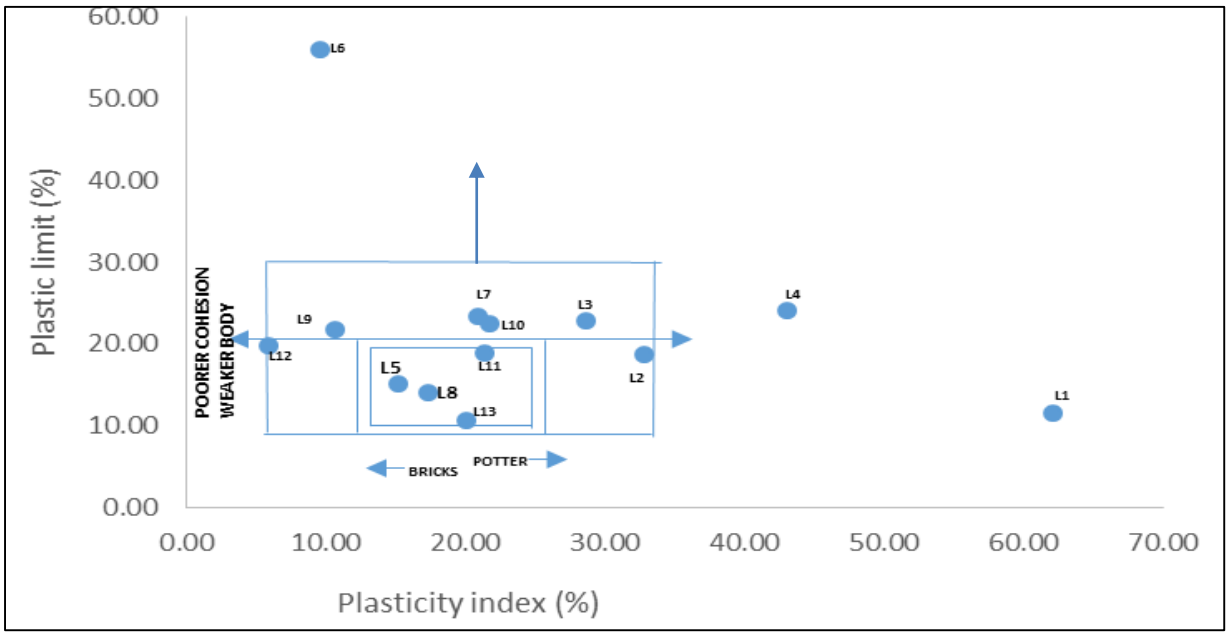

Figure 5.8: Workability chart showing possible industrial use of the studied clays.

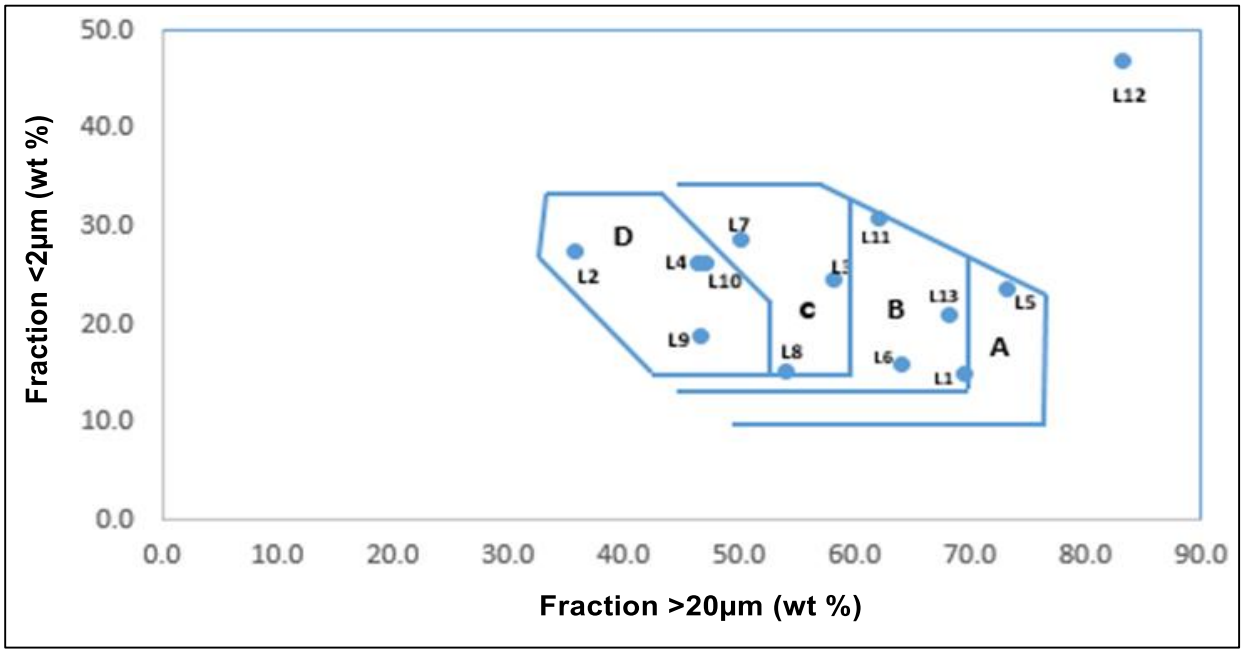

Figure 5.9: Winkler's chart showing possible clay application for (A) common bricks (B) vertically perforated bricks (C) roofing tiles and mansory bricks, and (D) hollow product.

CHAPTER SIX

CONCLUSIONS AND RECOMMENDATIONS

This chapter presents the summary of the dissertation and give some concluding and recommendation remarks.

6.1. Summary of the Study

Vhembe District has several clay deposits which are locally used in the making of burnt bricks and traditional ceramic pots however this traditional method of clay utilization do not take into account the chemical and mineralogical characteristics of clay being used. The increase in the market demand for clay products have been primarily driven by increase in civil and construction activities as well as a ceramic water filter factory in the area. This demand cannot be met with the traditional methods of manufacturing the products due to the paucity of scientific information on properties of the clay in the area. In response, there is a need to gain better understanding of the characteristics of clay in the Vhembe District and to establish the suitability of the variety of clay for different purposes.

In this context, the present study has been undertaken to investigate the provenance of clay sediments in the study area; determine the lithogeochemical, mineralogical and engineering properties of the major clay deposits in the study area and evaluate the suitability of the different clay deposits for various industrial uses. The research was systematically approached by locating the clay deposits during reconnaissance and field surveys. In the field, clay samples and rock outcrops within the study area were collected, labeled and taken to the laboratory for various analyses. The chemical, mineralogical, thermal and micro structural properties of the samples were determined using XRF, XRD, DTA-TGA and SEM respectively. The physical properties such color, CEC and soil pH were determined using Munsell colour chart, atomic absorption spectroscopy and soil pH meter respectively. The particle size distribution of the soil using sieves and hydrometer analyses and Atterberg limits tests provided a better understanding of the mechanical properties of the clays.

6.2. Conclusion

The following conclusions were made

- Petrologic and mineralogical characterizations of the studied rock surrounding the major clay deposits in Vhembe District revealed diverse rock types such as basalt, granodiorite and gneiss differentiated from subalkaline/tholeiitic magma composition. The plot of the highly incompatible and immobile elements such as Zr/Ti, Nb/Y, Th/Sc and Zr/Sc showed predominance of felsic compositional trend in most clay deposits. Mafic compositional trend in observed in Manini, Matsika, Tshipise and Lwamondo clay samples in discrimination function diagram. Mafic inclusion might have resulted from erosion of mafic to intermediate rock succession such as basalt, granodiorite and granite gneiss. This suggests that clay sediments were reworked by geological processes such as weathering.

- The relatively higher CIA value of 83.5 for clay deposits suggested an intense weathering, long transportation and depositional processes. This interpretation was further verified by the K/Cs values that were up to 6200 which allude to higher degree of clay weathering compared to the rock samples.

- The predominance of Al_2O_3 and TiO_2 contents in clay samples (13-22%) and the surrounding rock samples (3-12%) suggested a positive relationship which gave an indication that deposits also consists of input of detrital minerals or elements from local or surrounding rock suites. Although the value of SiO_2 content in rock samples are exceptionally higher when compared with clay samples, the ratio of SiO_2 / Al_2O_3in rock samples (9.2%) gave a higher value than clay samples (3.1%) thereby suggesting an ongoing desilicication and allitization processes. The Ce* anomalies value for most clay samples were above 1 and the higher value of LILE enrichment confirms an oxidizing depositional environments provenance with subduction zone geochemical domain.

- The mineralogical composition of studied clays from Vhembe District smectite (8.25 - 29.32%), kaolinite (14.91 - 59.26%) and chlorite (5.94 -16.54%) were major clay mineral types. These clay minerals were associated with quartz, feldspars, muscovite, talc, anatase and goethite. The mentioned clay mineral types occurred as combination of two or three in some of the sample while in other only one clay type was detected. Abundance of kaolinite with values ranging from >17.24% to >59% characterized Mashamba-

3<Mashamba-2<Doli<Matsika<Manini<Thengwe<Lwamondo in increasing order. In the mentioned samples, kaolinites constitute highest proportion among other clay minerals (*i.e.* smectite and chlorite) in each sample. Although, smectite showed highest content in Mukondeni (15.92%) and Mashamba-1 (29.32%) samples despite the presence of either kaolinite or chlorite in lower amount. Whilst kaolinite predominated Lwamondo, Doli, Matsika and Thengwe samples as the sole clay mineral type, chlorite also dominated Mavambe and Nandoni as well.

- The chemical composition result revealed that all the studied clay samples were rich in silica and alumina but with notable exception of samples from Lwamondo which had lowest silica content of 34% and highest alumina content of 22.4%. The fluxing oxides (Fo) of the clay samples included K_2O, N_2O, CaO, MgO, MnO and P_2O_5which varies slightly in content with average abundance ranging from 0.06% to 1.78%. Despite all other samples showing similarity in FO contents, Lwamondo clay sample has the lowest concentration of K_2O (0.46%), N_2O (0%), CaO (0.07%), MgO (0.09%) but highest in MnO (0.155%) and P_2O_5 (0.151%). The iron and TiO_2 content in all samples averages at 9.2% and 1.3% respectively with Lwamondo sample showing unusual iron content of above 25% and other samples contain less than 15%. This high content of iron oxide in Lwamondo clay sample makes the clay suitable for production of structural ceramics. In addition, the color of the ceramic bodies can be controlled by the relative abundances of hematite and goethite minerals. Clay samples of Mukondeni, Mashamba1, Mashamba-2 and Mashamba-3 whose Fe content were relatively low and exhibited grayish tonality with light intensity. The studied clay samples had hue/value/chroma from 2.5YR/5/8 to 10YR/5/1 with corresponding tonality of red to grey.

- Microanalysis using SEM revealed that the microstructure framework of all clay samples exhibited a porous skeleton structure owing to numerous tiny voids. These tiny pores present in the clay samples can generate strong suction activity to increase soil absorptive capacity. The composite results of SEM and CEC analyses their possible application in water filter and chemical fertilizer industries since they provide passage for water and soil cation mobility. Although the Cation Exchange Capacity (CEC) values of the studied clay samples widely varies from 15.37 to 83.16 meq/100g, soil pH exhibit similar and slightly basic values from 6.13 to 7.50. Samples from Muk, Mas1, Mas2 and Mas3 have relatively high CEC values above 60meq/100g compared to all other samples in which their CEC

values ranges between 15 and 44 meq/100g. The high CEC values and XRD result confirms that the raw clay materials contain considerable proportion of expansible clay minerals such as smectite and thereby encourage their utilization in ceramic industry.

- The particle size distribution curves demonstrated that the studied samples were clayey silt. This is consistent with the coefficient of gradation (C_c) and sorting (S_o) values which were found to be below 3 and above 1 respectively. Soils with C_c value less than 3 and S_o value above 1 are recognized as well graded and well sorted. In addition to the homogeneous effective sizes values (D_{10}) of all the studied clay samples, wide range coverage of the well graded and sorted particle sizes was attributed to silty textural pattern of the samples.

- Mechanical properties such as compressibility and plasticity were found to be high in clay samples from Mukondeni, Mashamba-1, Mashamba-2 and Mashamba-3. Although Lwamondo sample showed high compressibility while samples from Matsika and Nandoni showed medium compressibility. Clay samples from Doli, Mavambe, Siloam and Thengwe exhibited medium plasticity. The plasticity index of all studied clays ranged from 5.83 to 62.00 with liquid limit ranging from 31.34 to 73.62. Based on compressibility parameter, the workability chart showed that samples from Mukondeni, Mashamba-1, Mashamba-2, Mashamba-3, Nandoni, Matsika and Thengwe can be suitable for pottery-making. In the same vein, the Winkler's diagram showed that clay samples from Mashamba-2, Mavambe, Matsika can be suitable for manufacturing roofing tiles and masonry bricks while samples from Lwamondo, Thengwe, Mukondeni and Siloam can be used for producing vertically perforated bricks. Hollow products and common brick products can be produced from clay samples found Mashamba-1, Mashamba-2, Manini, Nandoni and Doli respectively.

- The relatively high weight loss in Doli (6.6%), Lwamondo (7.2%), Matsika (8.4%), Tshipise (6.2%) and Thengwe with the occurrence of thermal event at temperature above 950^{o}C despite low content of FO values was due to the predominance of kaolinite mineral and ferrous oxides. The absence of thermal events at temperature above 950^{o}C despite relatively high values of fluxing oxides in Mashamba-1 (5.7%) and Nandoni (6.7%) was due to the clay mineral type and chemical component present in the clay deposits. The thermal behavior of studied clay samples from Mukondeni, Mashamba-1, Mashamba-2

and Mashamba-3 showed relatively high shrinkage (>9%). The high shrinkage percentage could be owing to preponderance of smectite mineral. Other samples which are rich in kaolinite and chlorite minerals exhibited low shrinkage (<2%). The drying trends of the studied clay suggest their suitability for fast drying processes like soft and hard refractoriness and ceramics.

6.3. Recommendations

- The studied samples showed interesting properties for potential application in brick, pottery, refractory and water purification industries but their technological tests as compressive, flexural and absorptive tests need to be conducted as these tests will verify their practical application for brick, tile and other civil construction work.

- The kaolin and smectite-rich clays found in Lwamondo, Matsika, Mavambe Doli, Mashamba and Mukondeni can be used as extender, fillers and raw materials in production of paper, paint, plastics, sanitary and foot wares and water filter if chemically treated or modified.

- It is therefore recommended that technological and chemical modification tests be conducted in the study area to maximally harness the clay deposits for both academic and socio-economic development purposes.

REFERENCES

Agha, M.A., Ferrell, R.E., Hart, G.F., Abu El Ghar, M.S., Abdel-Motelib, A. (2013). Mineralogy of Egyptian bentonitic clays II: geologic origin. Clay and Clay Mineral. 61 (6), 551–565.

Akarish, A.M., El-Gohary, A.M., 2008. Petrography and geochemistry of Lower Paleozoic sandstones, East Sinai, Egypt: Implications for provenance and tectonic setting. Journal of African Earth Sciences 52, pp. 43-54.

Amidou, S. (2007). Infectious diarrhea in the Vhembe District of South Africa in the Era of HIV and AIDS from genomic to control. Unpublished PhD thesis, University of Venda, South Africa. pp. 66.

Annan, E., Kan-Dapaah, K., Azeko, S., Mustapha, K., Asare, J., Zebaze Kana, M., and Soboyejo, W. Clay Mixtures and the Mechanical Properties of Microporous and Nanoporous Ceramic Water Filters. Journal of Materials in Civil Engineering, October 2016, Vol. 28, No. 10.

Anthony R. West, Basic Solid-State Chemistry, 2nd Edition, Wiley, London, 2001, pp. 203-210.

Aramide, F.O., Alaneme K.K., Olubambi P.A., and Borode J.O. (2014). Characterization of some Clay Deposits in South West Nigeria. Leonardo Electronic Journal of Practices and Technologies Issue 25, July-December 2014, p. 46-57.

Astera, M. (2014). Cation Exchange Capacity in soils simplified. The ideal soil: A Handbook for the new agriculture.

Aye, E.A., Oyetunji, A. (2013). Metallurgical analysis of Ugunoda clay deposit, Nigeria for use as a refractory. International Journal of science and advanced technology 3(10), pp. 25-29.

Barker, O.B., Brandl, G., Callgha, C.C., Erikson, P.G and Van der Neut, M. (2006). The Soutpansberg and Water Groups and the Blouberg Formation. In: Johnson, M.R., Anhaesser, C.R. and Thomas, R.J. (2006). The Geology of South Africa, Geological Society of South Africa, Johannesburg and the Council of Geosciences, Pretoria, pp. 304-318.

Baiden, B.K, Agyekum, K., Ofori-Kuragu, J.K (2014). Perceptions on Barriers to the use of Burnt Clay Bricks for Housing Construction. Journal of Construction Engineering Volume 2014, Article ID-502961, 7 pages.

Bertolino, S.R.L., Zimmermann, U., Sattler, F (2007). Mineralog and Geochemistry of bottom sediments from water reservoirs in the vicinity of Cordoba, Argentina; environmental and health constraints. Applied Clay Sciences, 36, pp. 206-220.

Brake, N. Allahdadi, H., Adam.F (2016). Flexural strength and fracture size effects of pervious concrete, Constr. Build. Mater. 113 (2016) 536–543.

Brandl, G. (1981). The geology of the Messina area. Explanation sheet geological survey South Africa 2230 (Messina), Pp. 35.

Brandl, G. (1999). Soutpansberg Group. In Johnson. M.R. (Ed), Catalogue of South African Lithostratigraphic Units, South African Commission of Stratigraphy pp. 6-41.

Brandl. G. (2002). The geology of the Alldays area. Explanation sheet geological Survey South Africa, 2228 (Alldays), pp. 71.

Brencich, A. and Sterpi, E. (2006). Compressive strength of solid clay brick masonry: calibration ofexperimental tests and theoretical issues. Structural Analysis of Historical Constructions, New Delhi 2006.

British Geological Survey (2011). Mineral Planning factsheet: Natural Environment Research Council.

Boshoff, R. (2004). Formation of major fold types during distinct geological events in the Central Zone of the Limpopo Belt, South Africa. New structural, metamorphic and geochronological data. Unpublished M.Sc. Thesis, University of Pretoria South Africa.

Boussen S., Sghaier D., Chaabani F., Jamoussi B., and Bennour A. (2016). Characteristics and Industrial Application of the Lower Cretaceous clay deposits (Bouhedma Formation), Southeast Tunisia: Potential use for the manufacturing of ceramic tiles and bricks. Applied Clay Science 123, pp. 210-221.

Bumby, A.J. (2000). The Geology of Blouberg Formation, Waterberg and Soutpansberg Groups in the area of Blouberg Mountain, Northern Province, South Africa. University of Pretoria. Unpublished Thesis.

Burney, W.J. (2008). The effect of strength of brick on compressive strength of brick masonry. Process ASTM 2008; 28(Part II).

Carretero, M.I., Dondi, M., Fabri, M., Raimondo, M., (2002). The influence of shaping and firing technology on ceramic properties of calcareous and non-calcareous illitic-chloritic clays. Applied Clays Science 20, 301-306.

Celik, H., (2010). Applied Clay Science, 50, 245-254.

Christidis, G.E. (2013). Assessment of Industrial Clays. Developments in Clay Science Volume 5, 2013, Pp. 425-449.

Chryssikos, G.D., Gionis, V., Kacandes, G.H., Stathopoulou, E.T., Suárez, M., García-Romero, E., Sánchez del Rio, M. (2009) Octahedral cation distribution in palygorskite. American Mineralogist: 94: pp.200-203

Correi, S.L., Hotza, D., Segadae, S.A., 2004. Simultaneous optimization of linear firing shrinkage and water absorption of triaxial ceramic bodies using experiments design. Ceramics. International. 30,917-922.

Cultrone, G., De La Torre, M.J., Sebastian, E.M., Cazalla, O., and Roddriguez-Navarro, (2000). Behaviour of Brick Samples in Aggressive Environments: Water Air and Soil Pollution 119, pp. 191-207.

Dacosta, F.A., Muzerengi, C., Mhlongo, S.E., and Mukwevho G.F. (2013). Characterization of Clay for Water Filters at Mukondeni Village, Limpopo Province, South Africa. ARPN Journal of Engineering and Applied Sciences. Vol. 8, No. 1. pp. 927-932.

Darweesh, H.H.M., Wahsh, M.M.S. and Negim, E.M. (2012). Densification and Thermomechanical Properties of Conventional Ceramic composites containing two different Industrial byproducts. American-Eurasian Journal of Scientific Research 7 (3): 123-130.

Darweesh, H. H. M and El-Meligy, M. G. (2014). Non–Conventional Light–Weight Clay Bricks from Homra and Kraft Pulp Wastes. Journal of Chemistry and Materials Research Vol. 1 (4), 2014, 123–129.

Das, B.M. (2006). Principles of Geotechnical Engineering. 5th Edition. Nelson, a division of Thomson Canada Limited. p. 592.

Deer, W.A., Howie, R.A., Zussman, J. (2005). Rock forming minerals, sheet silicates: Micas, volume 3A, 2nd edition.

Dies, R.W. (2003). Development of Ceramic Water filters for Nepal. Unpublished M.Sc Thesis. Department of Civil and Environmental Engineering. Massachusetts Institute of Technology. p. 170.

Diko, M.L., Ekosse G.E., Ayonghe S.N., and Ntasin, E.B. (2011). Physical characterization of clayey materials from tertiary volcanic cones in Limbe (Cameroon) for ceramic applications. Applied Clay Science 51, pp. 380-384.

Djangang, C.N., Elimbi, A., Melo, U.C., Lecomte, G.L., Nkoumbou, C., Soro. J., Bonnet, J.P., Blanchart, P., Njpwouo, D. (2008). Sintering of clay-chamotte ceramic composites for refractory bricks. Ceramics International 34, 1207-1213.

Ehrmann, W., Schmiedl, G., Hamann, Y., Kuhnt, T., Hemleben, C., Siebel, W. (2007). Clay Minerals in late glacial and Holocene sediments of the northern and southern Aegean Sea. Palaeogeogr. Palaeoclimatol. Palaeoecol. 249, 36–57.

Elert, K., Cultrone, G., Navarro, C. R., Pardo, E. S. (2003) Durability of Bricks used in the Conservation of Historic Buildings – Influence of Composition and Microstructure, Journal of Cultural Heritage 4, pp. 91-99.

Elzea, J.M., Murray, H.H., (1994). Bentonite. In: Carr, D.D. (Ed.), Industrial Minerals and Rocks. 6th edn. Society for Mining, Metallurgy and Exploration, Littleton, CO, pp. 233-246.

Ekosse, G.E. (2000). The Makoro Kaolin deposit, southeastern Botswana: its genesis and possible industrial applications. Applied Clay Science 16, 301-320.

Ekosse, G.E. (2001). Provenance of the Kgwakgwe Kaolin deposit, southeastern Botswana and its possible utilization. Applied Clay Science 20, pp.137-152.

Ekosse, G.E. (2005). X-ray powder Diffraction Patterns of Clays and Clay Minerals in Botswana. Associated Printers, Gaborone. pp. 78.

Ekosse, G.E., (2010). Kaolin deposits and occurrences in Africa: Geology, mineralogy and utilization. Applied Clay Science 50, pp. 212-236.

Galan, E., Aparicio. P., Fernandez-Caliani, J.C., Miras, J., Marquez, M.G., Fallick, A.E., Clauer, N. (2016). New insights on mineralogy and genesis of kaolin deposits: The Burela kaolin deposit (Northwestern Spain). Applied Clay Science 131 pp.14–26.

Garcia-Romero, E., Suarez, M. (2010). The chemical composition of sepiolite and palygorskite. Clays and Clay Minerals: 58: pp.1-20.

Ghandour, I.M., Abd El-Hameed, A.T., Faris, M., Marzouk, A., Maejima, W. (2004). Textural, Mineralogical and microfacies characteristics of the lower Paleogene succession at the Nile Valley and Kharga Oasis Regions, Central Egypt. Journal of Geoscience. 47(4), 39–53.

Goldberg, K., Humayun, M (2010). The applicability of the chemical index of alteration as a paleoclimatic indicator example from the Permian of the Parana Basin, Brazil. Palaeography, Palaeoclimatology, Palaeoecology 293 pp. 175-183.

Gualtieri, A.F., Ferrari, S. (2006). The use of illitic clays in the production of stoneware tile ceramics. Applied Clay ScienceVolume 32, Issues 1–2, April 2006, Pp. 73–89.

Guggenheim, S. and Martin, R.T. (1995). Definition of Clay and Clay Mineral: Joint Report of the AIPEA Nomenclature and CMS Nomenclature Committees. Clays and Clay Minerals. 43(2): pp. 255-256.

Hajjaji, M., Kacim, S., Boulmane, M. (2000). Mineralogy and firing characteristics of a clay from the valley of Ourika (Morocco). Applied Clay Science 21 (3-4) 203-212.

Haurine, F., Cojan, I., Bruneaux, M.A. (2016). Development of an industrial mineralogical framework to evaluate mixtures from reservoir sediments for recovery by the heavy clay industry: Application of the Durance system (France). Applied Clay Science xxx (2016) xxx–xxx

Heckroodt, R.O. (1991). Clay and Clay materials in South Africa. Journal of the South African Institute of Mining and Metallurgy, 91(10) pp. 343-363.

Horm, G.F.J. and Strydom, J.H. (1998). Clay. In: Wilson M.G.C and Anhaeussr C.R (Editor). The Mineral Resources of South Africa. 6th Edition. Council for Geoscience. pp. 106-135.

Humberto de Araújo, J., Francisco da Silva, N., Acchar.W, Gomes, U.U. (2004). Thermal decomposition of illite. Ibero-America Jourrnal of Materials. Mat. Res. vol.7 no.2

Ince, I. and Ozdemir, A. (2010). Soil Type Investigation of the Doganhisar Clays, Central Anatolia, Turkey**.** Ozean Journal of Applied Sciences 3(3), 357. Pp.1-6.

Jauhiainen S, Holopainen M, and Rasinmaki A. (2007). Monitoring peatland vegetation by means of digitized aerial photographs. Scandanavian Journal of Forest Research 22: 168–177.

Kabanda, T.A. (2003). Climate In: A First Synthesis of the Environmental, Biological and Cultural Assets of the Soutpansberg, pp.10-11.

Kabeto, K., Zenebe, A., Bheemalingeswara, K., Atshbeha, S.G and Amare, K. (2012). Mineralogical and Geochemical characterization of clay and lacustrine deposits of Lake Ashenge Basin, Northern Ethiopia: Implication for Industrial Applications. Momona Ethiopian Journal of Science (MEJS), V4 (2): pp. 111-129

Karaman, S., Gunal, H., and Ersahin, S., (2006). Assessment of clay bricks compressive strength using quantitative values of colour components. Construction and Building Materials. Science Direct 20, pp. 348–354.

Khalaf, F. M. and Venny, A. S. (2002); New Tests for Porosity and Water Absorption of Fired Clay Bricks, Journal of Materials in Civil Engineering, Vol. 32 (11), Kulka, 67-71

Khalfaoul, A., and Hajjaji, M. (2010). Assessment of the ceramic suitability of a raw clay. Ceramics-Silikaty 54 (4) pp. 295-302.

Khan, M. (2000). A brief summary of ceramic stains, test methods and applications. Int Ceram Rev 2000; 47(5): pp. 299–302.

Kleynhans, C.J, Thirion, C and Moolman, J. (2005). A Level I River Ecoregion classification System for South Africa, Lesotho and Swaziland. Report No. N/0000/00/REQ0104.

Kloprogge, J.T., Komarneni, S., Anonette, J.E (1999). Synthesis of smectite clay minerals: A Critical Review. Clays and Clay minerals vol 49, no. 5 pp. 529-554.

Kogel, J.E, Trivedi, N.C, Barker, J.M, Krukowski, S.T (2006). Industrial Minerals and Rocks: Commodities, Markets and Uses.

Kreissig, K., Nagler, Th.F. Kramers, J.D., Van Reenen, D.D. and Smit, C.A. (2000). An isotopic and geochemical study of the northern Kaapvaal Craton and the Southern Marginal Zone of the Limpopo Belt: are they juxtaposed terranes? Lithos, 50, 1-25.

Krammers, J.D., Kreissig, K. and Jones, M.Q.W. (2001). Crustal heat production and style of metamorphism: a comparison between two Archaean high-grade provinces in the Limpopo Belt, southern Africa. Precambrian Res., 112, 149-163.

Krammers, J.D., McCourt, S and Van Reenen, D.D. (2006). The Limpopo Belt. In: Johnson, M.R., Anhaeusser, C.R. and Thomasd, R.J. (Ed.) (2006). The Geology of South Africa. Geological Society of South Africa, Johannesburg and the Council of Geosciences, Pretoria, pp. 209-236.

Kumar, R. (2011). Development of low Bulk Density Fireclay Insulation brick. National Institute of Technology, Department of Ceramic Engineering. Unpublished pp. 1-3.

Lacassie, J.P., Herve, F., Roser, B (2006). Sedimentary provenance study of the post-Early Permian to pre-Early Cretaceous metasedimentary Duque de York Complex, Chile. Revista de la Geologia de Chile 33, pp.199-219.

Larbi J. A. (2004). Microscopy Applied to the Diagnosis of the Deterioration of Brick Masonry. Journal of Construction and Building Material18, pp.299-307.

Lee, W.E. (2000). Comprehensive Composite Materials, 4, 4.12, Elsevier Science Ltd., pp. 363-385.

Luo, J., Han, G., Xie, M., Cai, Z., Wang, X. (2015). Quaternised Chitosan/ Montmorillonite nanocomposite resin and its adsorption behavior. Iranian Polymer Journal vol 24, Issue 7, pp 531-539.

Narayanan, S.P., Sirajuddin M (2013). Properties of Brick Masonry for FE modeling. American Journal of Engineering Research (AJER). Volume-1 pp.06-11.

Nemakundani, B.M. (2009). Assessment of Environmental Effect of Waste Disposal Facilities and Development of Strategies for Rehabilitation of Abandon Nyala Magnesite Mine. Unpublished Mini-Dissertation, Department of Mining and Environmental Geology, University of Venda, pp.7.

Nesbitt, H.W., Young, G.M (1982). Early Proterozoic climates and plate motions inferred from major element chemistry of lutites. Nature 299, pp 715-717.

Nguetnkam, J.P., Kamga, R., Villieras, F., Ekodeck, G.E., Razafitianamaharavo. A., Yon. J., (2005). Assessment of the surface areas of silica and clay in acid leached clay materials using concepts of adsorption on heterogeneous surfaces. J Colloid Interface Sci., 289, pp. 104–114.

Nyakairu, G.W.A., Kurzweil, H and Koeberl, C. (2002). Mineralogical, geochemical and sedimentological characteristics of clay deposits from central Uganda and their applications. Journal of African Earth Sciences 35,123-134.

Mahmoudi, S., Bennour, A., Srasra, E., Zargouni, F (2017). Characterization firing behavior and ceramic application of clays from the Gabes region in South Tunisia. Applied Clay Science 135, pp. 215-225.

Mahmoudi, S., Srasra, E., and Zargouni, F. (2008). The use of Tunisian Barremian Clay in the traditional ceramic industry: Optimization of ceramic properties. Applied Clay Science 42, pp.125-129.

Manoharan, C. Sutharsan, P., Venkatachalapathy, R. (2012). Characteristics of some clay materials from Tamilnandu, India and their possible ceramic uses. Annamalai University, pp. 412-417.

Mark, U (2010). Characterization of Ibere and Oboro clay deposits in Abia State Nigeria for refractory applications. International Journal of Natural and Applied Sciences, 6(3), pp. 296-305.

M'barek-Jemai M.B., Sdiri, A., Salah, I.B., Aissa, L.B Bouaziz, S., Duplay, J. (2017). Geological and technological characterization of the Late Jurassic-Early Cretaceous clay deposits (Jebel Ammar, northeasternTunisia) for ceramic industry. Journal of African Earth Sciences 129 Pp 282-290.

Michael, A. (2011). Materials selection in mechanical design. Butterworth-Heinemann. pp. 40.

McLennan. S.M., Taylor, S.R. (1993). Geochemical evolution of the Archean shales from South Africa, Swaziland and Pongola supergroups. Precambrian Research 22, pp. 93-124.

McLennan. S.M., Hemming, S.R., McDaniel, D.K., Hanson, G.N (1993). Geochemical approaches to sedimentation, provenance and tectonic. Geological Society of America Special Paper, 284, pp. 21-40.

Middleton, B.J. and Bailey, A.K. (2009). Water Resources of South Africa. WRC Rep No TT381. Pretoria.

Mikelonis A.M, Lawler, D.F, Passalacqua. P (2016). Multilevel modeling of retention and disinfection efficacy of silver nanoparticles on ceramic water filters. Science of the Total Environment 566–567, pp. 368–377.

Momoh, A., Akinyemi, S. A., Ojo, O.J., Dibal, H.U., Odewumi, S.C (2013). Geochemical appraisal of major elements in geophagic clays from Vhembe District, South Africa. International Journal of Current Research, v.5 (01), pp169-179.

Momoh, A (2014). Assessment of selected toxic trace elements in geophagic clays from Vhembe District South Africa. Geology of Metals and Human Health Impacts, 154(14), pp 20.

Monteiro, S.N., Vieira, C.M.F. (2004). Influence of Firing Temperature on the Ceramic Properties of Clays from Campos dos Goytacazes, Brazil. Applied Clay Sciences 27(3–4), 229–234.

Montes, C., Mefi, A.J., Carvalho, A., Vieira-Coelho, A.C. (2016). Polygenetic processes in the genesis of clay deposits of Pocos de Caldas alkaline massif in southeastern Brazil. Applied Clay science 119, pp. 424-430.

Mosheni,H., Moradi, H., Behbahani, Reza., Moeeni, Majid (2017). Geochemistry of siliciclastic sediments of the Semnan Province and NE of Isfahan Province (Iran), implication for provenance. Georpersia 7 (1) pp.55-69.

Mukhopadhyaya, P., Kumaran, K., Normandin, N., Goudreau, P. (2002). Effect of surface temperature on water absorption coefficient of building materials.Journal of Thermal Envelope and Building Science, v. 26, no. 2, pp. 179-195.

Municipality, M., 2014. Investigation of climate conditions in Makhado Municipality Jurisdiction, pp. 13-20.

Munoz, V. P, Morales, O. M.P, Letelier, G.V, Mendívil, G.M.A (2016). Fired clay bricks made by adding wastes: Assessment of the impact on physical, mechanical and thermal properties. Construction and Building Materials 125 pp 241–252.

Murray, H.H. (2000). Traditional and new applications for kaolin, smectite, palygorskite:
A general overview. Applied Clay Sciences 17,pp. 207–221.

Murray, H.H. (2005). Applied clay mineralogy. Occurrences, Processing and Application of Kaolins, Bentonites, Palygorskite-sepiolite and common clays.

Murray, H.H. (2007). Applied Clay Mineralogy. Developments in Clay Science, vol. 2, Elsevier, Amsterdam, p. 180.

Murray, H.H, Keller, W.D., (1993). Kaolin, kaolin and kaolin. In: Murray, H.H., Bundy, W., Harvery,C. (Eds.), kaolin genesis and utilization: Special Publication, 1. Clay minerals Society, Boulder, Co, USA, pp. 1-24.

Obaje, S.O, Omada, J.I., Dambatta, U.A. (2013). Clays and their Industrial Applications: Synoptic Review. International Journal of Science and Technology. Volume 3 No.5, pp. 1-7.

Obam, Ogah, Odaleje, Otor Noel. (2015). Structural and Dimensional Properties of Burnt-Bricks Produced at Oju, Nigeria. International Journal of Scientific Engineering and Applied Science (IJSEAS) - Volume-1, Issue-8, pp. 1-13

Odoma, A.N., Obaje, N.G., Omada, J.I., Idakwo, S.O., Erbacher, J., 2013. Paleoclimate reconstruction during Mamu Formation (Cretaceous) based on clay mineral distributions.
IOSR Journal of Applied Geology and Geophysics. (IOSR-JAGG) 1 (5), 40–46.

Omotoyinbo, J.A., Oluwole,O.O. (2008). Working Properties of some selected refractory clay deposits in South Western Nigeria. Journal of Minerals and Materials Characterisation and Engineering, 7(3), pp. 233-245.

Pedergnana, A., Garcia-Anton, M.D., Olle, A. (2017). Structural study of two quartzite varieties from the Utrillas facies formation (Olmos de Atapuerca, Burgos, Spain): From a petrographic characterization to a functional analysis design. Quaternary International 433 (2017) 163-178.

Perold, J. (2006). Ceramic Parameters in the Financial Evaluation of Brick Clay Deposits with reference to two South African examples. South Africa: University of Pretoria, pp. 20-31.

Parriaux, A., (2009). Geology: Basics for Engineers.

Plappally, A.k, Yakub, I, Brown, L.C, Soboyejo, W.O, Soboyejo, A.B.O (2012). Physical Properties of Porous Clay Ceramic-Ware. Journal of Engineering Materials and Technology, Vol 133, pp.9

Ptacek, P., Soukal, F. Opravil, T. Havlica, J. Brandstetr, J. (2011). The kinetic analysis of the thermal decomposition of kaolinite by DTG technique. Powder TechnologyVolume 208, Issue 1, Pp. 20–25.

Post, J.E., Heaney, P.J. (2008) Synchrotron powder X-ray diffraction study of the structure and dehydration behavior of palygorskite. American Mineralogist: 93: pp.667–675.

Pruett, R. J (2016). Kaolin deposits and their uses: Northern Brazil and Georgia, USA. Applied Clay Science 131, pp. 3–13.

Rayner, J., Skinner, B., Lantagne, D (2013). Current practices in manufacturing locally-made ceramic pot filters for water treatment in developing countries. J. Water Sanit. Hyg. Dev. 3 (2), 252.

Refaey, Y, Boris. J, El-Shater, A.H, El-Hadda, A.A., Kalbitz, K., (2015). Clay minerals of Pliocene deposits and their potential use for the purification of polluted wastewater in the Sohag area, Egypt. Geoderma Regional 5 (2015) pp. 215–225.

Santos, A.E., Rossetti, D. (2006). Depositional model of the Ipixuna Formation (Late Cretaceous-Early Tertiary), Rio Capim Area, Northern Brazil. Latin American Journal of Sedimentology 13, 101-117.

Saidi, D. (2012). Importance and Role of Cation Exchange Capacity on the Physicals Properties of the Cheliff Saline Soils (Algeria). Procedia Engineering 33 pp 435 – 449.

Schaetzl, R.J., Anderson, S.N. (2005). Soils Genesis and Geomorphology. Cambridge University Press, Cambridge, UK.

Schroeder, P.A., Pruett, R.J., Melear, N.D. (2004). Crystal–chemical changes in an oxidative Weathering front in a Georgia kaolin deposit. Clay and Clay Mineral. 52, 211–220.

Sei, J., Morato, F., Kra. G.,Staunton, S., Quiquampoix, H., Jumas, J.C., and Oliver-Fourcade. J (2006). Mineralogical, crystallographic and morphological characteristics of natural kaolins from the Ivory Coast. Journal of African Earth Sciences 46, pp. 245-252.

Serry, M.A, Hegab O.A, and Abd El-Wahed A.G. (2015). Egyptian Smectite-rich clays for lightweight and heavy clay products. Periodico di Mineralogia, 84, 2, pp. 351-371.

Sheldon, N.D., Tabor, N.J., (2009). Quantitative Paleoenvironmental and Paleoclimatic reconstruction using paleosols. Earth Science Reviews pp.95,1-52.

Shriver, D.F and Atkins P. W. (2006). Shriver & Atkins' Inorganic Chemistry, 4th edition, Oxford University Press, Oxford 2006, pp. 189-190.

Straaten, V.P (200). Rocks for crops: agrominerals of sub-Saharan Africa, ICRAF, Nairobi, Kenya, pp. 338.

Traore, K., Kabre, T.S., Blanchart, P. (2000). Low temperature sintering of a pottery clay from Burkina Faso. Applied Clay Science 17, pp.279-292.

Wieffering, N.B and Fourie, N.B. (2009). Construction Materials Building, CPUT. Pearson Education South African (Pty) Ltd.

Wei. D., Zhu. B., Wang. T., Tian. M., Huang.X (2014). Effect of Cationic exchange Capacity of Soil on Strength of Stabilized Soil. Procedia - Social and Behavioral Sciences 141, Pp. 399 – 406.

Walter, P.L (2011). Economic geology. Principles and Practice: metals, minerals, coal and hydrocarbons. Introduction to formation and sustainable exploitation of mineral deposits. Chichester, west Sussex: Wiley Blackwell p.331.

APPENDICIES

APPENDIX A: MINERALOGICAL ANALYSIS RESULTS

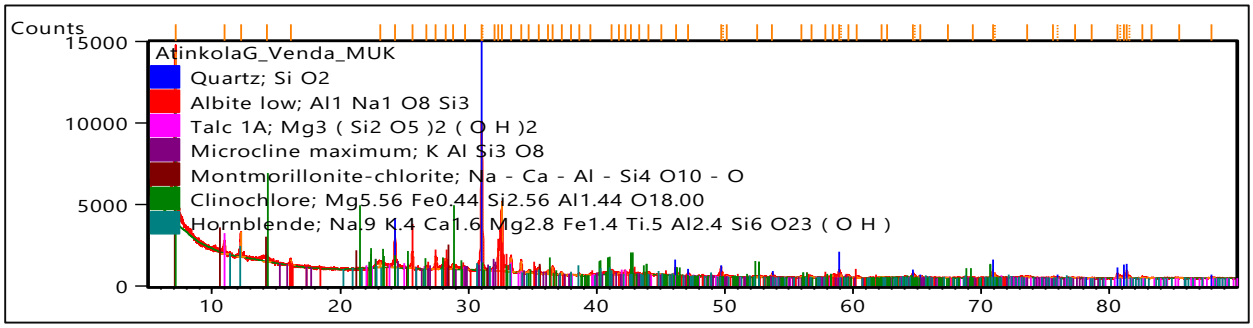

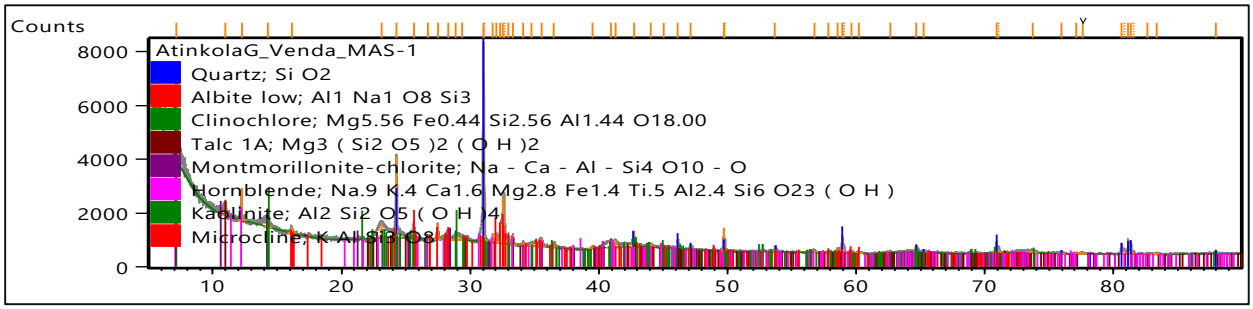

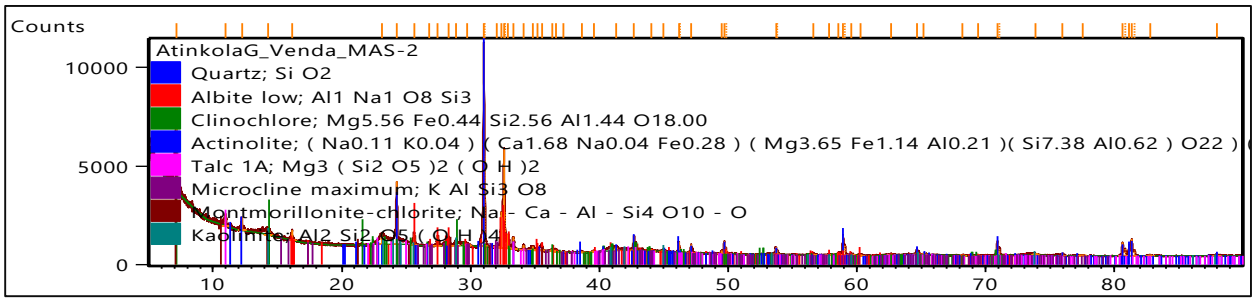

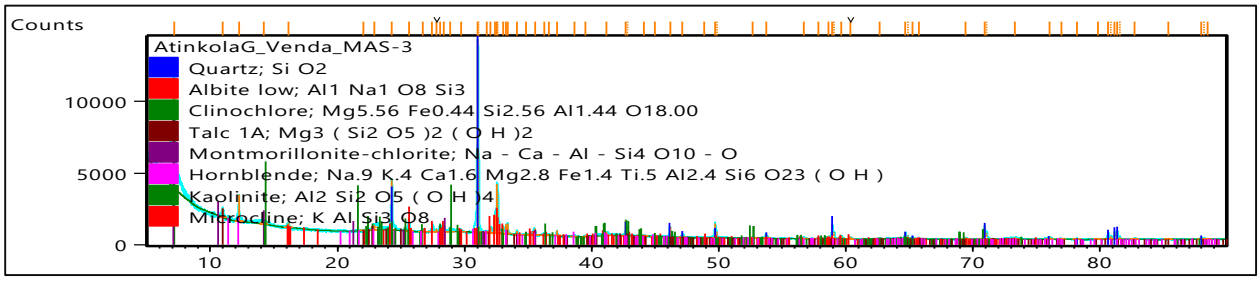

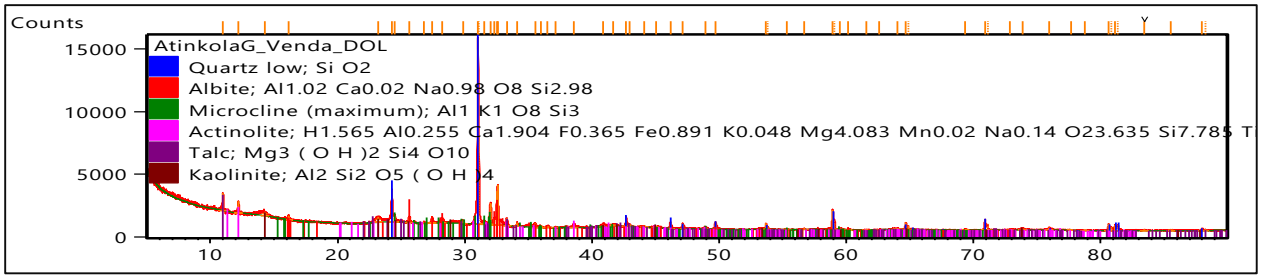

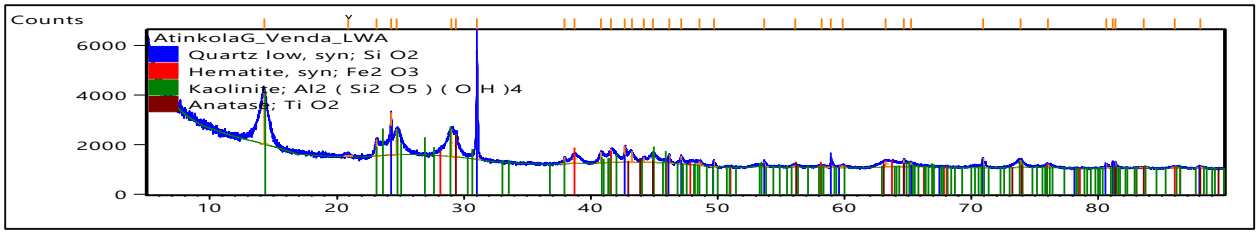

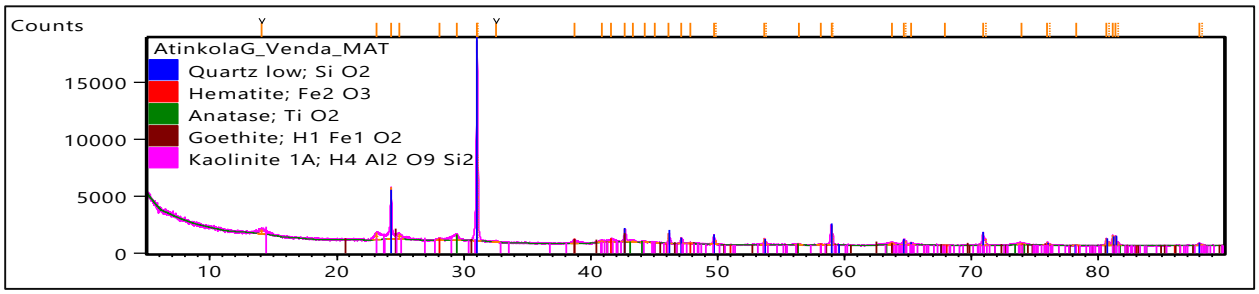

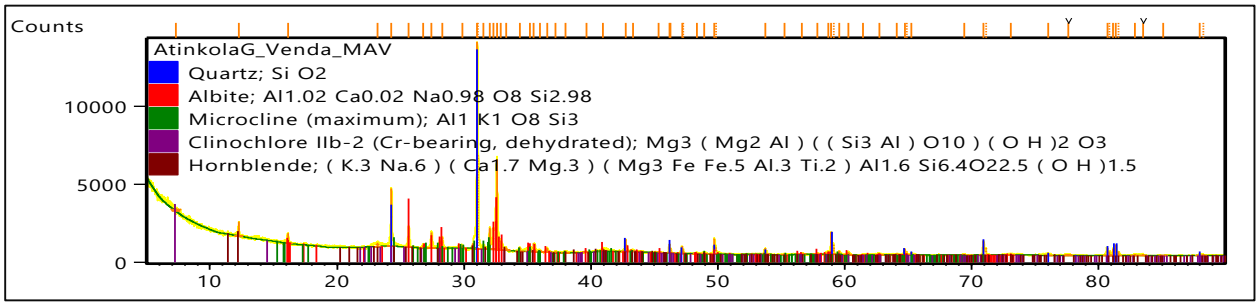

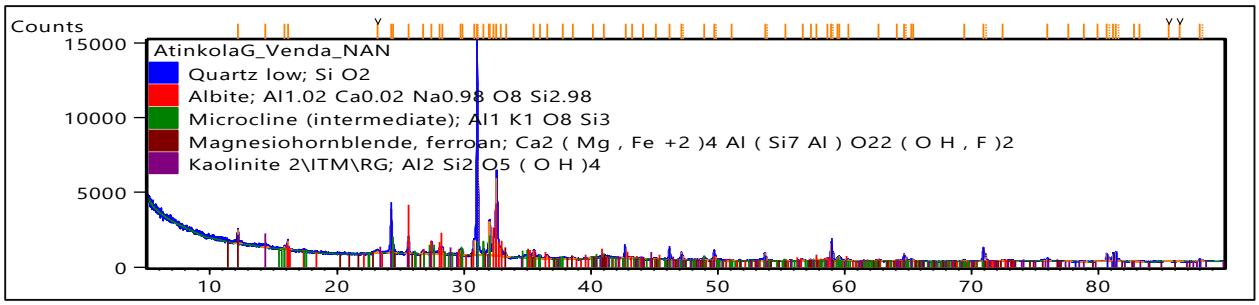

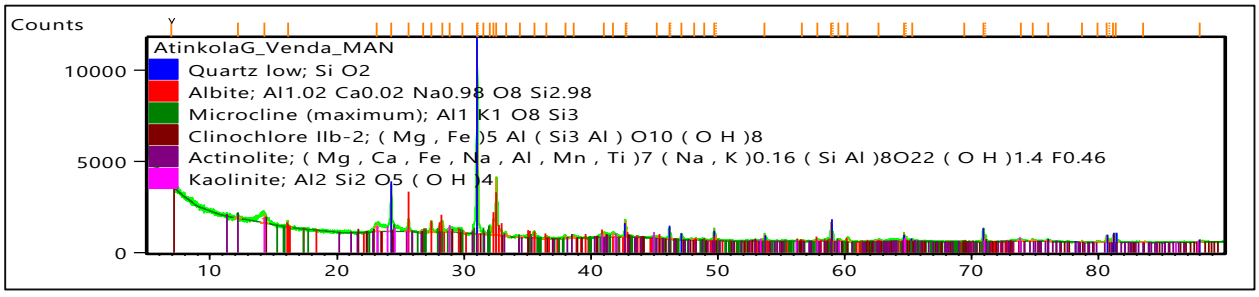

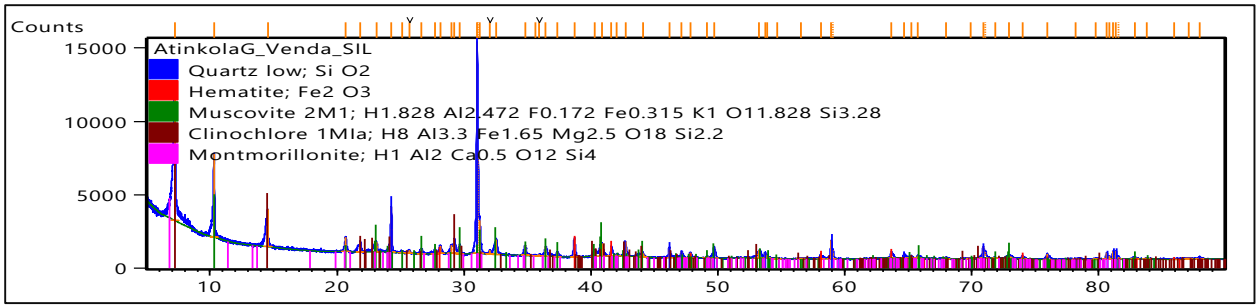

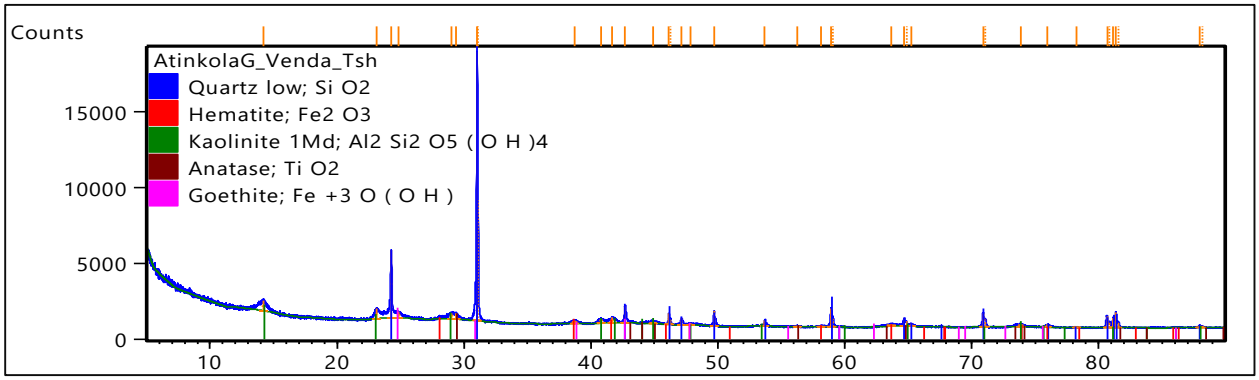

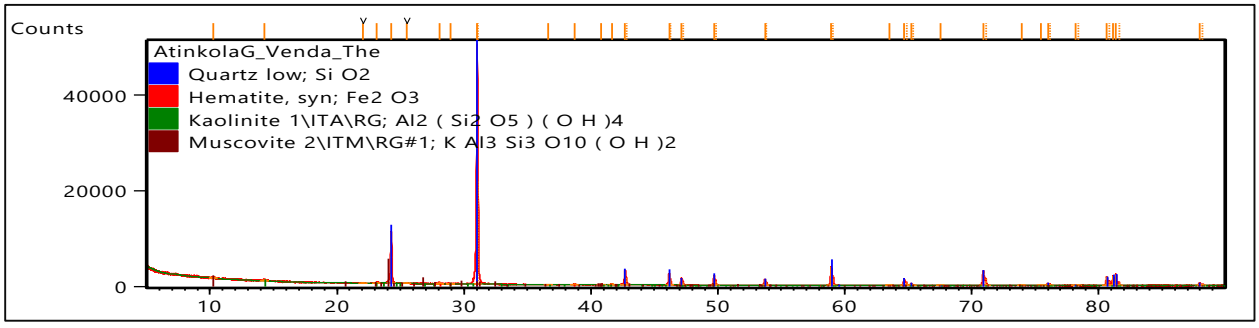

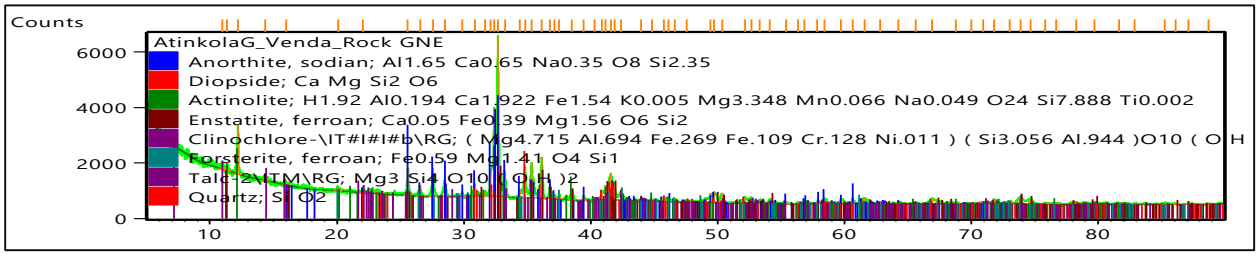

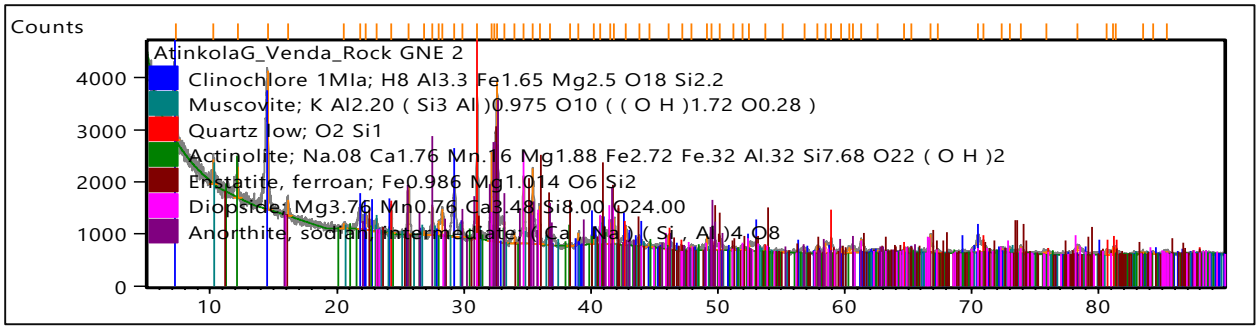

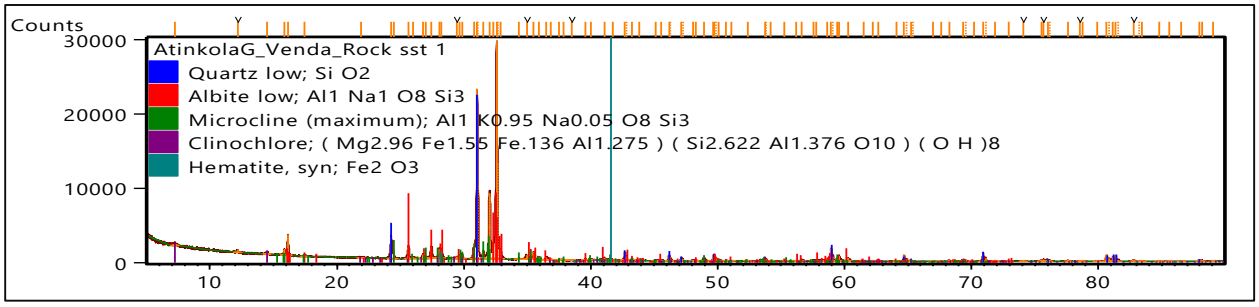

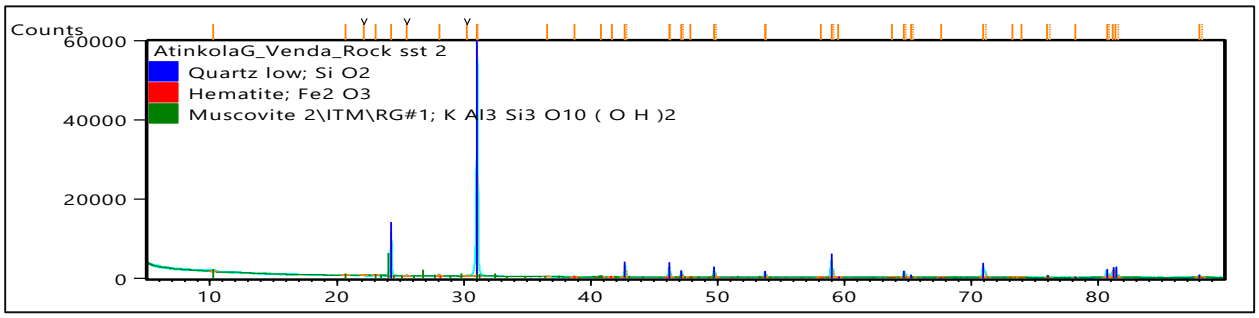

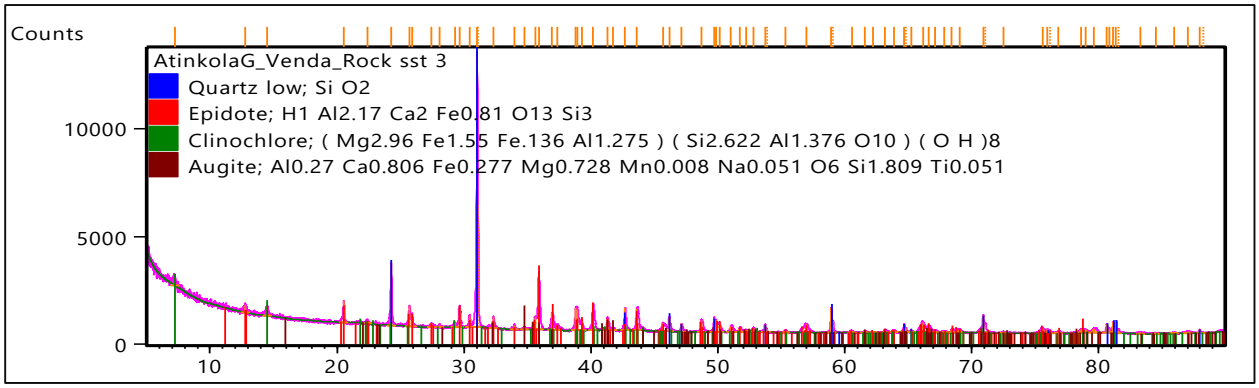

APPENDIX B: CHEMICAL ANALYSIS RESULTS

Sample (Clay)	SiO2 (%)	TiO2 (%)	Al2O3 (%)	Fe2O3 (%)	MnO (%)	MgO (%)	CaO (%)	Na2O (%)	K2O (%)	P2O5 (%)	Sc (PPM)	V (PPM)	Cr (PPM)	Co (PPM)	Ni (PPM)
Muk	51.05	0.631	14.28	5.99	0.095	3.1935	1.43	0.704	1.16	0.026	0.1	137.9	356.3	17.1	594.4
Mas 1	47.88	0.679	15.3	7.05	0.107	4.4049	2.14	0.676	0.85	0.03	0.2	150.3	432.3	19.3	732.1
Mas 2	49.61	0.546	16.08	5.85	0.073	2.9764	1.36	0.417	0.79	0.017	0.1	124.6	414.9	16.5	619.1
Mas 3	50.82	0.515	13.46	4.72	0.043	3.2974	1.17	0.339	0.75	0.023	0.1	117.4	350	12.7	539.6
Dol	46.85	1.039	17.61	7.37	0.084	1.3957	0.79	0.081	2.17	0.056	0.1	235.4	226.3	18.2	341.6
Lwa	34.1	3.844	22.41	25.5	0.155	0.0986	0.07	0	0.46	0.151	0	912.5	169.1	56.8	0
Mat	48.3	2.728	20.05	14.59	0.142	0.4217	0.3	0	0.6	0.079	0	614.6	227.3	33.8	136
Mav	54.11	0.92	14.29	5.89	0.082	1.1951	1.73	0.949	1.6	0.048	0.2	203.6	110.4	13.7	137.8
Nan	59.51	0.979	15.99	4.83	0.106	1.2996	1.22	1.315	3.04	0.091	0.1	211.6	113.9	11.6	176.8
Man	46.97	1.395	19.46	9.75	0.12	0.8057	1.3	0.128	1.27	0.058	0.1	306.1	139.6	22.3	169.6
Sil	48.62	1.088	13.48	11.14	0.124	3.5263	0.95	0.422	3.53	0.065	0.1	316.1	124.3	29.3	99.3
Tsh	42.07	1.879	16.14	13.62	0.169	0.3269	0.22	0	0.89	0.073	0	423	109.6	31.9	8.6
Thn	58.08	0.906	13.12	3.94	0.039	0.192	0.23	0	0.56	0.105	0	175	85.8	9.3	36.2

Sample (Clay)	Cu (PPM)	Zn (PPM)	Ga (PPM)	Ge (PPM)	As (PPM)	Rb (PPM)	Sr (PPM)	Y (PPM)	Zr (PPM)	Nb (PPM)	Mo (PPM)	Ag (PPM)	Cd (PPM)	Sn (PPM)	Sb (PPM)
Muk	59.5	81.8	18.4	1.4	3.1	51	307.2	16.7	157.5	4.3	1.6	0.4	0	2.8	0.2
Mas 1	74.2	75.9	17.9	1.2	2.2	43.9	235.2	16.6	142.3	4.4	1.6	0.4	0	1.6	0.3
Mas 2	47.4	49	18.6	1.2	2.7	34.9	233.7	12.3	164.4	3.4	1.8	0.2	0	1.7	0.3
Mas 3	33.9	48.2	16.6	1.2	2.2	30.8	229.9	10.2	149.9	5.7	1.8	0.6	0	2	0.5
Dol	60.6	58.7	18.1	1.2	3.4	74.7	181.6	18.9	147	6	0.3	0.5	0.1	1.6	0.3
Lwa	430.2	112.5	20.5	1.2	0.9	40.9	5.9	25	191.8	8.1	2.5	0.1	0	1.5	0.4
Mat	287.8	63	17.6	1.2	1.2	38.1	24.8	25.9	185	9.6	0.7	0.3	0	2	0.6
Mav	79.2	57.2	17.6	1.2	3.1	38.3	463.2	14.2	191.9	4.8	1.8	0.4	0	2.4	0
Nan	56.4	58.2	17.6	1.2	3.9	80.9	418.9	19.6	281.6	6.2	0.6	0.4	0	2.3	0
Man	134	61	20.1	1.2	2.7	36.1	310.9	14.9	190.7	4.7	0.3	0.4	0	2.7	0.3
Sil	181.1	113.5	14.2	1.2	1.2	102.8	43.1	26.8	97.4	4.1	1.2	0.3	0	1.6	0.3
Tsh	192	76.2	12.8	1.2	1.5	31.9	11	17.5	135	4.9	0.1	0.4	0	1.7	0.4
Thn	46.7	32.9	8.7	1.2	2.4	17.1	11.6	10.8	173.7	5.7	0.4	0.4	0.1	2.2	0.1

Sample (Clay)	Cs (PPM)	Ba (PPM)	La (PPM)	W (PPM)	Ta (PPM)	Hf (PPM)	Tl (PPM)	Pb (PPM)	Bi (PPM)	Ce (PPM)	Sm (PPM)	Eu (PPM)	Gd (PPM)	Tb (PPM)	Dy (PPM)
Muk	5.4	528.9	68.6	0	1	11.1	0.5	28.5	0.4	270.3	2.9	1	18.2	2.6	20.2
Mas 1	5.4	564.7	79.7	71.6	1.1	12.5	0.3	20.3	0.4	296.8	0	1.1	20.9	2.8	23.7
Mas 2	5.4	465.6	64.6	2.3	0.8	8.6	0.9	25.1	0.4	59.4	0	0.7	16.9	2.4	19.7
Mas 3	5.4	442.5	54.9	49.8	0.7	8.5	0.5	20.9	0.4	65	0	0.4	12.7	1.9	15.9
Dol	5.4	833.6	92.2	0	1	10.3	0.5	31.3	0.4	165.7	7.1	0.9	21.7	2.6	24.8
Lwa	38.7	2925.9	342.3	0	5	45	1.2	8.5	1	387.1	112.9	1.6	90.7	8	85.9
Mat	14.2	2093	198	0	3.4	33	0.7	13.4	0.7	261	54.1	1.4	50.4	4.7	49.2
Mav	5.4	745	71.5	12.4	1.2	11.1	0.4	28.6	0.4	130.7	0	0.8	16.7	1.9	19.8
Nan	5.4	788.5	64.9	0	0.9	12	0.4	36.6	0.5	426.9	0	1.1	14.5	1.6	16.3
Man	5.4	1099.3	123.5	17.6	1.8	18.3	0.5	25.5	0.4	156.8	12.2	1.2	29.7	3.1	32.8
Sil	5.4	869.9	128	11.2	2.3	24.3	0.2	8.1	0.5	148.7	20.4	1.3	33.7	4.3	37.5
Tsh	5.4	1460.2	171.4	0	2.4	27.4	0.4	14.2	0.6	191.2	37.1	1.7	44.2	4.7	45.9
Thn	5.4	734.2	53.4	0	0.8	10.5	0.3	21.9	0.5	69.5	0	0.4	10.1	1.4	13.3

Sample (Clay)	Ho (PPM)	Er (PPM)	Tm (PPM)	Yb (PPM)	Th (PPM)	U (PPM)	S (PPM)
Muk	N.A.	14.1	N.A.	226.5	2.2	0.7	18.2
Mas 1	N.A.	16.6	N.A.	278.5	3.3	1.7	32.1
Mas 2	N.A.	13.7	N.A.	235.3	15.7	1.3	18.6
Mas 3	N.A.	10.9	N.A.	204.6	12.4	1.2	30.8
Dol	N.A.	17.2	N.A.	135.8	5.5	2.1	46.7
Lwa	N.A.	59.6	N.A.	30	20.1	5.2	21.9
Mat	N.A.	34.6	N.A.	70.9	10.8	3.4	47.6
Mav	N.A.	13.9	N.A.	59	16.2	2.2	25.7
Nan	N.A.	11.3	N.A.	71.8	13	1.6	15
Man	N.A.	22.7	N.A.	76.2	38.2	1.1	39.2
Sil	N.A.	26.3	N.A.	52.4	7.1	3.2	12
Tsh	N.A.	31.2	N.A.	22.7	8	1.8	34.5
Thn	N.A.	8.9	N.A.	18.9	10.9	0	30.3

Sample (Rock)	SiO2 (%)	TiO2 (%)	Al2O3 (%)	Fe2O3 (%)	MnO (%)	MgO (%)	CaO (%)	Na2O (%)	K2O (%)	P2O5 (%)	Sc (PPM)	V (PPM)	Cr (PPM)	Co (PPM)	Ni (PPM)
Quarzitic sandstone	91.24	0.066	3.21	1.47	0.008	0.0949	0.05	0	0.78	0.018	0	13.2	21.2	3.5	4.7
Quarzite	43.08	0.375	11.32	8.16	0.141	10.1372	9.29	1.856	0.22	0.092	0.8	104.2	658.2	18.7	681.2
Granite Gneiss	42.06	0.904	12.37	10.89	0.172	5.3469	7.7	1.63	0.68	0.155	0.7	215.3	106.4	24.6	132.1
Basalt	55.62	1.059	10.33	9.74	0.086	1.6635	13.52	0.698	0.02	0.148	1.2	236.7	104.6	22.2	100.2
Granodiorite	65.02	0.095	12.72	0.63	0.008	0.1708	0.9	3.154	3.87	0.018	0.1	46.7	13.4	1.5	6.5

Sample (Rock)	Cu (PPM)	Zn (PPM)	Ga (PPM)	Ge (PPM)	As (PPM)	Rb (PPM)	Sr (PPM)	Y (PPM)	Zr (PPM)	Nb (PPM)	Mo (PPM)	Ag (PPM)	Cd (PPM)	Sn (PPM)	Sb (PPM)
Quarzitic sandstone	2.7	10	3.9	1.2	0.9	24.2	4	9.4	59.2	4.8	0.2	0.5	0.1	2.3	0.2
Quarzite	46.3	65.3	9.2	1.2	0	10.4	59.8	5.6	28	0.9	0	0.1	0	1.5	0.4
Granite Gneiss	198.6	110.1	12.1	1.2	0.5	23.3	115.9	13.9	79.4	4.1	0.1	0.1	0	1.4	0.4
Basalt	260.4	49.7	15.9	1.3	0.9	11.1	713.8	16.5	163.9	5.5	0.2	0.1	0	1.9	0.3
Granodiorite	0	32.9	21.8	1.2	5.2	80.3	702.1	10.8	142.8	0.5	0.1	0.3	0.1	2.4	0

Sample (Rock)	Cs (PPM)	Ba (PPM)	La (PPM)	W (PPM)	Ta (PPM)	Hf (PPM)	Tl (PPM)	Pb (PPM)	Bi (PPM)	Ce (PPM)	Sm (PPM)	Eu (PPM)	Gd (PPM)	Tb (PPM)	Dy (PPM)
Quarzitic sandstone	5.4	107.9	15.7	0	0.4	4.1	0.4	8.8	0.4	5.5	0	0.1	2.7	0.5	4.9
Quarzite	5.4	338.3	88.7	61.5	0.8	5.7	3	0	0.4	15.1	10.9	1.4	30.6	2.6	27.5
Granite Gneiss	5.4	733.1	125.8	0	2.5	19.8	2.7	4.8	0.5	71.9	18.9	1.7	36.6	3.4	36.7
Basalt	5.4	848.1	120.9	0	3.1	31.5	4.8	8	0.5	71.8	24.5	0.9	33.2	3.1	32.8
Granodiorite	5.4	129.6	5	0	0.3	2.4	1.4	48.4	0.4	76.7	0	0.1	0	0.2	2.1

Sample (Rock)	Ho (PPM)	Er (PPM)	Tm (PPM)	Yb (PPM)	Th (PPM)	U (PPM)	S (PPM)
Quarzitic sandstone	N.A.	3.5	N.A.	3.8	0	0	0
Quarzite	N.A.	19.2	N.A.	261.4	4.2	0.5	52.8
Granite Gneiss	N.A.	25.4	N.A.	64.1	7	1.3	50.8
Basalt	N.A.	23.1	N.A.	50.8	7.2	11.3	13.5
Granodiorite	N.A.	1.5	N.A.	3.3	0	2.4	0

LOCATION	SAMPLES	SiO_2 (%)	Al_2O_3 (%)	Fe_2O_3 (%)	MnO (%)	MgO (%)	CaO (%)	Na_2O (%)	K_2O (%)	CIW	CIA	k/Cs	SiO_2/Al_2O_3
Muk	Clay	51.0	14.3	6.0	0.1	3.2	1.4	0.7	1.2	87.0	81.3	2148.1	3.6
Mas1	Clay	49.6	16.1	5.9	0.1	3.0	1.4	0.4	0.8	90.0	86.2	1463.0	3.1
Mas2	Clay	47.9	15.3	7.1	0.1	4.4	2.1	0.7	0.9	84.5	80.7	1574.1	3.1
Mas3	Clay	50.8	13.5	4.7	0.0	3.3	1.2	0.3	0.8	89.9	85.6	1388.9	3.8
Dol	Clay	46.9	17.6	7.4	0.1	1.4	0.8	0.1	2.2	95.3	85.3	4018.5	2.7
Lwa	Clay	34.1	22.4	25.5	0.2	0.1	0.1	0.0	0.5	99.7	97.7	851.9	1.5
Mat	Clay	48.3	20.1	14.6	0.1	0.4	0.3	0.0	0.6	98.5	95.7	1111.1	2.4
Mav	Clay	54.1	14.3	5.9	0.1	1.2	1.7	0.9	1.6	84.2	77.0	2963.0	3.8
Nan	Clay	59.5	16.0	4.8	0.1	1.3	1.2	1.3	3.0	86.3	74.1	5629.6	3.7
Man	Clay	47.0	19.5	9.8	0.1	0.8	1.3	0.1	1.3	93.2	87.8	2351.9	2.4
Sil	Clay	48.6	13.5	11.1	0.1	3.5	1.0	0.4	3.5	90.8	73.3	6537.0	3.6
Tsh	Clay	42.1	16.1	13.6	0.2	0.3	0.2	0.0	0.9	98.6	93.5	1648.1	2.6
The	Clay	58.1	13.1	3.9	0.0	0.2	0.2	0.0	0.6	98.2	94.3	1037.0	4.4

CIA= 100 * [Al2O3/(Al2O3 + K2O + Na2O + CaO*)]; CIW= [Al2O3/(Al2O3 + CaO* + Na2O)]*100. CaO*= amount of CaO incorporated in the silicate fraction of samples. CIA/CIW= chemical index of alteration/weathering

Location	SiO_2 (%)	TiO_2 (%)	Al_2O_3 (%)	Fe_2O_3 (%)	MnO (%)	MgO (%)	CaO (%)	Na_2O (%)	K_2O (%)	P_2O_5 (%)
Quartzitic Sandstone	91.24	0.07	3.21	1.47	0.01	0.09	0.05	0.00	0.78	0.02
Quartzite	43.08	0.38	11.32	8.16	0.14	10.14	9.29	1.86	0.22	0.09
Granite Gneiss	42.06	0.90	12.37	10.89	0.17	5.35	7.70	1.63	0.68	0.16
Basalt	55.62	1.06	10.33	9.74	0.09	1.66	13.52	0.70	0.02	0.15
Granodiorite	65.02	0.10	12.72	0.63	0.01	0.17	0.90	3.15	3.87	0.02

	Muk	Thon	Mas	khan	Dol	Lwa	Mat	Mav	Nan	Man	Sil	Tsh	The
Rb (ppm)	51	44	35	31	75	41	38	38	81	36	103	32	17
Sr (ppm)	307	235	234	230	182	6	25	463	419	311	43	11	12
Ba (ppm)	529	565	466	443	834	2926	2093	745	789	1099	870	1460	734
K (ppm)	1	1	1	1	2	0	1	2	3	1	4	1	1
Zr (ppm)	158	142	164	150	147	192	185	192	282	191	97	135	174
Th (ppm)	2	3	16	12	6	20	11	16	13	38	7	8	11
U (ppm)	1	2	1	1	2	5	3	2	2	1	3	2	0
Ta (ppm)	1	1	1	1	1	5	3	1	1	2	2	2	1
Hf (ppm)	11	13	9	9	10	45	33	11	12	18	24	27	11
Nb (ppm)	4	4	3	6	6	8	10	5	6	5	4	5	6
Sc (ppm)	0	0	0	0	0	0	0	0	0	0	0	0	0
La (ppm)	69	80	4115	55	92	342	198	72	65	124	128	171	53
Ce (ppm)	270	297	59	65	166	387	261	131	427	157	149	191	70
Sm(ppm)	3	0	0	0	7	113	54	0	0	12	20	37	0
Eu(ppm)	1	1	1	0	1	2	1	1	1	1	1	2	0
Y(ppm)	17	17	12	10	19	25	26	14	20	15	27	18	11
Gd(ppm)	18	21	17	13	22	91	50	17	15	30	34	44	10
Tb(ppm)	3	3	2	2	3	8	5	2	2	3	4	5	1
Dy(ppm)	20	24	20	16	25	86	49	20	16	33	38	46	13
Er(ppm)	14	17	14	11	17	60	35	14	11	23	26	31	9
Yb(ppm)	227	279	235	205	136	30	71	59	72	76	52	23	19

LOCATION	SAMPLE	Zr/Sc	Th/Sc	Zr/Ti	Nb/Y	La/Sc	Ti/Zr	La/Sc	Ti/Zr
Muk	Clay	1575.00	22.00	315.00	0.26	686.0	31.8	686.0	31.8
Mas1	Clay	711.50	16.50	474.33	0.27	398.5	21.1	398.5	21.1
Mas2	Clay	1644.00	157.00	182.67	0.28	646.0	54.7	646.0	54.7
Mas3	Clay	1499.00	124.00	299.80	0.56	549.0	33.4	549.0	33.4
Dol	Clay	1470.00	55.00	294.00	0.32	922.0	34.0	922.0	34.0
Lwa	Clay	1918.00	201.00	159.83	0.32	3423.0	62.6	3423.0	62.6
Mat	Clay	1850.00	108.00	264.29	0.37	1980.0	37.8	1980.0	37.8
Mav	Clay	959.50	81.00	479.75	0.34	357.5	20.8	357.5	20.8
Nan	Clay	2816.00	130.00	704.00	0.32	649.0	14.2	649.0	14.2
Man	Clay	1907.00	382.00	381.40	0.32	1235.0	26.2	1235.0	26.2
Sil	Clay	974.00	71.00	487.00	0.15	1280.0	20.5	1280.0	20.5
Tsh	Clay	1350.00	80.00	337.50	0.28	1714.0	29.6	1714.0	29.6
The	Clay	1737.00	109.00	579.00	0.53	534.0	17.3	534.0	17.3
Quartzitic Sandstone	Rock	592.00	0.00	148.00	0.51	157.0	0.0	157.0	0.0
Quartzite	Rock	136.58	6.00	34.15	0.33	100.8	0.0	100.8	0.0
Granite Gneiss	Rock	35.00	5.25	9.33	0.16	110.9	0.1	110.9	0.1
Basalt	Rock	1428.00	0.00	102.00	0.05	50.0	0.0	50.0	0.0
Granodiorite	Rock	113.43	10.00	29.41	0.29	179.7	0.0	179.7	0.0

LOCATION	La(N)	Ce(N)	Sm(N)	Eu(N)	Gd(N)	Tb (N)	Dy(N)	Er(N)	Yb(N)	La/Yb(N)	Eu*(N)	(Sm+Gd)	Ce*(N)
Muk	186.92	282.45	12.55	11.49	59.48	44.83	53.02	56.63	913.31	0.20	0.32	72.03	7.84
Mas1	217.17	310.14	0.00	12.64	68.30	48.28	62.20	66.67	1122.98	0.19	0.37	68.30	9.08
Mas2	176.02	62.07	0.00	8.05	55.23	41.38	51.71	55.02	948.79	0.19	0.29	55.23	2.25
Mas3	149.59	67.92	0.00	4.60	41.50	32.76	41.73	43.78	825.00	0.18	0.22	41.50	3.27
Dol	251.23	173.15	30.74	10.34	70.92	44.83	65.09	69.08	547.58	0.46	0.20	101.65	3.41
Lwa	932.70	404.49	488.74	18.39	296.41	137.93	225.46	239.36	120.97	7.71	0.05	785.15	1.03
Mat	539.51	272.73	234.20	16.09	164.71	81.03	129.13	138.96	285.89	1.89	0.08	398.91	1.37
Mav	194.82	136.57	0.00	9.20	54.58	32.76	51.97	55.82	237.90	0.82	0.34	54.58	5.00
Nan	176.84	446.08	0.00	12.64	47.39	27.59	42.78	45.38	289.52	0.61	0.53	47.39	18.83
Man	336.51	163.85	52.81	13.79	97.06	53.45	86.09	91.16	307.26	1.10	0.18	149.87	2.19
Sil	348.77	155.38	88.31	14.94	110.13	74.14	98.43	105.62	211.29	1.65	0.15	198.44	1.57
Tsh	467.03	199.79	160.61	19.54	144.44	81.03	120.47	125.30	91.53	5.10	0.13	305.05	1.31
The	145.50	72.62	0.00	4.60	33.01	24.14	34.91	35.74	76.21	1.91	0.28	33.01	4.40

APPENDIX C: PARTICLE SIZE DISTRIBUTION CURVES

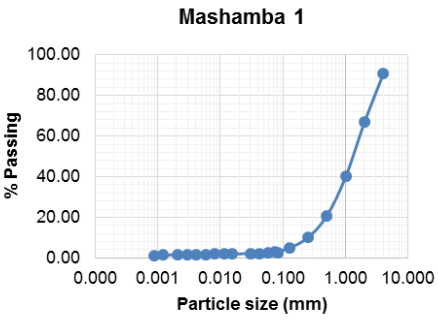

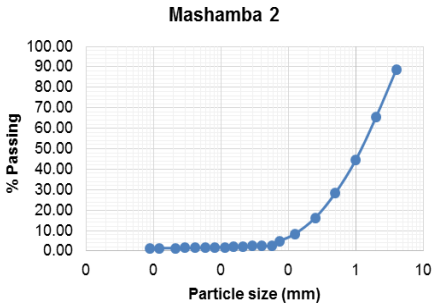

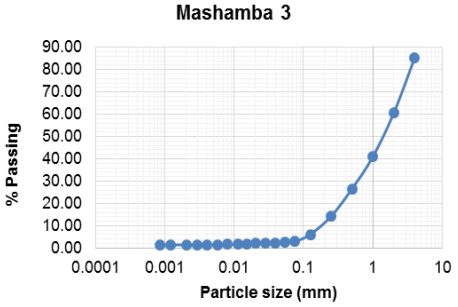

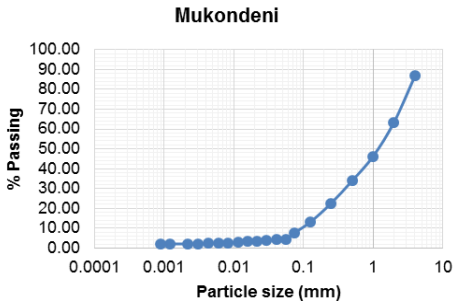

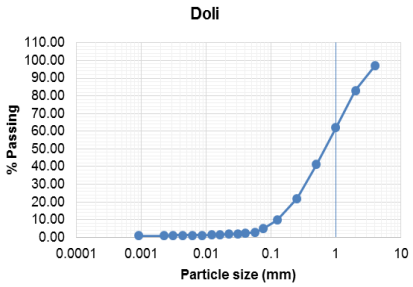

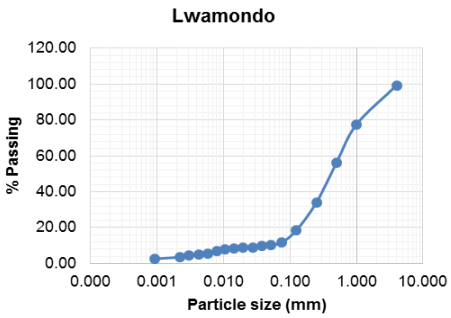

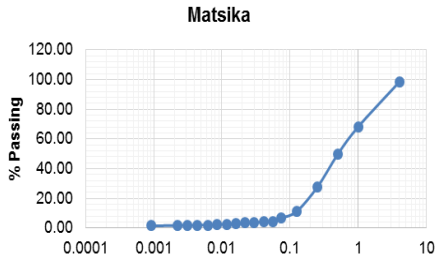

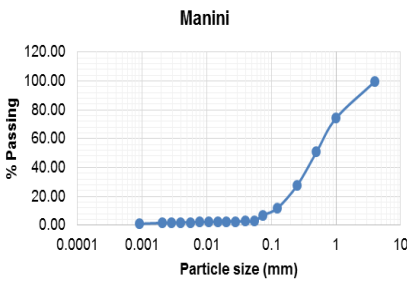

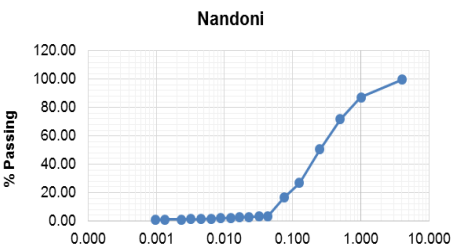

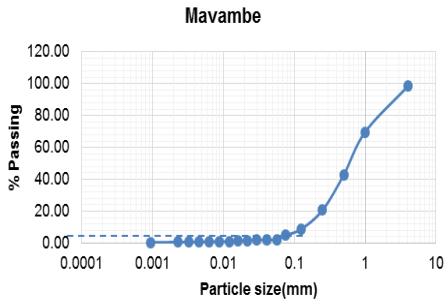

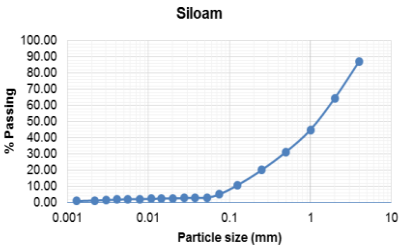

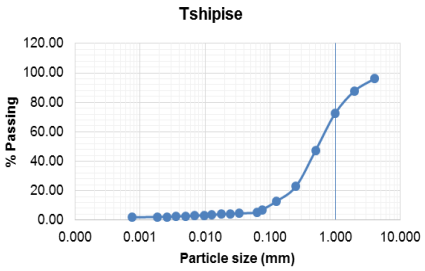

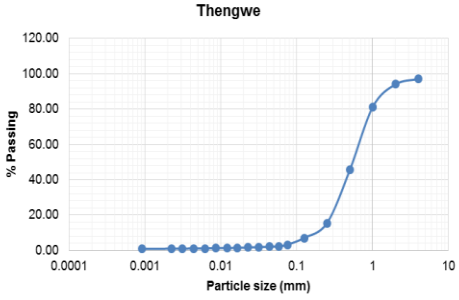

APPENDIX D: ATTERBERG LIMIT RESULTS

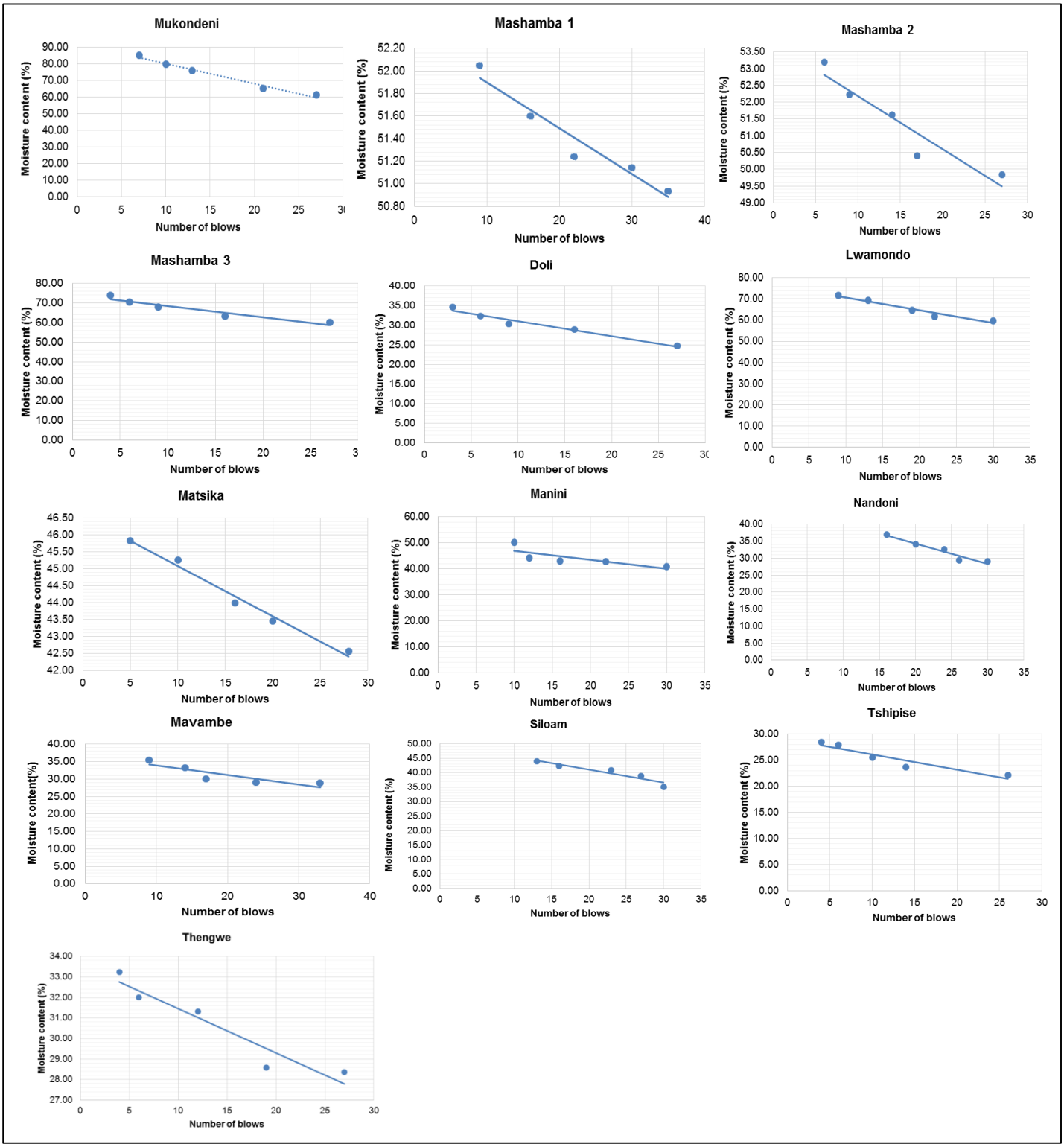

APPENDIX E: DTA-TGA (THERMOGRAPHS) CURVES

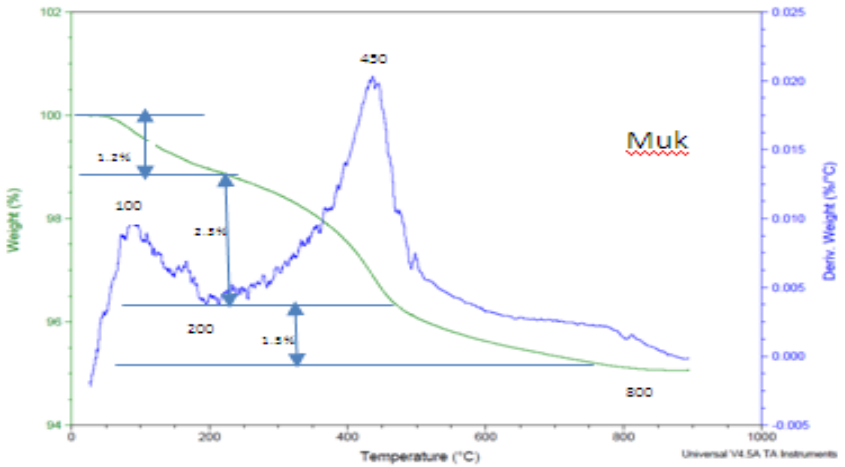

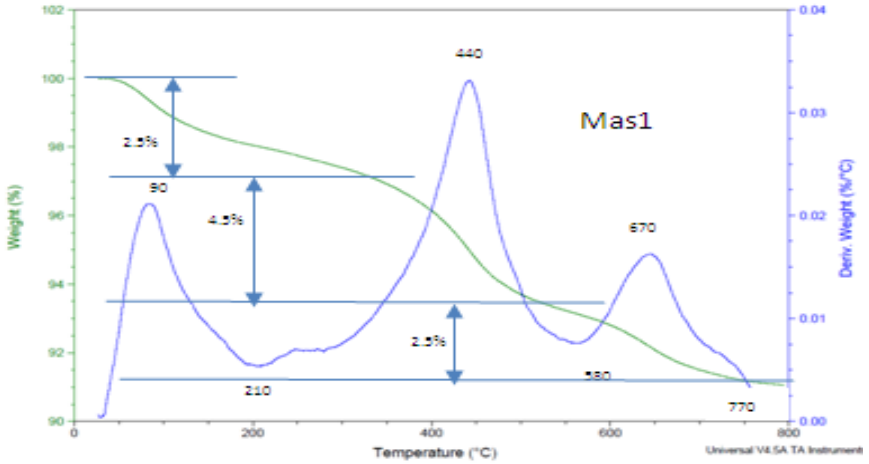

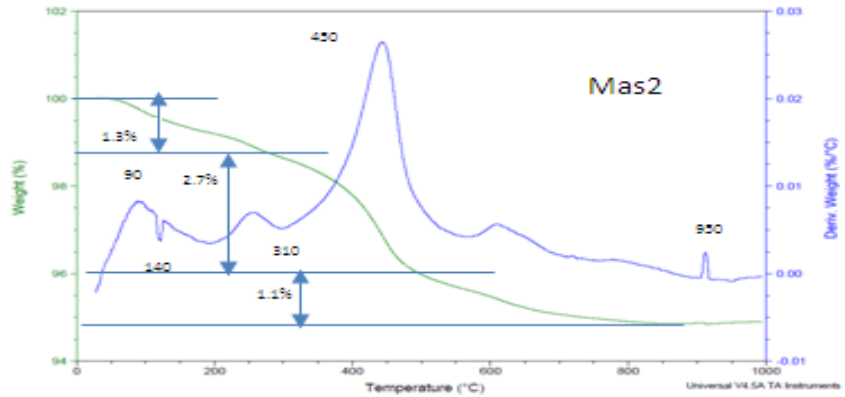

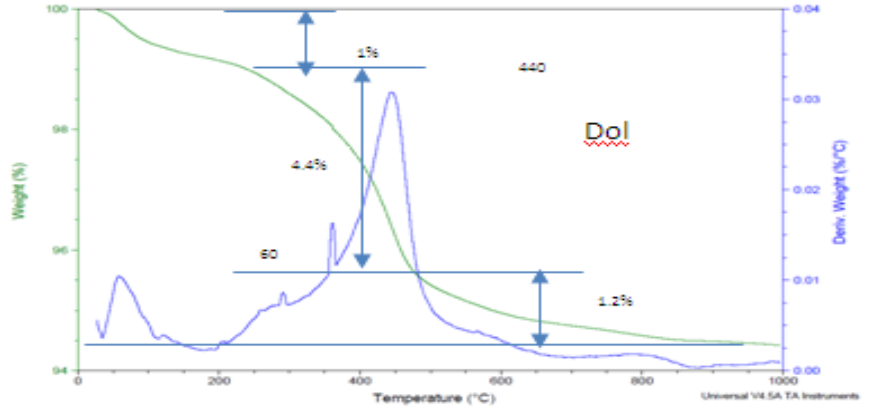

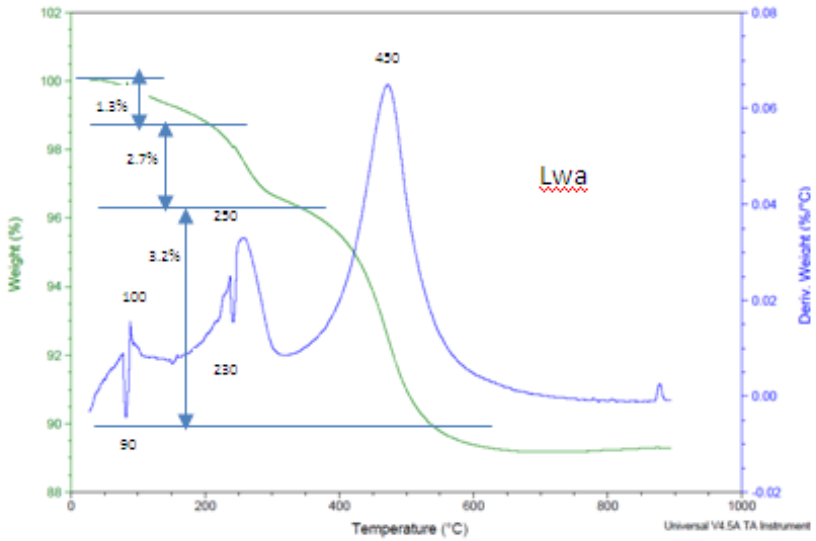

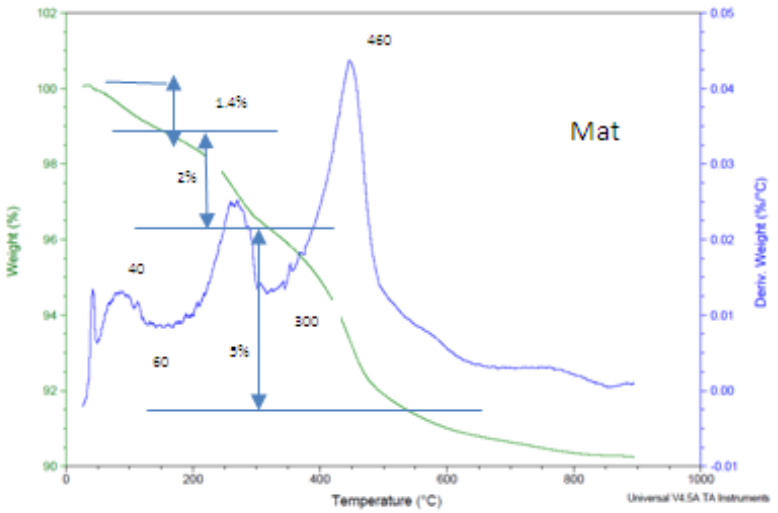

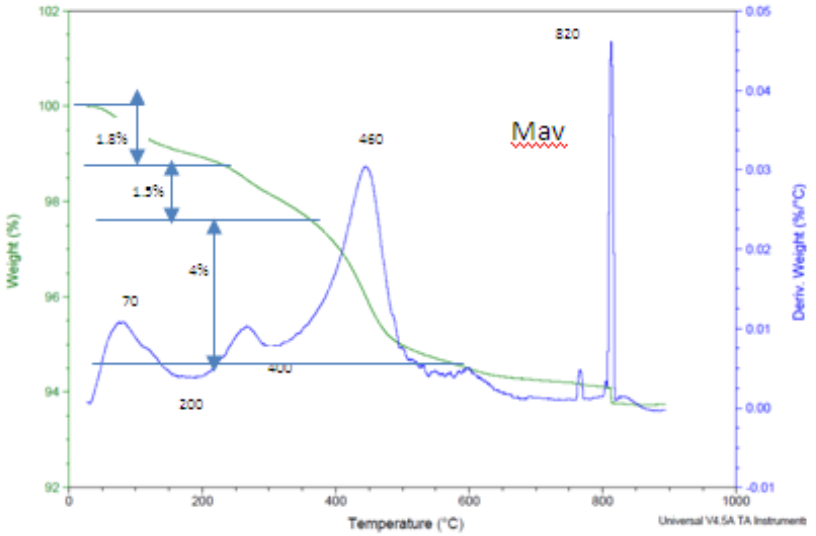

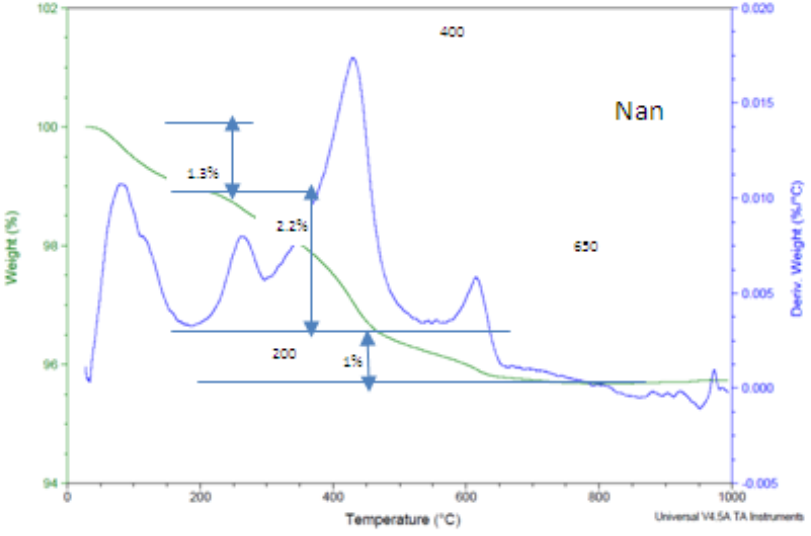

б